Free Fermion Systems: Topological Classification and Real-Space Invariants

by

Zhi Li

Bachelor of Science, Peking University, 2014

Master of Science, University of Pittsburgh, 2016

Submitted to the Graduate Faculty of

the Dietrich School of Arts and Sciences in partial fulfillment

of the requirements for the degree of

Doctor of Philosophy

University of Pittsburgh

2020

UNIVERSITY OF PITTSBURGH

DIETRICH SCHOOL OF ARTS AND SCIENCES

This dissertation was presented

by

Zhi Li

It was defended on

July 30th 2020

and approved by

Roger S.K. Mong, Department of Physics and Astronomy, University of Pittsburgh

David Pekker, Department of Physics and Astronomy, University of Pittsburgh

Jeremy Levy, Department of Physics and Astronomy, University of Pittsburgh

Andrew R. Zentner, Department of Physics and Astronomy, University of Pittsburgh

Di Xiao, Department of Physics, Carnegie Mellon University

Dissertation Director: Roger S.K. Mong, Department of Physics and Astronomy,

University of Pittsburgh

Free Fermion Systems: Topological Classification and Real-Space Invariants

Zhi Li, PhD

University of Pittsburgh, 2020

One of the major progress of modern condensed matter physics is the discovery of topological phases beyond Landau's paradigm–phases that are characterized by topology besides symmetries. In this thesis, we address topological phases of free fermionic systems by considering their topological classification and real-space invariants.

Although the theory for topological classification is fairly complete in momentum space, essentially based on the topological classification of fiber bundles, the theory in real space is more difficult. In this thesis, we discuss a formula for the $\mathbb{Z}_2$ invariant of topological insulators. As a real-space formula, it is valid with or without translational invariance. Moreover, our formula is a local expression, in the sense that the contributions mainly come from quantities near a point. It is the local nature of this invariant that guarantees the existence of gapless mode on the boundary. Based on almost commute matrices, we provide a method to approximate this invariant with local information. The validity of the formula and the approximation method is rigorously proved.

The topological classification problem can be extended to non-Hermitian systems, an effective theory for systems with loss and gain. In this thesis, we propose a novel framework towards the topological classification of non-Hermitian band structures. Different from previous K-theoretical approaches, this approach is homotopical, which enables us to find more topological invariants. We find that the whole classification set is decomposed into several sectors, based on the braiding of energy levels. Each sector can be further classified based on the topology of eigenstates (wave functions). Due to the interplay between energy level braiding and eigenstates topology, we find some torsion invariants, which only appear in the non-Hermitian world. We further prove that these new topological invariants are unstable, in the sense that adding more bands will trivialize these invariants.

Table of Contents

List of Tables

List of Figures

Preface

First of all, I would like to sincerely thank my advisor, Dr. Roger Mong, for everything related and not related to physics during the five years. It is hard to imagine a smooth graduate career without his advice, encouragement, and forgiveness. A large part of $\{\text{my understanding}\} \cap \{\text{truth}\}$ on condensed matter physics is based on inspiring discussions with him (the wrong part belongs to myself!). I especially would like to thank his tolerance and support when I spent time on many "not even wrong" ideas.

I also thank everyone who has helped me through discussions or collaborations: Ira Rothstein, David Pekker, Kiumars Kaveh, Beni Yoshida, Timothy Hsieh, Kang Yang, Liujun Zou, Yixiang Liu. Special thanks to Yuchi He, my six-year roommate at Pittsburgh and ten-year friend since undergraduate. Discussions with him really helped me a lot, although we never co-author any publication (I am sure we will). His passion for physics always inspires me.

Thanks to many friends who have shared happiness and sadness with me: Yuchi He, Yufeng Shen, Keping Xie, Peiyuan Huang, Niping Yan. Special thanks to my girlfriend Luxi Wang, for her emotional supports and many more that only she fully understands. Memories with them are the most valuable asset for me during these years.

Last but not least, thanks to my parents, for their continuing support. Thanks for keeping the place, home, where I can have a rest no matter how far I am flying. I feel lucky and honored to be your son.

1.0 Introduction

A central problem in condensed matter physics is to understand different phases of matter. The most important insight, initiated by Landau one century ago [1], dubbed the Landau-Ginzburg paradigm, is that different phases are associated with different symme-tries, and phase transitions are associated with symmetry breaking or symmetry restoration [2].

Four decades ago, people started to realize that there are new kinds of phases beyond the Landau-Ginzburg paradigm, which are characterized by topological invariants besides symmetries [3, 4]. One of the most well-known examples is the integer quantum Hall effect [5], where the states responsible for the interesting phenomena (such as the quantized Hall conductance and the stable gapless chiral edge modes) do not break any symmetry, and the distinction between different phases lies in some quantized invariants which have deep connections with topology [3].

Those phases are now called "topological phases", the study of which has become one of the most important research directions in modern condensed matter physics. In this thesis, we will discuss topological phases of free fermion systems.

1.1 Topological Band Theory

While the complete classification of topological phases is still unknown (although a lot of progress has been made, especially for gapped systems), a formal theory for translation-ally invariant gapped non-interacting systems, based on topological band theory, have been established.

As an example, let us consider a two-band tight-banding model in two dimensions (2D) without any symmetry restrictions except particle number conservation, with the following
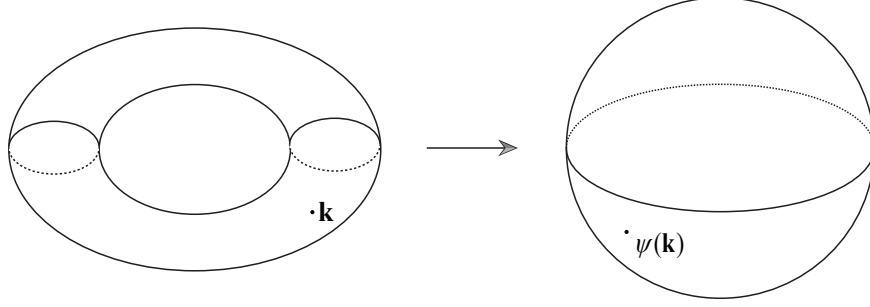
Figure 1: Topological origin of Chern insulator. The filled state for each $\mathbf{k}$ corresponds to a point on the Bloch sphere. The map from Brillouin zone torus T^2 to Bloch sphere S^2 might be topologically nontrivial.

Hamiltonian (set chemical potential $\mu = 0$):

$$H_{\text{full}} = \sum_{\mathbf{x},\mathbf{y}} \phi_{\mathbf{x}}^{\dagger} H_{\mathbf{x}-\mathbf{y}} \phi_{\mathbf{y}} = \int_{\text{BZ}} \frac{d^2\mathbf{k}}{(2\pi)^2} \phi_{\mathbf{k}}^{\dagger} H(\mathbf{k}) \phi_{\mathbf{k}}. \tag{1.1}$$

Here, $\phi_{\mathbf{x}} = (a_{\mathbf{x}1}, a_{\mathbf{x}2})^T$ is the column vector of annihilation operators at site $\mathbf{x}$, with subscipts 1 and 2 corresponding two orbitals in that site (and therefore two bands). After the Fourier transformation, each $H(\mathbf{k})$ is a 2×2 Hermitian matrix with one positive eigenvalue and one negative eigenvalue. The integral is taken over the Brillouin zone BZ, which is a two-dimensional torus T^2 in this case.

We assume that each $H(\mathbf{k})$ has a positive eigenvalue and a negative eigenvalue. Therefore, there is a spectral gap at 0 where the chemical potential μ locates at. According to the standard band theory [6], this is an insulating state.

However, once we consider the eigenvector (instead of eigenvalue) of $H(\mathbf{k})$, things might become nontrivial. For example, consider the eigenvectors $\psi(\mathbf{k})$ of $H(\mathbf{k})$ associated with the negative eigenvalue (physically, the filled state). $\psi(\mathbf{k})$ can be regarded as a point on the Bloch sphere S^2 [7], since we could always normalize it and its phase is unimportant. Therefore, we have defined a map, which assigns a state $\psi(\mathbf{k})$ to each momentum $\mathbf{k}$ in the Brillouin zone, see Fig. 1:

$$\mathbf{k} \in T^2 \mapsto \psi(\mathbf{k}) \in S^2. \tag{1.2}$$

2

The key point is: it is not always possible for two continuous maps from T^2 to S^2 to transform into each other by continuous deformation (homotopy). More precisely, continuous maps from T^2 to S^2 are topologically classified by a "mapping degree" [8], which is an integer. Intuitively, this topological invariant measures how many times the image of T^2 covers S^2, considering the orientation. An equivalent point of view is as follows. The assignment Eq. (1.2) defines a complex line bundle over T^2 [9, 10, 11]. This line bundle can be classified by some characteristic numbers, in this case, the Chern number (the Chern number here is exactly equal to the mapping degree mentioned above):

$$C = \frac{1}{4\pi} \int_{T^2} d^2k \ \vec{\psi} \cdot (\frac{\partial \vec{\psi}}{\partial k_1} \times \frac{\partial \vec{\psi}}{\partial k_2}), \tag{1.3}$$

where $\vec{\psi}$ in regarded as a vector in $\mathbb{R}^3$, $\cdot$ and $\times$ are inner and outer products of vectors. Therefore, we call an insulator with nonzero Chern number a "Chern insulator" and say that Chern insulators have a $\mathbb{Z}$ classification.

The topological phenomena in Chern insulator are essentially the same as those in integer quantum Hall effect, characterized by quantized Hall conductance and gapless chiral edge modes. In this situation, Eq. (1.3) becomes the famous TKNN formula [3] for the Hall conductance:

$$\sigma_H = \frac{e^2}{2\pi\hbar}C, \tag{1.4}$$

where C is the Chern number for filled band as defined above. Haldane realized that the same topology can also be realized without magnetic field [12], which may also be called anomalous quantum Hall effect.

The above example illustrates the key idea of topological band theory: the band structure, with eigenstates taken into consideration (not only energy levels), may possess some topological properties, which gives rise to a topological classification.

1.2   The Periodicity Table and Topological Invariants

While the above example considers the case with no symmetry, it is natural to take symmetries into consideration. A well-known example is the topological insulator (TI), which

is a topologically nontrivial system in two-dimension (2D) with time-reversal symmetry, theoretically proposed in Ref. [13, 14], and experimentally realized in Ref. [15]. It is characterized by the gapless helical edge modes protected by the time-reversal symmetry [16], and the band-crossing in the language of topological band theory. The topological invariant, in this case, is a $\mathbb{Z}_2$ number which we call Kane-Mele invariant.

Depending on the existence/nonexistence of various symmetries and their actions on the Hilbert space, free fermionic systems are classified into ten classes [17]. This is called the ten-fold way. Depending on the symmetries and dimensions, systems are classified by a topological invariant valued in $\mathbb{Z}$ or $\mathbb{Z}_2$ [18, 19, 20, 21]. More interestingly, the ten classes and dimensions can be organized in a nice way, called the periodicity table (see Tab. 5), where different topological invariants show nice periodic feature. This will be the main theme of Chapter. 2.

As mentioned above, a common feature of free-fermionic topological phases is the existence of protected gapless boundary modes. An argument for the boundary modes goes as follows: since the system is topological on one side and trivial on the other side, there must be some gapless modes localized along the boundary to separate two parts, otherwise, two phases can be connected without a phase transition. Firstly, since there is generally no Brillouin zone for systems with boundaries, there must be some real-space notion of topological versus trivial (instead of topological band theory as discussed above). Secondly, the above argument is not always valid, as there do exist some examples dubbed gappable boundaries. To make this argument more rigorous, we need the distinction of topological phase and trivial phase to be locally detectable, so that two sides of the boundary are indeed different.

In Chapter. 3, we will discuss some examples of real-space local formula for topological invariants. While the topological band theory is not valid in real space, one can still get useful results from noncommutative geometry/topology considerations [22, 23, 24, 25] or from physical considerations such as scattering theory [26] or boundary Anderson delocalization [19]. The real-space invariants may manifest itself as a trace formula [27, 28, 29], or some more general (Fredholm, mod 2 Fredholm, Bott, etc) indexes [30, 31, 32, 33, 34, 35, 36, 37, 38].

Once such formulas have been established, they can also be applied to systems with disorder, where the classification is believed to be robust [18, 39, 40]. Indeed, it is exactly

because this stability (for classification and for the edge mode) that people hope topological phases will be useful in real life, where disorders are inevitable.

1.3   Non-Hermitian Topological Band Structures

Non-Hermitian Hamiltonian can emerge as an effective description of open systems with gain and loss [41] or as an extension of conventional Hermitian quantum mechanics [42, 43, 44]. Inspired by the great success in topological phases for Hermitian systems, there have been lots of works focusing on the topological aspects of non-Hermitian systems, see Ref. [45, 46, 47, 48, 49] and references therein for details.

While some frameworks and techniques can be easily extended to the non-Hermitian case, there is one more subtlety, coming from the fact that non-Hermitian matrices may have complex eigenvalues.

For example, consider a translationally invariant one-dimensional system with two bands. We again work in momentum space and assume $E_1(k) \neq E_2(k)$ for all k (this condition is a natural generization of gapness in the Hermitian case). The difference between non-Hermitian world and Hermitian world is: it is possible that $E_1(2\pi) = E_2(0)$. If one follows the spectrum when k goes around the Brillouin zone (a circle S^1 in this case) starting from $E_1(0)$, one may go to $E_2(0)$ instead of going back to $E_1(0)$, see Fig. 2(a). In this case, we do not have a good notion of "upper band" and "lower band". Instead, two bands essential combines into one band.

Whether $E_1(2\pi) = E_1(0)$ or $E_1(2\pi) = E_2(0)$ is clearly a topological distinction. It reflects the fact that energy levels may braid with each other as the momentum k varies. Naturally, if more bands are given, one will expects more general braiding patterns of energy levels, see Fig. 2(b). The braiding phenomenon also becomes more complex in higher dimensions, at least because there are more directions for the momentum to vary[1]. Moreover, as we will show, the topological property of energy levels may have some "interferences" with the

---

[1]One may wonder whether there is "higher-dimensional braiding" which cannot be decomposed into products of one-dimensional braiding. We will see essentially there is not.
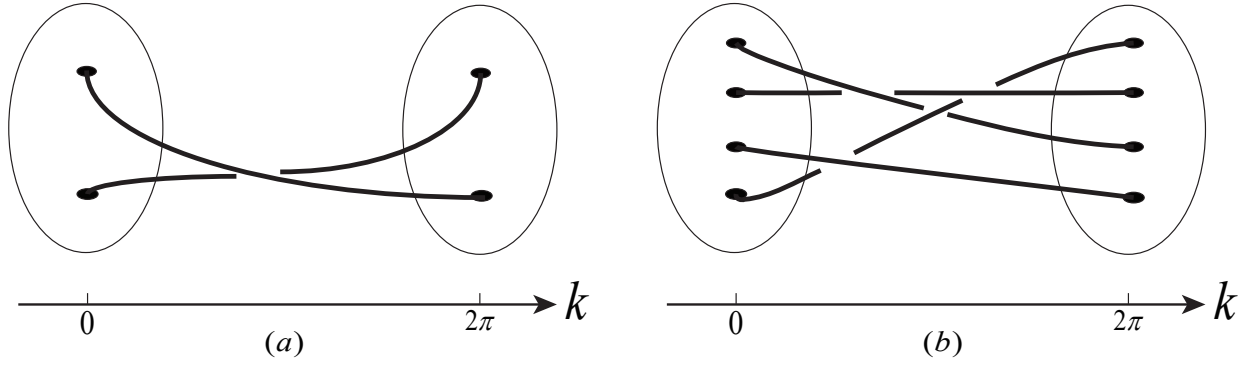
Figure 2: (a) $\mathbb{Z}_2$ braiding of energy levels. In this figure, the disk is the complex energy plane, with two spectra points in it; k is the Bloch momentum, $k = 0$ and $k = 2\pi$ should be identified. (b) A more complicated braiding pattern with four bands.

topological property of states, which provide new topological invariants and/or change the nature of previous Hermitian topological invaraints.

1.4   Organization of This Thesis

This thesis is organized as follows.

Chapter. 2 reviews the ten-fold way and the K-theoretical periodicity table for Hermitian topological insulators and superconductors. While the results are more or less well-known, we will derive the results from the first principle, with special emphasis on mathematical generality. The treatment in this chapter is largely based on [18, 20].

Chapter. 3 considers the computation of topological invariants in position space instead of momentum space. We will find that topological invariants are essentially local[2]. Part of this chapter is based on [29].

In Chapter. 4, we consider the topological classification of non-Hermitian band struc-tures. We will consider the braiding phenomenon in higher-dimensions and for more bands.

---

[2]Different from topological-ordered systems where order parameters are non-local.

6

More importantly, we will consider the interplay between energy level topology and states topology, based on rigorous algebraic-topological calculations. We will see that, in the existence of non-trivial braidings, the topological classification contains some novel torsion invariants. We will further prove that these new topological invariants are unstable, in the sense that adding more bands will trivialize these invariants. Discussions in this chapter are based on [50].

In Chapter. 5, we briefly summarize this thesis and provide some questions for further developments.

2.0 K-**Theoretical Classification of Topological Insulators and Superconductors**

In this chapter, we review the ten-fold way and the K-theoretical periodicity table for Hermitian topological insulators and superconductors. While the results are more or less well-known, we will try to derive the results from the first principle, with special emphasis on mathematical generality. For this purpose, we will use the "most suitable" mathematical tools at will. For a review of relevant mathematics, see Appendix A.

We first consider symmetries in quantum mechanics and explain a $\mathbb{Z}_2 \times \mathbb{Z}_2$ classification [20]. We emphasize that these two $\mathbb{Z}_2$ gradings are natural consequences of general principles of quantum mechanics. They come from the distinction between linear and antilinear, and the time-orientation issue, which are in principle applicable to any quantum systems.

We then derive the ten-fold way classification of quantum systems [17]. We again emphasize that this classification is valid for any quantum mechanical systems in any dimensions, bosonic or fermionic, interacting or not.

In Sec. 2.2.3.3, we derive the famous periodicity table for topological insulators and superconductors [18, 19, 21]. We note that, to be in accordance with the spirit of 2.1, the symmetries are labeled by real quantum symmetries, namely, operators that act on the physical Hilbert space and with real physical consequences. We found that it is important to consider particle number conservation [18], since its existence/absence will lead to different classifications.

2.1 Quantum Symmetries

2.1.1 Wigner's Theorem

Consider a quantum mechanical system described by the projective Hilbert space $P\mathcal{H}$, the ray space of Hilbert space $\mathcal{H}$. A point $l \in P\mathcal{H}$ corresponds to a pure state $\psi \in \mathcal{H}$ with

phase information omitted, and we will use the notation l_ψ. According to the Born rule, the probability of finding l_{ψ_1} in a state l_{ψ_2} is given by:

$$P(l_{\psi_1}, l_{\psi_2}) = |\langle \psi_1 | \psi_2 \rangle|^2. \tag{2.1}$$

This is a well-defined pairing on $P\mathcal{H}$.

A symmetry is a change of our point of view that does not change the results of possible experiments. Therefore, we have the following:

Definition 2.1 (Symmetry). A symmetry of quantum system is a bijection s of $P\mathcal{H}$ such that:

$$P(l_1, l_2) = P(s(l_1), s(l_2)), \tag{2.2}$$

for any $l_1, l_2 \in P\mathcal{H}$. We denote the group of s satisfying as $\mathrm{Aut}\,(P\mathcal{H})$, with Aut for automorphism.

The following important theorem [51, 52] tells that any symmetry transformation can be lifted to the original Hilbert space $\mathcal{H}$.

Theorem 2.1 (Wigner). A symmetry can be induced by a unitary transformation or an antiunitary transformation $U : \mathcal{H} \to \mathcal{H}$ such that:

$$s(l_\psi) = l_{U\psi} \tag{2.3}$$

We remark that there can be operators which is neither unitary nor antiunitary that induces symmetries on $P\mathcal{H}$. For example, define $U\psi = e^{i\theta(\psi)}\psi$ where $\theta(\cdot)$ is an arbitrarily complicated function. Wigner's theorem says that any such lifting can be made unitary or antiunitary with such state-dependent phase.

Formally speaking, we denote the group of unitary transformation on $\mathcal{H}$ as $U(\mathcal{H})$, denote the group of unitary and antiunitary transformations as $\mathrm{Aut}\,(P\mathcal{H})$. Then we have the following exact sequence of group homomorphism [53]:

$$1 \longrightarrow U(\mathcal{H}) \longrightarrow \mathrm{Aut}\,(\mathcal{H}) \xrightarrow{\phi} \mathbb{Z}_2 \longrightarrow 1, \tag{2.4}$$

where $\phi = -1$ means a transformation is antilinear. Wigner's theorem says that the homomorphism $\mathrm{Aut}\,(\mathcal{H}) \to \mathrm{Aut}\,(P\mathcal{H})$ defined by Eq. (2.3) is surjective.

Moreover, it is easy to see any unitary or antiunitary transformation that induces identity on $P\mathcal{H}$ must be a phase. Therefore, we have the following exact sequence:

$$1 \longrightarrow U(1) \longrightarrow \text{Aut}(\mathcal{H}) \xrightarrow{\pi} \text{Aut}(P\mathcal{H}) \longrightarrow 1. \tag{2.5}$$

Note that since $U(1) \subset U(\mathcal{H})$, the homomorphism ϕ factorizes through $\text{Aut}(P\mathcal{H})$. This means that whether a symmetry can only be lifted as either unitary or antiunitary, but not both.

2.1.2 Symmetries Compatible with Dynamics

In this thesis, we will assume relevant physics takes place in a trivial space-time background (as always in non-gravitational physics), therefore we will have a notion of time such that $t \in \mathbb{R}$.

Normally, any physical symmetry operation s is natually associated with a $\mathbb{Z}_2$ number which tells us whether the operation reverses (if $\tau = -1$) the orientation of time [20]:

$$\tau(s) \in \mathbb{Z}_2. \tag{2.6}$$

It is clear by definition that this τ is a group homomorphism.

By definition, a dynamics of a quantum system is a unitary operator group generated by a Hermitian Hamiltonian H:

$$U(t) = \exp(-itH). \tag{2.7}$$

We will assume time-translational symmetry, hence H is time-independent. The unitary $U(t)$ also induces an isometry on the ray space $P\mathcal{H}$. We say a symmetry s is campatible with the dynamics $U(t)$ if the following diagram commute:

$$\begin{array}{ccc} P\mathcal{H} & \xrightarrow{s} & P\mathcal{H} \\ \downarrow{\scriptstyle U(\tau(s)t)} & & \downarrow{\scriptstyle U(t)} \\ P\mathcal{H} & \xrightarrow{s} & P\mathcal{H} \end{array} \tag{2.8}$$

Therefore, when lifted to $\mathcal{H}$, we have:

$$\tilde{s}^{-1}U(t)\tilde{s} = U(\tau(s)t)e^{-i\theta_s(t)}, \tag{2.9}$$

10

with $\theta_s(t) \in \mathbb{R}$. It is easy to show that:

$$\theta_s(t_1) + \theta_s(t_2) = \theta_s(t_1 + t_2). \tag{2.10}$$

Hence $\theta_s(t) = \theta_s t$, with some continuity assumptions.

In terms of the Hamiltonian, we have:

$$\tilde{s}^{-1} H \tilde{s} = \phi(s)\tau(s)H + \phi(s)\theta_s \overset{\text{def}}{=} \chi(s)H + \theta(s). \tag{2.11}$$

To simplify the notation, we have defined $\chi = \phi\tau$.

Theorem 2.2. We can always set $\theta(s) = 0$ without loss of generality.

Proof. For $\forall s$ such that $\chi(s) = 1$, the above equation would imply the spectrum of H has a translational symmetry and in particular, unbounded from below. This situation would be unphysical since it usually means the system is unstable[1]. Therefore $\theta(s) = 0$ whenever $\chi(s) = 1$.

For $\forall s, t$, we have:

$$\chi(st)H + \theta(st) = (\tilde{s}\tilde{t})^{-1}H\tilde{s}\tilde{t} = \chi(s)\chi(t)H + \chi(s)\theta(t) + \theta(s), \tag{2.12}$$

and therefore:

$$\theta(st) = \chi(s)\theta(t) + \theta(s). \tag{2.13}$$

For $\forall s, t$ such that $\chi(s) = \chi(t) = -1$, we get $\theta(s) = \theta(t)$. Set this value to be θ.

Now consider $H - \frac{1}{2}\theta$. We have:

$$\tilde{s}^{-1}(H - \frac{1}{2}\theta)\tilde{s} = \chi(s)H + \theta(s) - \frac{1}{2}\theta = \chi(s)(H - \frac{1}{2}\theta). \tag{2.14}$$

The last equation holds no matter whether $\chi s = 1$ or -1. Therefore, by the substitution $H - \frac{1}{2}\theta \to H$, we can make $\theta(s) = 0$ for $\forall s$. $\square$

To summarize, if the symmetry s on $P\mathcal{H}$ is compatible with the dynamics generated by H, then s and H commutes or anticommute depending on the value of $\chi(s)$:

$$\tilde{s}H = \chi(s)H\tilde{s}. \tag{2.15}$$

---

[1]It is interesting to consider possible exceptions of this folklore.

2.1.3 The $\mathbb{Z}_2 \times \mathbb{Z}_2$ Grading of Symmetries, Twisted Representation

From the above subsections, we see that there are two natural Z_2 grading on the symmetry group (now viewed as a subgroup of $\mathrm{Aut}\,(P\mathcal{H})$), namely, ϕ and χ.

Depending on the value of ϕ and χ, there are four possibilities. It turns out all four possibilities are physically realizable.

- $\chi = 1, \phi = 1$. Linear and time-orientation preserving. For example, some ordinary internal symmetries.

- $\chi = 1, \phi = -1$. Antilinear and time-orientation reversal. For example, ordinary time-reversal symmetry T, and we have $[\tilde{T}, H] = 0$.

- $\chi = -1, \phi = -1$. Antilinear and time-orientation preserving. For example, particle-hole symmetry C, and we have $\{\tilde{C}, H\} = 0$.

- $\chi = -1, \phi = 1$. Linear and time-orientation reversal. For example, for the combination of $S = CT$, and we have $\{\tilde{CT}, H\} = 0$. A physical example is the sublattice symmetry, or chiral symmetry.

We emphasize that the two gradings are both very natural. They come from the distinction between linear and antilinear (a natural consequence of Wigner's theorem), and the time-orientation issue (inevitable as long as we have a notion of time and $t \in \mathbb{R}$). Therefore, for example, while the physical particle-hole symmetry C seems somewhat special (as special as a fine-tuned internal symmetry), it is essential to take symmetries of this grading type into consideration.

2.1.4 Twisted Extenstion and Twisted Representation

In most cases, we know the symmetry in an "abstract" form: we known the symmetries form a group, but we do not know exactly how it acts on the Hilbert space or ray space. For example, for a single particle in three dimensions, the system possesses a $SO(3)$ symmetry due to space rotation, but it is not clear by default that how $SO(3)$ acts on the Hilbert space[2].

---

[2]It is exactly due to the formalism developed here that a particle could have $\frac{1}{2}$ spin.

We say the quantum system has a symmetry group G, if there G acts on $P\mathcal{H}$ as symmetries (namely, Eq. (2.2) is satisfied). In other words, there is a homomorphism $\rho : G \to \text{Aut}\,(P\mathcal{H})$. Note that then ϕ can be defined on G. This makes G a Z_2-graded group[3], and ρ is grading preserving. With these data, we can pullback [53] the sequence Eq. (2.5) to the following commuting diagram:

$$
\begin{array}{ccccccccc}
1 & \longrightarrow & U(1) & \longrightarrow & \tilde{G} & \xrightarrow{\pi} & G & \longrightarrow & 1 \\
& & \Big\| & & \Big\downarrow{\tilde{\rho}} & & \Big\downarrow{\rho} & & \\
1 & \longrightarrow & U(1) & \longrightarrow & \text{Aut}\,(\mathcal{H}) & \xrightarrow{\pi} & \text{Aut}\,(P\mathcal{H}) & \longrightarrow & 1.
\end{array}
\tag{2.16}
$$

The first line is a ϕ-twisted extension of G by $U(1)$, in the sense that for $\forall e^{i\theta} \in U(1)$ and $\forall \tilde{g} \in \tilde{G}$ we have (this is clear seen by the commutativity of the above diagram):

$$
\tilde{g} e^{i\theta} = e^{i\theta\phi(g)} \tilde{g}.
\tag{2.17}
$$

It is a central extension iff $\phi(g) = 1$ for $\forall g \in G$. The original bigrading (ϕ, χ) of G also naturally extends to a bigrading of $\tilde{G}$ defined in Eq. (2.16), since $U(1)$ is connected.

We note that the same symmetric group G may have different homomorphisms ρ into $\text{Aut}\,(P\mathcal{H})$, and thus may give rise to different extensions $\tilde{G}$. They should be regarded as different quantum theories, since G acts on $P\mathcal{H}$ in different manners.

Moreover, if the Hamiltonian H is gapped at 0, there is a natural $\mathbb{Z}_2$-grading of the Hilbert space $\mathcal{H} = \mathcal{H}_0 \oplus \mathcal{H}_1$ given by eigenspaces of H with positive and negative eigenvalues. It is easy to check that the $\tilde{\rho}$ is a (ϕ, χ)-twisted representation of $\tilde{G}$ on the $\mathbb{Z}_2$-graded Hilbert space $\mathcal{H}$, in the sense that:

- $\tilde{\rho}(\tilde{g})$ is antilinear if $\phi(\tilde{g}) = -1$,
- $\tilde{\rho}(\tilde{g})$ is odd (flip the grading of $\mathcal{H}$) if $\chi(\tilde{g}) = -1$.

Abstractly, we say a gapped quantum system has a symmetry group G, if there is a twisted extension $\tilde{G}$ and a (ϕ, χ)-twisted representation of $\tilde{G}$ on $\mathcal{H}$. If we insist $\chi = 1$, we can forget the $\mathbb{Z}_2$-grading of the Hilbert space, then we obtain a ϕ-twisted representation on a non-graded Hilbert space.

---

[3]The odd part can be be empty.

2.2 The Three-Fold Way and the Ten-Fold Way

In this section, we consider the ensemble of Hamiltonians compatible with a given symmetry. The purpose is two-fold:

1. It often happens in physics that we are aware of the symmetry without the knowledge of the detailed interaction. Interestingly, by considering a random Hamiltonian in such an ensemble, one can still obtain useful information [54].

2. The classification of topological phases of matter depends on the symmetries. It is obviously useful to understand the ensemble of all possible Hamiltonians before going on.

The three-fold way [55] and ten-fold way [17] refer to (a minimal) classifications of possible symmetry actions. By classification, we mean the classification of symmetry group G, the twisted extension $\tilde{G}$, and the twisted representation $\tilde{\rho}$. Fixing the symmetry, the ensemble of Hamiltonians is also fixed.

We emphasize that the considerations here are completely general and does not refer to any specific setup. Therefore, the classifications here valid for any quantum mechanical systems in any dimensions, bosonic or fermionic, interacting or not.

2.2.1 The Three-Fold Way

In this subsection, we fix χ to be 1. For any symmetry group G, we have the following sequence (the last homomorphism may not be surjective):

$$1 \longrightarrow G_0 \longrightarrow G \xrightarrow{\phi} K \longrightarrow 1, \tag{2.18}$$

where K is a subgroup of $\mathbb{Z}_2 = \{1, T\}$, where T means anti-linear and time-orientation reversal.

A twisted extension of G gives rise to a central extension of G_0, which is somewhat less interesting. Therefore, we consider the case $G = K$.

If $K = \{1\}$, then there is no twist and the extension is unique: $\tilde{K} = U(1)$.

If $K = \{1, T\}$, then:

Theorem 2.3. There are two inequivalent twisted extensions of $\{1, T\}$, with $\phi(T) = -1$.

Proof. Choose a lift $\tilde{T}$ of T, then $\pi(\tilde{T}^2) = T^2 = 1$ so $\tilde{T}^2 = \alpha \in U(1)$. Note that $\alpha \tilde{T} = \tilde{T}^3 = \tilde{T}\alpha$ and also $\alpha \tilde{T} = \tilde{T}\alpha^{-1}$ since $\phi(T) = -1$, so α must be 1 or -1.

If $\alpha = 1$ then $\tilde{T}^2 = 1$ and the extension group will be

$$\tilde{K} = \{z, z\tilde{T} | z \in U(1), z\tilde{T} = \tilde{T}z^{-1}, T^2 = 1\}, \tag{2.19}$$

which is isomorphic to $O(2)$.

If $\alpha = -1$ then $\tilde{T}^2 = 1$ and the extension group will be

$$\tilde{K} = \{z, z\tilde{T} | z \in U(1), z\tilde{T} = \tilde{T}z^{-1}, T^2 = -1\}. \tag{2.20}$$

Moreover, it is easy to see that any lift $\tilde{T}$ of T must be squared to the same value for a fixed extension. Indeed, any lift of T must be of the form $\lambda\tilde{T}$ where $\lambda \in U(1)$. Since $\tilde{T}$ is anti-unitary, we have:

$$(\lambda\tilde{T})^2 = \lambda\bar{\lambda}\tilde{T}^2 = \tilde{T}^2. \tag{2.21}$$

Therefore, the above two extensions are distinct. $\qquad\square$

Following the above discussion, we have obtained a three-fold way classification of symmetry action of $\mathbb{Z}_2$ and its subgroup $\{1\}$, see Tab. 1.

class	A	AI	AII
T		+1	−1

Table 1: The three-fold way. Here the second line presents the value of $\tilde{T}^2$ in the extension, with empty means T is not a known symmetry and we only consider the subgroup $\{1\}$.

15

2.2.2 The Ten-Fold Way

Now we consider the general case. Similar to the above, we consider possible subgroups of $\mathbb{Z}_2 \times \mathbb{Z}_2$ and their twisted extensions.

The group $\mathbb{Z}_2 \times \mathbb{Z}_2$ can be presented as $\{1, C, T, CT\}$ (denoted by $\mathbb{Z}_{2,2}$ in the following), where ϕ grading for both C and T is -1. It has 4 proper subgroups: $\{1\}$, $\{1, C\}$, $\{1, T\}$, and $\{1, CT\}$.

- For $K = \{1\}$, the twisted extension is unique.
- For $K = \{1, C\}$ or $\{1, T\}$, according to the above subsection, each has two inquivalent extension.
- For $K = \{1, CT\}$, since $\phi(CT) = 1$, there is actually no twist. The central extension of K is unique. This is because the group cohomology $H^2(\mathbb{Z}_2, U(1)) = 0$. Or more explicitly, any lifting $\tilde{C}T$ can be made $\tilde{C}T^2 = 1$ by multiplication with a phase.
- For $K = \mathbb{Z}_{2,2}$. As above, $\tilde{C}T^2$ can always be made to 1 without changing the value of $\tilde{C}^2$ and $\tilde{T}^2$. Therefore, depending on the values of $\tilde{C}^2$ and $\tilde{T}^2$, there are four possibilities.

Therefore, we have obtained a ten-fold way classification of symmetry action of $\mathbb{Z}_2 \times \mathbb{Z}_2$ and its subgroups, see Tab. 2. The last line tells us which subgroup of $\mathbb{Z}_2 \times \mathbb{Z}_2$ we are considering.

2.2.3 Gapped Hamiltonian Ensembles, Clifford Algebra

In this subsection, we will answer the following problem: what is the ensemble of gapped Hamiltonians that are compatible with the above (twisted) actions of various symmetries? It turns out that the above extensions of the $\mathbb{Z}_2 \times \mathbb{Z}_2$ group are closely connected to Clifford algebras, and we will be able to answer the question with this connection.

2.2.3.1 Kitaev's Approach [18] As an example, let us consider the extension of $\{1, T\}$ with $\tilde{T}^2 = -1$. We will regard the Hilbert space $\mathcal{H}$ as a real vector space with a complex structure J, $J^2 = -1$. T being antilinear means:

$$\{\tilde{T}, J\} = 0. \tag{2.22}$$

16

T	C	S	Symmetry	Clifford	Gapped Hamiltonian	Cartan's label	AZ label
			$\{1\}$	$\mathbb{C}l_0$	$\mathbb{Z} \times BU$	AIII	A
		$+1$	$\{1, CT\}$	$\mathbb{C}l_1$	U	A	AIII
$+1$			$\{1, T\}$	$Cl_{0,0}$	$\mathbb{Z} \times BO$	BDI	AI
$+1$	$+1$	$+1$	$\mathbb{Z}_{2,2}$	$Cl_{0,1}$	O	D	BDI
	$+1$		$\{1, C\}$	$Cl_{0,2}$	O/U	DIII	D
-1	$+1$	$+1$	$\mathbb{Z}_{2,2}$	$Cl_{0,3}$	U/Sp	AII	DIII
-1			$\{1, T\}$	$Cl_{0,4}$	$\mathbb{Z} \times BSp$	CII	AII
-1	-1	$+1$	$\mathbb{Z}_{2,2}$	$Cl_{3,0}$	Sp	C	CII
	-1		$\{1, C\}$	$Cl_{2,0}$	Sp/U	CI	C
$+1$	-1	$+1$	$\mathbb{Z}_{2,2}$	$Cl_{1,0}$	U/O	AI	CI

Table 2: The ten-fold way. Here ± 1 represents the value of $\tilde{g}^2$ in the extension, where $g = T$ or C or S, with empty means g is not a known symmetry. The column "Clifford" tells us for which Clifford algebra $\mathcal{H}$ is a module. Euivalently, it tells us the correct Clifford extension problem we should ask (for example, $Cl_{0,3}$ means the Clifford extension problem $Cl_{0,3} \to Cl_{0,4}$). The column "Gapped Hamiltonian" tells which symmetric space the space of gapped Hamiltonians is. "Cartan's label" is the label for that symmetric space while "AZ" label is the label for that symmetric class that often seen in the literature.

The symmetry requires:

$$[\tilde{T}, H] = 0, \tag{2.23}$$

and H being a complex linear operator requires:

$$[J, H] = 0. \tag{2.24}$$

The above equations are equivalent to:

$$\{\tilde{T}, J\} = \{\tilde{T}, J\tilde{T}H\} = \{J, J\tilde{T}H\} = 0. \tag{2.25}$$

Up to homotopy, we can assume $H^2 = 1$ and equivalently $(J\tilde{T}H)^2 = -1$. It is then clear that $e_1 = \tilde{T}, e_2 = J$ generate a real representation of Clifford algebra $Cl_{2,0}$, and the question is to find the space of possible $e_3 = J\tilde{T}H$ so the representation can be extended to a representation of Clifford algebra $Cl_{3,0}$.

This type of "Clifford extension problem" [56] is discussed in the appendix A.3, where it is showed that the question is equivalent to finding the space of e_5 such that a $Cl_{0,4}$-module into a $Cl_{0,5}$-module. The final answer, in this case, is the symmetric space[4] $\mathrm{Grad}^{0,4} \cong \mathbb{Z} \times Sp/Sp \times Sp = \mathbb{Z} \times BSp$.

2.2.3.2 Freed-Moore's Approach

[20] An alternative point of view is as follows. We regard $\mathcal{H}$ as a complex vector space. Then the antilinear $\tilde{T}$ with $\tilde{T}^2 = -1$ is a quaternionic structure which makes $\mathcal{H}$ a quaternionic vector space. $[\tilde{T}, H] = 0$ means H is $\mathbb{H}$-linear. Its ± 1 eigenspaces determines a symplectic gradation of $\mathcal{H} = \mathcal{H}_0 \oplus \mathcal{H}_1$ and are therefore specified by $\mathbb{Z} \times BSp$.

Formally, there is an equivalence between $\mathbb{H}$-vector space and $Cl_{0,4}$ modules, due to $Cl_{0,4} \cong \mathbb{H}(2)$. The fact that $\mathcal{H}$ has a quaternionic structure implies that $\mathcal{H}$ induces an ungraded module[5] for $Cl_{0,4}$. The gradation $\mathcal{H} = \mathcal{H}_0 \oplus \mathcal{H}_1$ makes the $Cl_{0,4}$-module graded. Therefore, to classify H is the same as to classify the gradation of $\mathcal{H}$, which is then equivalent to classify the gradation of $Cl_{0,4}$-modules.

Therefore, one goes back to the same question as in Kitaev's approach: extension from $Cl_{0,4}$-module to $Cl_{0,5}$-module.

Following either approach, one can similarly work out gapped Hamiltonian ensembles (symmetric spaces) and corresponding Clifford algebras (under which $\mathcal{H}$ is a Clifford module) for other symmetry classes. The results are listed in Tab. 2.

2.2.3.3 Comments on Zero-Dimensional Classification

We note that we could get a classification for general gapped zero-dimensional Hamiltonian (not just free fermions) follow-

---

[4]Note that this is the symmetric space of class CII, while the usual terminology for this symmetry class is AII! The later convention comes from another connection between symmetric spaces and Clifford algebras: tangent spaces of symmetric classes give the ensemble of Hamiltonian compatible with symmetries without gapped condition [17]. Two nomenclatures are related by a shift.

[5]The induced module is $\mathcal{H} \oplus \mathcal{H}$.

ing the above discussions. For a Hilbert space of fixed dimension, it is just $[pt, \mathrm{Grad}^{p,q}(\mathbb{R}^D)]$. For Hilbert space with arbitrary finite dimension, the result will be $\mathrm{Rep}^{p,q}$, the set of graded representation compatible with symmetries indicated by p, q.

However, this will not be an Abelian group yet, and we will not get the usual K theoretic classification even if we take its Grothendieck group (see Appendix A.4) respected to the natural monoid structure. This is because the natural "addition" for many-body Hilbert spaces is not compatible with the definition of usual K. In physics, we consider the tensor products of Hilbert spaces when combining two systems, while in K theory we are considering direct sums. See Sec. 2.3.1 for more discussions.

2.3 Classification of Free Fermionic Systems in Arbitrary Dimensions

2.3.1 General Comments on Classification

A classification problem, formally speaking, is to classify elements of a set according to some equivalence relations. In many condensed matter physics problems, the set is taken to be the set of Hamiltonians H with a suitably defined "energy gap", and H_1 and H_2 are equivalent if and only if they can be continuously connected while keeping the gap open.

The space of Hamiltonians may also be reduced by imposing some constraints. Accordingly, the classification results will generally be changed, since

- the constraints may eliminate some old class,
- an old class may split into several new classes, if two objects that are used to be able to continuously connected may not be able to be connected with each other anymore due to the constraints.

One example is the classification of free fermionic systems in this chapter. Another famous example is the symmetry protected topological phase (SPT)[6] [57, 58].

In general, the classification result will just be a set without any interesting structures. However, if there is a monoid structure, one may naturally take its Grothendieck group,

---

[6]Or symmetry protected trivial phase.

resulting in an abelian group, which seems more regular. This procedure modifies the original equivalence relation into "stably equivalence relation": if $x + z$ is equivalent to $y + z$, then x is also equivalent to y is the stable sense.

The main example of this procedure is the classification of free fermionic systems. Here, the monoid structure is given by the direct sum of "one-particle Hilbert space" (this notion is valid only for free systems). Physically, two band structures are stably equivalent if they are equivalent upon adding another band structure z on top of both.

We remark that taking the Grothendieck group is not the only way to get an Abelian group structure. For example, if the Brillouin zone is a sphere, then some classification spaces are automatically groups, since the homotopy groups π_k for $k \leq 2$ is Abelian. In this way, one can get some "nonstable" topological invariants, for example, the Hopf invariant [59].

2.3.2 Free Fermionic Hamiltonians

A free fermionic system, by definition, has the second-quantized Hamitonian with only quadratic terms. Since we are going to consider both insulators and superconductors (which violates particle number conservation), it is convenient to introduce Majorana opeators [60]:

$$c_{2j-1} = a_j + a_j^\dagger, \quad c_{2j} = \frac{a_j - a_j^\dagger}{i}. \tag{2.26}$$

Under this transformation, the original fermionic anticommutation relations become:

$$c_m^\dagger = c_m, \quad \{c_m, c_n\} = 2\delta_{mn}. \tag{2.27}$$

The second-quantized Hamiltonian on the full Hilbert space has the the following form:

$$H_{\text{full}} = \frac{i}{4} \sum_{m,n} A_{m,n} c_m c_n. \tag{2.28}$$

In this equation, an i is introduced so that we can assume A_{ij} is an anti-symmetric real matrix without loss of generality. Moreover, this constraint uniquely determines A_{ij} for a given Hamiltonian H_{full} and operator basis $\{c_m\}$.

20

2.3.2.1 Symmetry Actions For free fermion systems, we will assume relevant symmetries are induced by their actions in the one-particle space by second quantization.

Let us denote the symmetry on the full Hilbert space by $\mathcal{U}$, the assumption amounts to say:

$$\mathcal{U} c_m \mathcal{U}^\dagger = U_{m,n} c_n. \tag{2.29}$$

The m, n above are indexes in mode space $\mathcal{M}$, which is a real $2n$-dimensional space if one has n usual fermion operators.

Taking the Hermitian conjugation, we see $U_{m,n}$ must be real. Moreover, $\mathcal{U}$ being unitary or antiunitary implies the anticommutation relation is preserved:

$$S_{m,n} S_{k,l} \{c_n, c_l\} = 2\delta_{m,k}, \tag{2.30}$$

which is then equivalent to $UU^T = 1$. Therefore, S is real orthogonal.

The symmetry-dynamics compatiblility condition $\mathcal{U} H_{full} \mathcal{U}^\dagger = \chi(\mathcal{U}) H_{full}$ becomes:

$$U^T A U = \chi(\mathcal{U}) \phi(\mathcal{U}) A = \tau(\mathcal{U}) A. \tag{2.31}$$

In the above equation, the extra $\phi(\mathcal{U})$ factor comes from the $\frac{i}{4}$ prefractor and the possibility for $\mathcal{U}$ to be antilinear.

On the full Hilbert space $\mathcal{H}$, $\tilde{S}^2$ is generally neither 1 nor -1. For example, if $\tilde{S}^2 = -1$ on a one-particle state $|\psi\rangle \in \mathcal{H}$, then it will act as 1 on $|\psi\rangle \otimes |\psi\rangle \in \mathcal{H}$. We will assume[7] that $\tilde{U}^2$ acts as either 1 or -1 on the one-particle space, namely:

$$\mathcal{U}^2 c_m \mathcal{U}^{\dagger 2} = \pm c_m. \tag{2.32}$$

This implies $U^2 = \pm 1$.

For both linear symmetries and antilinear symmetries, U is always a real orthogonal matrix, acting on the "mode space". The difference is hidden in the following way. Consider the effect of $c \to ic, c^\dagger \to -ic^\dagger$. It will induce an orthogonal transformation Q on $\{c_m\}$ with

$$Q^2 = -1. \tag{2.33}$$

---

[7]It is obviously just an assumption. There's nothing wrong to formally consider a fermionic system with two fermions, $\tilde{S}^2 = 1$ for one and $\tilde{S}^2 = -1$ for the other.

Therefore, it is a complex structure on the (real) mode space, namely, $\mathcal{M} = W_{\mathbb{R}}$ where W is $\mathbb{C}$-linear space. If $\tilde{S}$ is linear, we will have:

$$[Q, U] = 0. \tag{2.34}$$

If $\tilde{S}$ is antilinear, we will have:

$$\{Q, U\} = 0. \tag{2.35}$$

Note that, however, the Hamiltonian does not necessarily compatible with the complex structure, since it would imply particle number conservation. If it is indeed the case, as for insulators, we will have:

$$[Q, A] = 0. \tag{2.36}$$

In this case, we will be able to regard iA as a Hermitian matrix on W, which is exactly the one-particle Hamiltonian H. The symmetry actions are:

$$U^{\dagger} H U = \chi(\mathcal{U}) H, \tag{2.37}$$

where U is now regarded as a unitary or anti-unitary operator on W. This is formally the same as Eq. (2.15) on the full Hilbert space.

To summarize, for free fermionion systems, discussions on the full Hilbert space $\mathcal{H}$ can be translated into the real mode space $\mathcal{M}$ together with a complex structure Q. The results are summarized in Tab. 3.

Symmetry	Action on A	Action on H	Linearity	Extensions
Time	$T A T^T = -A$	$T H T^{\dagger} = H$	$\{Q, T\} = 0$	$T^2 = \pm 1$
Particle-Hole	$C A C^T = A$	$C H C^{\dagger} = -H$	$\{Q, C\} = 0$	$C^2 = \pm 1$
Chiral	$S A S^T = -A$	$S H S^{\dagger} = -H$	$[Q, S] = 0$	$S^2 = 1$

Table 3: Symmetries for free fermionic systems. In the A column, A is real anti-symmetric as in the Majorana representation, T, C, S are real orthogonal matrices. The H column is only valid if the system conserves particle number; under this assumption, H is Hermitian, T, C, S are unitary or antiunitary operators.

2.3.3 Ten-Fold Way with(out) Particle Number Conservation

For classification purposes, one needs to first classify symmetry actions. As emphasized several times, it just depends on general principals of quantum mechanics. One still considers subgroups of $\{1, C, T, CT\}$ and different twisted extensions. Therefore, the ten-fold way discussed previously still applies here.

Within each symmetry class, one needs to classify all matrix A (equivalently, the Hamiltonian) that is real anti-symmetric and is consistent with the symmetry actions. However, there is a subtlety here. If we assume no relation between A and Q, there will be no difference for a $S^2 = 1$ system and a $T^2 = 1$ system, since they both give the same constraints on A: real anti-symmetric and anticommuting with the symmetry matrix (the matrix T and S are of course different, but the classification results will be the same). Therefore, to get a more complete classification, one needs to consider whether Q is compatible with A or not [18]. This is also physically reasonable since insulators and superconductors are by definition very different physical systems.

For insulators, Q is compatible with A so we can work on complex Hamiltonians. In this case, we can repeat the analysis in Sec. 2.2.3, this time on the one-particle Hilbert space. Therefore, the results of classifying spaces apply here.

For systems where Q is not known to be conserved[8], the analysis is different. This is because previous analyses consider representations and compatible $\mathbb{C}$-linear Hamiltonians on complex Hilbert spaces, while for our case, the underlying space is the real mode space $\mathcal{M}$[9].

We first consider $\{1\}$ with no other symmetries. We will need to find all A that is gapped, real anti-symmetric. Without gapped condition, it just lives in the Lie algebra $\mathfrak{o}(N)$, the tangent space class D symmetric space. So it would be in class D under the AZ convention. The space of gapped ones is then homotopy to the DIII symmetric space, following Tab. 2.

We can also work in Kitaev's approach. We can flatten the spectrum by assuming $A^2 = -1$ if it is gapped. The answer is then immediate by noticing that A defines an orthogonal complex structure, so the answer is O/U. More generically, this is the $Cl_{0,0} \to Cl_{1,0}$ extension

---

[8]It could be, but just not known.
[9]One could consider the complexification $\mathcal{M}_{\mathbb{C}}$ and extend the Hamiltonian $\mathbb{C}$-linearly. But one needs to be careful since this procedure introduces more structures.

problem, which maps to $Cl_{0,2} \to Cl_{0,3}$ problem. The solution this again DIII symmetric space O/U as shown in Tab. 2.

Another example is the case where $T^2 = -1$. We have:

$$T^2 = -1, A^2 = -1, \{T, A\} = 0, \tag{2.38}$$

so it is a $Cl_{1,0} \to Cl_{2,0}$ extension problem, which is the same as $Cl_{0,3} \to Cl_{0,4}$ extension. The answer for gapped Hamiltonians is the symmetric space AII. Under AZ convention, the correct AZ label should be DIII.

AZ label	T	C	S	Clifford	Gapped A	new AZ label
A				$Cl_{0,2}$	DIII	D
AIII			+1	$Cl_{1,2}$	D	BDI
AI	+1			$Cl_{1,2}$	D	BDI
BDI	+1	+1	+1	$Cl_{0,2}$	DIII	D
D		+1		$(Cl_{0,0})^2$	BDI^2	AI^2
DIII	−1	+1	+1	$Cl_{1,3}$	DIII	D
AII	−1			$Cl_{0,3}$	AII	DIII
CII	−1	−1	+1	$Cl_{0,4}$	CII	AII
C		−1		$\mathbb{C}l_0$	CI	A
CI	+1	−1	+1	$Cl_{1,1}$	BDI	AI

Table 4: The AZ classfication classes for each AZ symmetry class. Here, "AZ label" means the AZ label for symmetry actions, where "symmetry" means real, physical symmetry that acts on the physical Hilbert space. "new AZ label" means the AZ label one should refer to in order to find the correct classification for that symmetry class. AI^2 means the classification problem decomposed into two independent problems, each results in an AI classification.

In Tab. 2.3.3, we summarize the Clifford extension problem for each case and their AZ label for classification. The first four columns indicates real symmetries[10] for the quan-

---

[10]Particle-hole symmetries in BdG Hamiltonians are redundancies instead of real symmetries.

tum system. The point is: to get the classification for the symmetry class indicated by (T^2, C^2, S^2), one needs to look up in literatures by the new AZ label.

2.3.4 Classification in Zero Dimension: $K^*(pt)$

Now, the classification for zero-dimensional free fermionic systems follows immediately from discussions above and those in Sec. 2.2.3.

Indeed, we already know the spaces of gapped Hamiltonians are $\text{Grad}^{p,q}$ with p, q determined by the symmetries. Also note that the notion of stably equivalence for free systems is in accordance with the definition $\text{Grad}^{p,q}$ as a limit for those in finite dimensional spaces. Therefore, the final classification is simply:

$$[pt, \text{Grad}^{p,q}], \tag{2.39}$$

which is isomorphic to $K^{p-q}(pt)$, due to the fact that $\{\text{Grad}^{p,q}\}$ is a K theory spectrum.

Equivalently, from the discussions in Appendix A.5.2, we know the answer to the Clifford extension problem is by definition given by Karoubi's $K^{p,q}(pt)$, which in turn is isomorphic to $K^{p-q}(pt)$.

2.3.5 Classification in Higher Dimensions: KR Theory

2.3.5.1 Going to Momentum Space
For translationally invariant systems, we have:

$$H_{\text{full}} = \frac{i}{4} \sum_{\mathbf{x},\mathbf{y},m,n} A_{\mathbf{x}-\mathbf{y},m,n} c_{\mathbf{x},m} c_{\mathbf{y},n}, \tag{2.40}$$

where $\mathbf{x}, \mathbf{y}$ are position indexes and m, n are now "orbital" indexes. Going to momentum space by a Fourier transform on $c_{\mathbf{x},m}$, we will have:

$$H_{\text{full}} = \int \frac{d\mathbf{k}}{(2\pi)^d} \frac{i}{4} \sum_{m,n} A_{m,n}(\mathbf{k}) c_{-\mathbf{k},m} c_{\mathbf{k},n}. \tag{2.41}$$

The real anti-symmetric condition in position space now translates into:

$$A_{m,n}(\mathbf{k}) = -A_{n,m}(\mathbf{k}), \quad A_{m,n}(\mathbf{k}) = \overline{A_{m,n}(-\mathbf{k})}, \tag{2.42}$$

namely, anti-symmetric covariantly real.

Let us also translate symmetry actions Eq. (2.29)-Eq. (2.31) into momentum space. To do so, we will assume that relavant symmetries are local, in the sense that:

$$U_{m\mathbf{x},n\mathbf{y}} = U_{m,n}\delta_{\mathbf{x},\mathbf{y}}, \tag{2.43}$$

where by abuse of notations we have use the same letter U. U is still a real orthogonal matrix.

A little calculation shows:

$$\mathcal{U}c_m(\mathbf{k})\mathcal{U}^\dagger = U_{m,n}c_n(\phi(\mathcal{U})\mathbf{k}),$$
$$U^T A(\mathbf{k})U = \tau(\mathcal{U})A(\mathbf{k}) \tag{2.44}$$

Unlike what one might expected, under Majorana representation, $\mathbf{k}$ does not go to $\mathbf{k}$ even for time-reversal symmetry.

AZ label	T	C	S	Symmetry	Clifford	$d=0$	$d=1$	$d=2$	$d=3$
A				$\{1\}$	$\mathbb{C}l_0$	$\mathbb{Z}$		$\mathbb{Z}$	
AIII			$+1$	$\{1, CT\}$	$\mathbb{C}l_1$		$\mathbb{Z}$		$\mathbb{Z}$
AI	$+1$			$\{1, T\}$	$Cl_{0,0}$	$\mathbb{Z}$			
BDI	$+1$	$+1$	$+1$	$\mathbb{Z}_{2,2}$	$Cl_{0,1}$	$\mathbb{Z}_2$	$\mathbb{Z}$		
D		$+1$		$\{1, C\}$	$Cl_{0,2}$	$\mathbb{Z}_2$	$\mathbb{Z}_2$	$\mathbb{Z}$	
DIII	-1	$+1$	$+1$	$\mathbb{Z}_{2,2}$	$Cl_{0,3}$		$\mathbb{Z}_2$	$\mathbb{Z}_2$	$\mathbb{Z}$
AII	-1			$\{1, T\}$	$Cl_{0,4}$	$\mathbb{Z}$		$\mathbb{Z}_2$	$\mathbb{Z}_2$
CII	-1	-1	$+1$	$\mathbb{Z}_{2,2}$	$Cl_{3,0}$		$\mathbb{Z}$		$\mathbb{Z}_2$
C		-1		$\{1, C\}$	$Cl_{2,0}$			$\mathbb{Z}$	
CI	$+1$	-1	$+1$	$\mathbb{Z}_{2,2}$	$Cl_{1,0}$				$\mathbb{Z}$

Table 5: Periodicity table for free fermionic systems. d is the space dimension. Z or $\mathbb{Z}_2$ is the group that topological invariant values in.

2.3.5.2 Periodicty Table Since Clifford operators U does not alter $\mathbf{k}$, the symmetries make relevant bundles a Clifford module. The $A(k)$ that one tries to find, should satisfy

Eq. (2.42). Mathematically this means $A(k)$ is an extra Clifford operator that is compatible with a Real structure— a Real bundle morphism. The problem in hand exactly corresponds to Karoubi's description of $KR^{p,q}(X)$, where X comes with a Real structure $\mathbf{k} \to -\mathbf{k}$, originally due to Eq. (2.42). Therefore:

Theorem 2.4 (Classification). Free fermionic systems in d dimension with AZ label corresponds to (p, q) are classified by $KR^{p,q}(X)$, where X is the Brillouin zone with a Real structure $\mathbf{k} \to -\mathbf{k}$.

We will consider the case $X = \bar{S}$, where the bar indicates the Real structure. Using the properties discussed in Appendix A.7, we have:

$$KR^{p,q}(\bar{S}^d) = KR^{p+d,q}(pt) = KO^{0,q-p-d}(pt). \qquad (2.45)$$

Note the importance of the Real structure. Otherwise for S^d we would get $KO^{0,q-p+d}(pt)$, which is a wrong answer.

In Tab. 5 we list the results for $d = 0, 1, 2, 3$. This is the famous periodicity table for free fermionic systems [18, 19, 21]. In this table, d is the space dimension, Z or $\mathbb{Z}_2$ is the group that topological invariant values in. The first two rows are called complex classes since the corresponding Clifford algebra are complex algebras; the other eight rows are called real classes for similar reasons.

The periodicity comes from both the Bott periodicity and the fact that we are using the sphere as the Brillouin zone and therefore one has the suspension isomorphism: according to Eq. (2.45), it is the latter property that ensures a shift of dimension is equivalent to a shift of symmetry class. Indeed, if one works with $X = T^2$, the Brillouin zone for lattice systems, one will get some "weak invariant" [18, 61, 62, 63] and the result will not be periodic.

3.0   Topological Invariants in Real Space

According to the discussions in the previous chapter, at least in translationally invariant cases, free fermionic systems are classified into 10 classes, within which systems are classified by a topological invariant valued in $\mathbb{Z}$ or $\mathbb{Z}_2$. Indeed, one can further get many analytical formulas for the topological invariants by working in momentum space and (essentially) considering some vector bundles (with symmetries) over the Brillouin zone [19, 21, 64].

While the classification is believed to be robust against disorder [39, 40, 18], there is no traditional notion of the Brillouin zone with disorder. Therefore, one must find real-space formulas for topological invariants. This will be generally more difficult than finding formulas in momentum space. Nevertheless, one can still get useful results from noncommutative geometry/topology considerations [22, 23, 24, 25], which may manifest itself as a (Fredholm, mod 2 Fredholm, Bott, etc) index [27, 30, 31, 32, 33, 34, 35, 36, 37, 38] (although some of them are abstract definitions and do not tell us how to calculate them efficiently); or from physical considerations such as scattering theory [26] or boundary Anderson delocalization [19].

There is another motivation to find real-space topological invariants. A common argument for the boundary gapless modes goes as follows: since the system is topological on one side and trivial on the other side, there must be some gapless modes localized along the boundary to separate two parts. Firstly, since there is generally no Brillouin zone for systems with boundaries, there must be some real-space notion of topological versus trivial. Secondly, the above argument is not always valid, as there do exist some examples dubbed gappable boundaries. To make this argument more rigorous, we need the distinction of topological phase and trivial phase to be locally detectable, so that two sides of the boundary are indeed different. It means that the real-space topological invariant should be local, see Eq. (3.15) and below for more discussions.

In this chapter, we will review some index theorems as examples of real-space topological invariants. We will also review an interesting approach based on almost commuting matrices [31]. It turns out the obstruction for making almost commuting matrices commute coincide

with some topological invariants. Finally, in Sec. 3.4, we discuss a local formula for the Kane-Mele invariant in real space.

3.1 Filled-Band Projection, Two-Point Correlator, and Flat-Band Hamiltonian

Before going on, we provide some general discussions one the filled-band projection, two-point correlator, and the flat-band Hamiltonian.

For free fermionic system, we can effectively consider the one-particle Hilbert space and the one-particle Hamiltonian $H_{\mathbf{x},\mathbf{y}}$. The indexes of the matrix are valued in a lattice, for exmaple, $\mathbb{Z}^d$ where d is the dimension. We will require that $H_{\mathbf{x},\mathbf{y}}$ (as an operator on the one-particle Hilbert space) is gapped, in the since that:

$$\exists \delta, \text{ such that } \mathrm{spec}(H) \subset \mathbb{R}\backslash(-\delta, \delta). \tag{3.1}$$

With this requirement, one can spectral-flatten the Hamiltonian by making all positive eigenvalues to be 1 and negative eigenvalues to be -1, and keeping the eigenvectors invariant. This procedure has been used several times in Chapter 2. After this procedure, we will get a spectral-flattened Hamiltonian $\bar{H}$, and a filled-band projection $P = \mathcal{P}_-(H)$ such that:

$$\bar{H} = 1 - 2P, \quad P = \oplus_{\lambda<0} P_\lambda, \tag{3.2}$$

where P_λ is the projection matrix on the eigenspace of H with eigenvalue λ.

It turns out that the filled-band projections (a one-particle notion) are equal to the ground state two-point correlators (a many-body notion). Indeed, without loss of generality, one can just work in the basis where the one-particle Hamiltonian H is diagonal (for example, the $\mathbf{k}$ basis, if the system is translationally invariant), then it is obvious that projection equals two-point correlator.

In this section, all formulas work with P, since it contains all information of the eigenvectors (as well as whether it is filled or empty), which are enough to determine the topology.

3.2 Index Theorems

3.2.1 Relative Index of a Pair of Projections

In this subsection we collect interesting results on a pair of projections (P, Q), where P, Q are Hermitian idempotent operators [27, 65]. Geometrically, they are about two closed subspaces in a Hilbert space [66].

Theorem 3.1. Dewnote $A = P - Q$ and $B = 1 - P - Q$, then the following statements follow from straightforward calculation, and are valid even for infinite-dimensional Hilbert space:

(1) $A^2 + B^2 = 1$, $AB + BA = 0$;

(2) A^2 commute with P and Q;

(3) $Ax = x$ iff $Px = x$ and $Qx = 0$, $Ax = -x$ iff $Px = 0$ and $Qx = x$;

(4) $Bx = x$ iff $Px = Qx = 0$, $Bx = -x$ iff $Px = Qx = x$.

To build up intuitions, one may diagonize A. The above theorem implies the following decomposition of the Hilbert space:

- $P = 1, Q = 1$ subspace, so that $A = 0, B = -1$;

- $P = 1, Q = 0$ subspace, so that $A = 1, B = 0$;

- $P = 0, Q = 1$ subspace, so that $A = -1, B = 0$;

- $P = 0, Q = 0$ subspace, so that $A = 0, B = 1$;

- $\lambda \in (-1, 0) \cup (0, 1)$ eigenvalues of A must come in pairs and B switches (invertibly) between them. Moreover, there exists basis such that:

$$A = \begin{bmatrix} \lambda & 0 \\ 0 & -\lambda \end{bmatrix}, B = \begin{bmatrix} 0 & -\sqrt{1-\lambda^2} \\ -\sqrt{1-\lambda^2} & 0 \end{bmatrix},$$
$$P = \frac{1}{2} \begin{bmatrix} 1+\lambda & \sqrt{1-\lambda^2} \\ \sqrt{1-\lambda^2} & 1-\lambda \end{bmatrix}, Q = \frac{1}{2} \begin{bmatrix} 1-\lambda & \sqrt{1-\lambda^2} \\ \sqrt{1-\lambda^2} & 1+\lambda \end{bmatrix}.$$

(3.3)

30

Assuming $P - Q$ is compact[1], define the relative index between P and Q as:

$$\text{Ind}(P, Q) = \dim \text{Ker}(P - Q - 1) - \dim \text{Ker}(Q - P - 1). \tag{3.4}$$

According to the above analysis, it counts the difference of dimensions where $P = 1, Q = 0$ and $P = 0, Q = 1$. For finite-dimensional spaces, it also counts the difference between $\dim(P)$ and $\dim(Q)$, since $P = Q = 1$ blocks and $\lambda \in (-1, 0) \cup (0, 1)$ blocks have equal contributions to the dimensions. Moreover,

Theorem 3.2. If $(P - Q)^{2n+1}$ is trace class for some $n \in \mathbb{N}$, then for $\forall m \geq n$:

$$\text{Ind}(P, Q) = \text{Tr}[(P - Q)^{2m+1}]. \tag{3.5}$$

As a corollary, if $P - Q$ is trace class, then even if $\dim(P)$ and $\dim(Q)$ are infinite, we still have $\text{Tr}(P - Q) \in \mathbb{Z}$.

Note that in general, $\dim(P)$ and $\dim(Q)$ are not finite (more seriously but physically relevant, $P - Q$ is not even trace class), the above formalism provides a way to compare the difference of two dimensions. It is interesting that we have obtained a quantized trace.

3.2.2 Flow of a Unitary

For any unitary U_{ij}, we draw a directed graph associate with it. Each index i corresponds to a point. For each ordered pair (i, j) we imaging a flow from j to i with intensity $|U_{ij}|^2$, and a flow from i to j with intensity $|U_{ji}|^2$. The net flow from j to i is:

$$f_{ij} = |U_{ij}|^2 - |U_{ji}|^2. \tag{3.6}$$

Obviously, for each point, total flow in=total flow out=1, so[2]

$$(\partial f)_j = \sum_i f_{ij} = 0. \tag{3.7}$$

Now assume the indexes are valued in $\mathbb{Z}$, and U is quasi-diagonal in the sense that:

$$U_{ij} \leq C|i - j|^{-d} \text{ for large enough } d. \tag{3.8}$$

---

[1]Or more generally, if (P, Q) is a Fredholm pair.
[2]This is a cycle condition.

For any cut at $\eta \in \mathbb{R}$, the total flow across η from left to right is independent on η. This because otherwise the flow will accumulate or dissipate at some points, a contradiction with "total flow in=total flow out". This quantity is defined as the flow of the unitary U [28]:

$$\mathcal{F}(U) = \sum_{i \geq \eta, j < \eta,} f_{ij}, \forall \eta \in \mathbb{R}. \tag{3.9}$$

A nice feature of this quantity is its locality. Since U_{ij} decays fast enough as $|i-j| \to \infty$, $f_{i,j}$ will be small as long i or j (not neccesarry for both) is far from η. This means $\mathcal{F}(U)$ can be well approximated by only summing over i, j near η, with precision guranteed by Eq. (3.8).

Interestingly, the flow $\mathcal{F}(U)$ of a unitary U must be an integer. Indeed, consider $\eta = 0$, define Π as the projection on $\mathbb{N}$, then:

$$\mathcal{F}(U) = \text{Tr}((1 - \Pi)U^{\dagger}\Pi U) - \text{Tr}((1 - \Pi)U\Pi U^{\dagger}) = \text{Tr}(U^{\dagger}\Pi U - \Pi). \tag{3.10}$$

Note that $U^{\dagger}\Pi U$ is also a projection[3], the above equation is just $\text{Ind}(U^{\dagger}\Pi U, U)$, which must be an integer.

For finite-dimensional projections, $\text{Tr}(U^{\dagger}\Pi U - \Pi) = \text{Tr}(U^{\dagger}\Pi U) - \text{Tr}(\Pi) = 0$. This is because for a finite system, there is no space for a net flow (no Hilbert hotel). However, in infinite dimensions, there could be a nonzero flow. The simplest example is $U_{i+1,i} = 1$, then $\mathbb{F}(U) = 1$, and indeed $U^{\dagger}\Pi U$ is the projection on $[-1, \infty)$, which has "one more dimension" compared to Π.

The quantization of $\mathcal{F}(U)$ have a topological origin. Assuming U is translational invariant. One can show that Π can be replaced by X by replacing the trace over all indexes by the trace per cell:

$$\mathcal{F}(U) = (tr)(U^{\dagger}XU - U) = \text{tr}(U^{\dagger}[X, U]). \tag{3.11}$$

In momentum space, this is just the winding number of $\det(U(k))$:

$$\mathcal{F}(U) = \frac{i}{2\pi} \int_0^{2\pi} \text{tr}(U^{\dagger}dU). \tag{3.12}$$

---

[3]For this to be true, it is important for U be a unitary, not just a isometry.

3.2.3 Chern Number of a Projection

Given a projection operator P with indexes in $\mathbb{Z}^2$. Assuming P is quasidiagonal[4] in the sense of Eq. (3.8). We define a 2-chain by associate the following number for each triple (j, k, l):

$$h_{jkl} = 12\pi i (P_{jk} P_{kl} P_{lj} - P_{jl} P_{lk} P_{kj}). \tag{3.13}$$

They are real numbers which are totally antisymmetric in indexes. They also satisfy and a chain condition:

$$(\partial h)_{kl} = \sum_j h_{jkl} = 0. \tag{3.14}$$

Similar to Eq. (3.9), we define the Chern number of P as [28]:

$$\nu(P) = 12\pi i \sum_{j \in A} \sum_{k \in B} \sum_{l \in C} (P_{jk} P_{kl} P_{lj} - P_{jl} P_{lk} P_{kj}), \tag{3.15}$$

where this time the space is devided into three parts ABC since we are in 2D (instead of two parts in 1D), see Fig. 3(b).

(a) (b) (c)
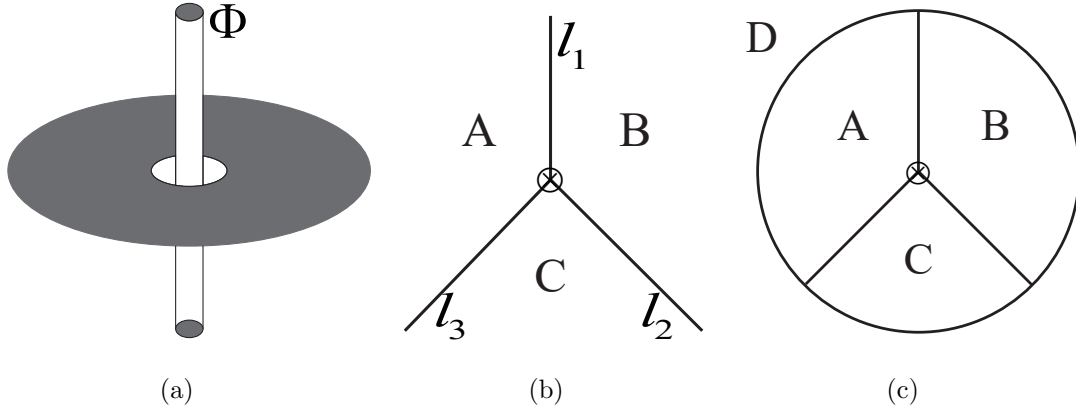
Figure 3: (a) Insert a flux in the hole. (b) Divide the plane into three regions A, B, C. The intersection point is where a flux will be inserted. (c) Truncate the plane with a circle. Denote the region outside the circle by D. The intersection point is where a flux will be inserted.

---

[4]Unlike U, where it can be strictly finite width even if $\mathcal{F}(U) \neq 0$, there is a No-Go theorem saying that if $\nu(P) \neq 0$ then P cannot be of finite width, see Sec. 3.3.1 and Appendix B.

Similar to $\mathcal{F}(U)$, $\nu(P)$ is also a local quantity, in the sense that it can be well approximated by only summing over j, k, l near the trijunction. For example, one may truncate the plane with a circle as in Fig. 3(c) and do the same summation (with A, B, and C now finite).

More remarkably, this quantity enjoys similar properties as $\mathcal{F}(U)$: it is invariant under slight changes of boundaries between ABC, and it is also quantized. The first property is due to the chain condition Eq. (3.14). For the second property, let us define Π_A as the projection on region A and similarly for B, C, then:

$$\nu(P) = 4\pi i \operatorname{Tr}\left(\left[P\Pi_A P, P\Pi_B P\right]\right). \tag{3.16}$$

This equation also shows $\nu(P)$ is invariant even if one rotates the boundaries or if the regions have some finite overlap. Note that they cannot have an infinite overlap, see below.

Now define Π_x (and Π_y) to be the projection on the right (and upper) half plane. The above equation can be used to show:

$$\nu(P) = 2\pi i \operatorname{Tr}\left(\left[P\Pi_x P, P\Pi_y P\right]\right). \tag{3.17}$$

Define $U = \exp(2\pi i P\Pi_y P)$. It commutes with P. We have:

$$
\begin{aligned}
\operatorname{Ind}(U^\dagger \Pi_x U, \Pi_x) &= \operatorname{Tr}(U^\dagger \Pi_x U - \Pi_x) \\
&= \operatorname{Tr}\left(U^\dagger P\Pi_x P U - P\Pi_x P + U^\dagger(1-P)\Pi_x(1-P)U - (1-P)\Pi_x(1-P)\right) \\
&= \operatorname{Tr}(U^\dagger P\Pi_x P U - P\Pi_x P) \\
&= \int_0^{2\pi} \operatorname{Tr}\left(\frac{d}{d\phi}(e^{-i\phi P\Pi_y P}P\Pi_x P e^{i\phi P\Pi_y P})\right) \\
&= 2\pi i \operatorname{Tr}\left(\left[P\Pi_x P, P\Pi_y P\right]\right) \\
&= \nu(P).
\end{aligned}
\tag{3.18}
$$

The first equation is because the trace exists[5]; the second equation is because $[U, P] = 0$; the third equation is because $U = 1$ in the $P = 0$ block.

---

[5]This is why we must use Π_x, Π_y instead of Π_A, Π_B! Otherwise one will get $\nu(P) \in 2\mathbb{Z}$ instead of $\mathbb{Z}$, which is a wrong. To be precise, no points at infinity are close to the boundaries to both regions. It is this property that make the trace exists.

In the translational invariant case, one can similarly replace Π_x, Π_y by X, Y and calculate $\nu(P)$ by taking trace per cell:

$$\nu(P) = 2\pi i \ \mathrm{tr}\big(P\,[[X,P],[Y,P]]\,\big). \tag{3.19}$$

In momentum space, this indeed goes back to the integral representation Eq. (1.3) of Chern number.

3.3   Almost Commuting Matrices

There is another interesting approach for real-space topological invariants [31]. This approach is based on the intuition that trivial insulators can be deformed into "atomic insulators" where electrons are fully localized while topological insulators cannot.

3.3.1   Physical Motivation: Localized Wannier Functions

Let us assume that our system is put on the sphere $S^2 \subset \mathbb{R}^3$ whose radius equals 1.

It is a basic intuition that if all electrons are localized near the lattices, then the system is an insulator. From band theory, we know that eigenstates usually have a fixed momentum and therefore not localized. Nevertheless, the intuition is still valid in many cases, provided that we think about Wannier functions instead of eigenstates.

Given a projection P, a set of Wannier function is a basis $\{v^a\}$ of ImP such that each v^a has some localization property. Here, by localization, we mean the wavefunction v^a is mainly supported near its real-space center. To be precise, we define

$$x^a = \langle v^a | \, X \, | v^a \rangle \tag{3.20}$$

to be the x-coordinate of its center (and similarly we have y^a, z^a, etc). Here, X is a diagonal matrix (in real space) with diagonal element $X_{ii} = x_i$, the coordinate of lattice i. There might be different meaning of localization:

- (exponential localization) $\exists C$ such that $|v_i^a| \le C e^{-|i-x^a|/l}$ ($l \ll 1$).

- (localization) Define $X' = \sum_a x^a |v^a\rangle \langle v^a|$, then

$$\forall \omega \in \text{Im} P, \|(X - X')\omega\| \leq l \|\omega\|. \tag{3.21}$$

In the second definition, $X |v^a\rangle = \sum_a X |v^a\rangle \langle v^a|\omega\rangle$ while $X' |v^a\rangle = \sum_a x^a |v^a\rangle \langle v^a|\omega\rangle$. So the definition is indeed a kind of localization property saying that v^a is localized near x^a. If can be proved that, under technical assumptions, exponential localization implies localization (with different length scale l).

Here is how the notion of localization comes into play with topological physics. If all eigenstates are really localized, the system must be a trivial insulator. Therefore, it is reasonable to claim the following rough correspondence:

$$\text{localized Wannier functions} \longleftrightarrow \text{topologically trivial.} \tag{3.22}$$

This correspondence can be made precise. For example, it can be shown that a system is trivial iff the Wannier functions can be made exponentially localized [67]. For strictly localized Wannier functions, there is a stronger no-go result [68], see Appendix B. Moreover, for strictly localized Wannier cannot exist even if we allow the basis to be overcompleted [69].

Now let us consider the matrix X', Y', Z'. One has:

$$X'^2 + Y'^2 + Z'^2 = P^2, \quad [X', Y'] = [Y', Z'] = [Z', X'] = 0. \tag{3.23}$$

For gapped systems, one can prove that the above equations are approximately true for PXP, PYP, PZP:

$$\left\| (PXP)^2 + (PYP)^2 + (PZP)^2 - P^2 \right\| < \delta,$$
$$\left\| [PXP, PYP] \right\|, \left\| [PYP, PZP] \right\|, \left\| [PZP, PXP] \right\| < \delta. \tag{3.24}$$

Concentrating on the $P = 1$ subspace, then P^2 above can be repalced by I. It can be regarded as a "blurred representation" of a unit sphere, where PXP, PYP, PZP are some noncommuting coordinates.

36

This condition Eq. (3.21) implies that the almost commuting triple (PXP, PYZ, PZP) is close to a exactly commuting tripe (X', Y', Z'). It can be shown that the converse is also true. Therefore, we finally arrives at the following (rough) correspondence:

$$\text{topologically trivial} \longleftrightarrow PXP, PYP, PZP \text{ can be made commute.} \tag{3.25}$$

We can also put the system on the torus, and use two unitaries U, V as coordinates matrices. Then we need to consider whether it is possible to make almost commuting almost unitaries PUP, PVP into commuting unitaries.

3.3.2 Bott Index

While almost commuting Hermitian pair can always be made commute [70, 71], there is an obstruction to make a triple of commuting Hermitian matrices commute [31].

Indeed, consider the matrix:

$$B(H_1, H_2, H_3) = \begin{bmatrix} H_3 & H_1 - iH_2 \\ H_1 + iH_2 & -H_3 \end{bmatrix}, \tag{3.26}$$

and define the following Bott index as:

$$\text{bott}(H_1, H_2, H_3) = \frac{1}{2} \text{Tr} \left(f_0(B(H_1, H_2, H_3)) \right). \tag{3.27}$$

Here, $f_0(x) = \text{sgn}(x)$. If H_1, H_2, H_3 exactly mutually commute and $H_1^2 + H_2^2 + H_3^2 = 1$, then it is easy to show that eigenvalues of $B(H_1, H_2, H_3)$ come into pairs of ± 1. Therefore $\text{bott}(H_1, H_2, H_3) = 0$. In general, the Bott index equals the number of positive eigenvalues minus n, where n is the size of H_i.

It can be proved that $\text{bott}(H_1, H_2, H_3)$ is stable under small perturbations. Therefore, $\text{bott}(H_1, H_2, H_3) = 0$ is a necessary condition to make an almost commuting Hermitian triple commute. Moreover, the inverse proposition is also true. Therefore, the Bott index is the only obstruction to make almost commuting Hermitian triple commute.
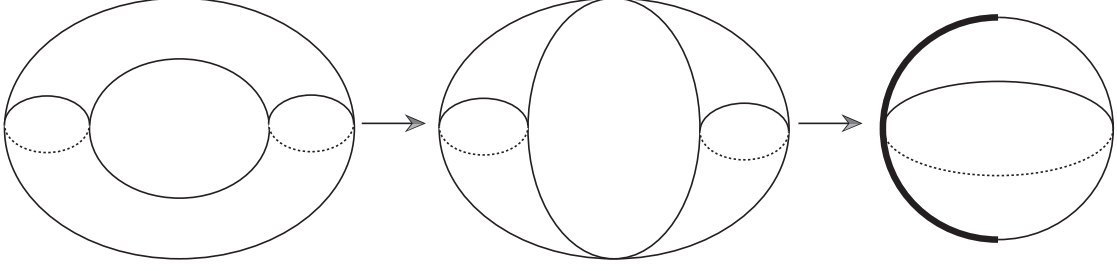
Figure 4: A nice map from torus to sphere. We first glue two circles on the torus into two points, then map the right half onto the sphere where the two points corresponds to two poles. The left half is mapped to a single longitude. The purpose of this construction is to make sure f_i in Eq. (3.28) are functions in one variable.

For a pair of almost commuting unitaries (U, V), a similar index exists by reducing the problem to the commuting triple case. Let (f_1, f_2, f_3) induces a map[6] $T^2 \to S^2 \subset \mathbb{R}^3$:

$$(e^{2\pi i\theta_1}, e^{2\pi i\theta_2}) \to (f_1(e^{2\pi i\theta_1})\cos(\theta_2) + f_2(\theta_1), f_1(e^{2\pi i\theta_1})\sin(\theta_2), f_3(e^{2\pi i\theta_1})). \tag{3.28}$$

The matrix version of this map is:

$$(U, V) \to (f_1(U)\cos(\theta_V) + f_2(U), f_1(U)\sin(\theta_V), f_3(U)). \tag{3.29}$$

Note that it is important for f_i to be functions in one variable, otherwise $f_i(U, V)$ is not well-defined unless they commutes exactly. The function f_2 is instroduced for techinical reason and satisfies $f_1^2 + f_2^2 + f_3^2 = 1, f_1 f_2 = 0$. See Fig. 4 for an illustration of the idea behind this map.

Similar to Eq. (3.26), consider:

$$Q(U, V) = \begin{bmatrix} f_3(U) & f_2(U) + i f_1(U) V^\dagger \\ f_2(U) + iV f_1(U) & -f_3(U) \end{bmatrix}, \tag{3.30}$$

---

[6]Due to topological difference, the map cannot be a homeomorphism. However, one only need its mapping degree equals 1.

and define the Bott index as:

$$\kappa(U, V) = \frac{1}{2} \operatorname{Tr}(f_0(Q(U, V))). \tag{3.31}$$

If U, V exactly commute, then $\kappa(U, V) = 0$. By the same logic as above, $\kappa(U, V)$ is an obstruction to make a pair of almost commuting unitaries commute. Moreover, one can show that the inverse is also true.

The above index have a more topological explanation. Consider the following path in the complex plane:

$$t \to \det((1 - t)UV + tVU). \tag{3.32}$$

It starts at $\det(UV) = 1$ and ends at $\det(VU) = 1$. If $[U, V]$ is small enough, the the path cannot pass 0, so we can define a winding number $\omega(U, V)$. If $[U, V]{=}0$, then the path always stay at 1, so $\omega(U, V) = 0$. It turns out that under technical assumptions,

$$\kappa(U, V) = \omega(U, V). \tag{3.33}$$

3.3.3 Topological Origin of Bott Index

Here we briefly comment on the mathematical origin on how the Bott index is constructed and why it is related to almost commuting matrix problem [72, 73].

Consider the general problem of finding commuting matrices in an algebra R. Any commuting triple $(H_1, H_2, H_3) \in R^3$ naturally induces a homomorphism ψ from $C(S^2)$ to R, by mapping $f(x_1, x_2, x_3) \in C(S^2)$ to $f(H_1, H_2, H_3)$ (it is well defined iff H_i mutually commutes, essentially by simultaneously diagonalization). With ψ in hand, it is natural to consider the induced map on the algebraic K_0 groups [74]:

$$\psi_* : K_0(C(S^2)) \to K_0(R). \tag{3.34}$$

Due to the Serre-Swan duality, $K_0(C(S^2)) \cong K^0(S^2) \cong \mathbb{Z} \oplus \mathbb{Z}$. Here the first $\mathbb{Z}$ factor is the dimension and the second $\mathbb{Z}$ factor is the Chern number of a (virtual) bundle $[E] \in$

$K^0(S^2)$. A well-known example for nontrivial bundle over S^2 is given by the following projection:

$$\frac{1}{2} \begin{bmatrix} 1 + x_3 & x_1 - ix_3 \\ x_1 + ix_2 & 1 - x_3 \end{bmatrix} \in M_2(C(S^2)). \tag{3.35}$$

Therefore, the above projection corresponds to a nontrivial element in $K_0(C(S^2))$. This is called a Bott element, which induces the Bott periodicty:

$$\tilde{K}^0(S^2) \cong K^0(pt) = \mathbb{Z}. \tag{3.36}$$

Considering the image of this Bott element under ψ_* in $K_0(R)$ will induce our Bott index.

It is now clear that the obstruction for making almost commuting matrices commute has a topological origin, which is a nontrivial bundle over the sphere S^2. However, one should note that here the sphere is in real space, instead of momentum space.

3.4 Real-Space Invariant for Topological Insulators

A topological insulator (TI), first proposed by Kane and Mele in Ref. [13], is an example of nontrivial systems for AII class in two-dimension (2D). It is characterized by the gapless helical edge modes protected by the time-reversal symmetry [16], and the band-crossing in the language of topological band theory. The topological invariant, in this case, is a $\mathbb{Z}_2$ number which we call Kane-Mele invariant, see Refs. [13, 75, 76, 62, 77, 78] for more details.

In this section, we discuss a formula for the Kane-Mele invariant, which remains valid with disorder [29]. It has two useful features:

- It is purely topological, in the sense that we discard many geometrical information or choices such as distances and angles [see Eq. (3.51)].
- Similar to Eq. (3.15), the input of our formula is the projection P. Also similar to Eq. (3.15), our formula is essentially a local expression, in the sense that the contribution mainly comes from quantities near a point.

3.4.1 Intuition: Flux Insertion and Topological Invariant

In this section, we put Chern insulator/topological insulator on a punctured plane and insert fluxes at the origin [see Fig. 3(a)]. We will explain how the physics of flux insertion is related to topological invariant. This section aims to explain our intuition and provide a physical derivation of our formula, hence, some statements here may not very rigorous. We will establish our results carefully in the following sections.

Recall the simple case, Chern insulators, which can be realized in integer anomalous quantum Hall systems. In this case, we have the well-known Thouless charge pump [79]: when a flux unit is adiabatically inserted, it induces an annular electric field, which in turn produces a radial electric current due to the Hall effect. As a result, electrons are pushed away from (or close to, depending on the sign of the current) the origin for "one unit". In Fig. 5 we draw the band structure for boundary states (near the puncture). Diagrammatically, when a flux unit is inserted, every occupied state moves toward top right to a lower level.
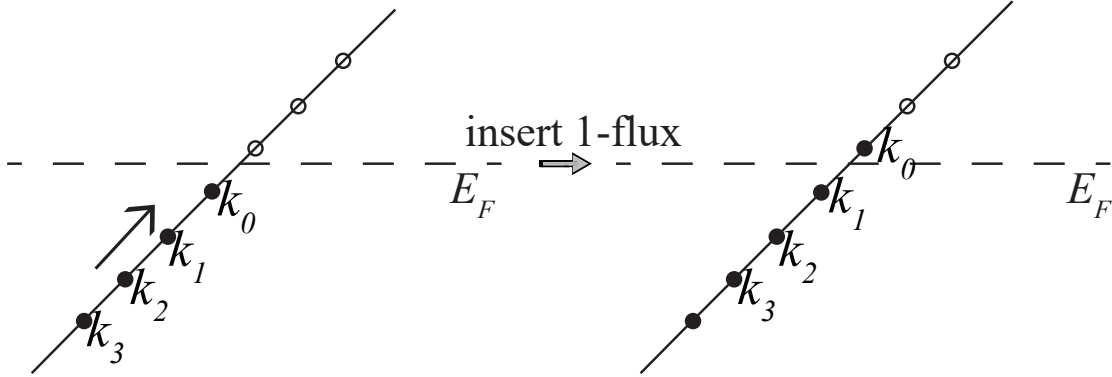
Figure 5: Band for boundary states of a Chern insulator. • means filled, ∘ means empty. After a unit flux insertion, every filled state moves towards top right to the next level. In this process, the label k_i is tight to the electron, not the level.

The many-body state after the flux insertion is not the ground state, because there is a filled state above the Fermi level. Compared to the ground states, we can see that the new ground state has one less electron (k_0 electron in Fig. 5) than the old one (note that we are doing $\infty - \infty$, see comments below). The difference of the number of electrons in ground

states is exactly the Chern number. This is the idea behind Ref. [27]:

$$\text{Chern number} = \text{Ind}(P, P') = \dim \text{Ker}(P - P' - 1) - \dim \text{Ker}(P - P' + 1), \qquad (3.37)$$

where P/P' is the projection operator onto filled states before/after the flux insertion, Ind is the relative index for a pair of projections, which intuitively counts the difference of their ranks (dimension of eigenvalue 1 subspace, number of filled levels in physics). Since the rank is just $\text{Tr}(P)$ and $\text{Tr}(P')$, one may expect

$$\text{Ind}(P, P') \sim \text{Tr}(P - P'). \qquad (3.38)$$

This formula is indeed correct if $\text{Tr}(P - P')$ is well-defined—if $(P - P')$ is trace class [80]. This is not the case for nontrivial Chern insulator though: $\text{Ind}(P, P')$ is still well-defined [27], but one needs a more complicated formula to evaluate it, which is essentially Eq. (3.15).

Now we turn to topological insulators. In this case, we adiabatically insert a $\frac{1}{2}$-flux quanta. As shown in Fig. 6, what happens is: energies for left-movers increase, while energies for right-movers decrease. If we assume (without loss of generality) the Fermi level is right below an empty state, the ground state after the flux insertion will have one more electron than before. We want to count the number of extra electrons to determine the Kane-Mele invariant ν_{KM} (mod 2).

To do this, we first count the number of electrons in a finite disk with radius r (the system is still on an infinite plane, we just draw a virtual circle to define a disk). Due to time-reversal symmetry, topological insulators have zero total Hall conductance, so the number of electrons inside the disk remains unchanged under adiabatic flux insertion. However, there is a vertex state (k_0^R in Fig. 6) that is left empty, so in the new ground state the number of electrons in the disk is increased by 1:

$$\Delta \langle \text{No. electrons in a (large) disk} \rangle = 1 = \nu_{\text{KM}} \ (\text{mod } 2), \qquad (3.39)$$

where $\langle \rangle$ means ground state expectation value (note again that ground states before and after the flux insertion are different).
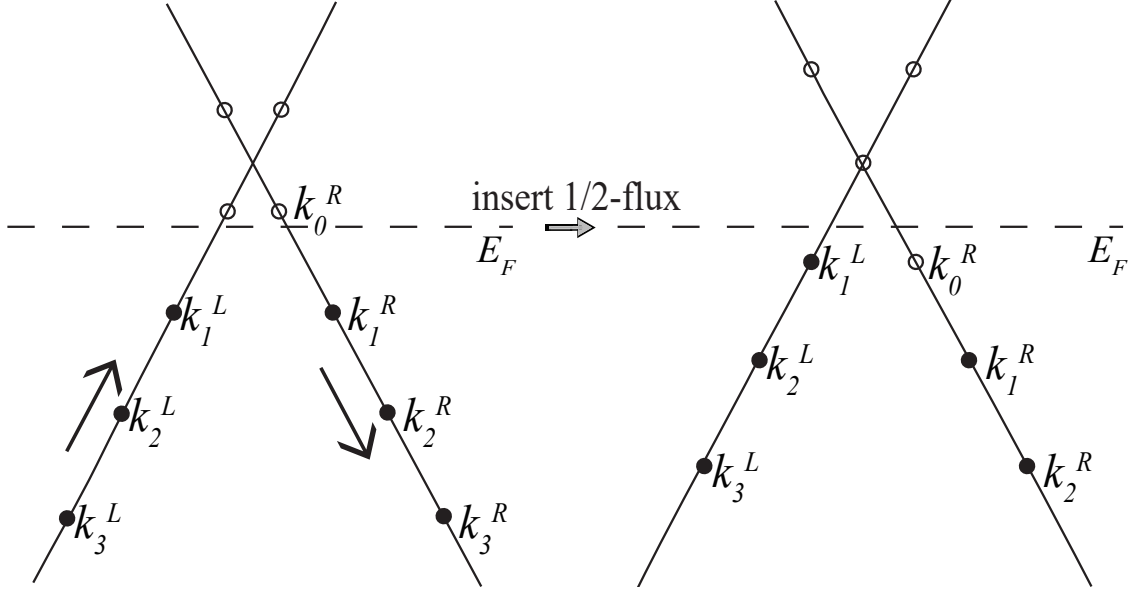
Figure 6: Band for boundary states in a topological insulator. After a half flux insertion, we get one more state under the Fermi level, which is geometrically near the vertex (flux).

Since P is the projection onto filled states, $H_0 = 1 - 2P$ can be regarded as a spectral-flattened Hamiltonian (filled$= -1$, empty$= 1$). Denote $H_{\frac{1}{2}}$ to be the Hamiltonian after flux-insertion, consider $Q = \frac{1}{2}(1 - H_{\frac{1}{2}})$ and corresponding projection matrix $\overline{Q}$ (see Sec. 3.4.2 for details). We have

$$\langle N_r \rangle \text{ (before)} = \langle \sum_{|i|<r} a_i^\dagger a_i \rangle = \text{Tr}(P_r),$$

$$\langle N_r \rangle \text{ (after)} = \text{Tr}(\overline{Q}_r), \qquad (3.40)$$

$$\Delta \langle N_r \rangle = \text{Tr}\,\overline{Q}_r - \text{Tr}\,P_r = \text{Tr}(\overline{Q}_r - Q_r).$$

Here N_r is the number of electrons in disk r, $P_r, \overline{Q}_r$ is the truncation of $P, \overline{Q}$ ($\overline{Q}_r$ means $(\overline{Q})_r$: spectral flatten before truncation). The last equation is because P and Q have the same diagonal elements (see Sec. 3.4.2) and they are finite matrices.

Thus, we expect

$$\nu_{\text{KM}} = \lim_{r\to\infty} \Delta \langle N_r \rangle = \lim_{r\to\infty} \text{Tr}(\overline{Q}_r - Q_r) \sim \text{Tr}(\overline{Q} - Q) \pmod 2. \qquad (3.41)$$

43

One may want to apply the same idea to Chern insulators. This will just lead to $0 = 0$. Indeed, we still have

$$\Delta \langle \text{No. electrons in a (large) disk} \rangle = \lim_{r \to \infty} \text{Tr}(\overline{Q}_r - Q_r). \tag{3.42}$$

However, there will always be an electron go into (or out of) the disk adiabatically, which compensates the lost (or extra) state, so $\Delta\langle\text{No. electrons in disk}\rangle$ in the left-hand side is always 0 in this case. This can also be seen from the (large) gauge equivalence between the two systems before and after a unit flux insertion. For the right-hand side, since $Q = P'$ in this case is already a projection, $\overline{Q} = Q$, so the r.h.s is 0. The difference between topological insulators and Chern insulators is as follows: in the former case the number of electrons through the boundary r is 0 in average (because of zero Hall conductance), while in the latter it is nonzero and is essentially the Chern number.

As a side note, one may also consider the insertion of a unit flux and consider the difference between two ground states. A direct application of the relative index Eq. (3.37) gives 0. However, one may note that two terms (dimension of the kernel) in Eq. (3.37) come from left movers and right movers separately and therefore one can define the $\mathbb{Z}_2$ index with one kernel. This is the idea behind Ref. [36].

3.4.2 Formula for Infinite System

In this section, we will carefully define the quantities in our main formula Eq. (3.41) and show its well-definedness.

The input of our formula will be the single-body projection operator P, which is related to the spectrum-flattened Hamiltonian $H_0 = 1 - 2P$. For gapped states, P decays at least exponentially [81]:

$$P_{\mathbf{x},\mathbf{y}} < C_1 e^{-C_2|\mathbf{x}-\mathbf{y}|}. \tag{3.43}$$

According to the Peierls substitution [82], if we insert a $\frac{1}{2}$-flux at a vertex, the new (single-body) Hamiltonian can be written as $H_{\frac{1}{2}} = 1 - 2Q$, where

$$Q_{\mathbf{x},\mathbf{y}} = s_{\mathbf{x},\mathbf{y}} P_{\mathbf{x},\mathbf{y}}. \tag{3.44}$$

Here $s_{\mathbf{x},\mathbf{y}}$ are phases such that for any loop $l = (\mathbf{x}_1, \mathbf{x}_2, \cdots, \mathbf{x}_n = \mathbf{x}_1)$, we have

$$s_l \overset{\text{def}}{=} \prod_{i=1}^{n} s_{\mathbf{x}_i,\mathbf{x}_{i+1}} = \begin{cases} -1, & \text{if the vertex is in the loop} \\ 1, & \text{otherwise} \end{cases}. \tag{3.45}$$

These phases can be chosen as follows: we divide the plane into three regions, as in Fig. 3(b).

Let $n_{\mathbf{x},\mathbf{y}}$ to be the number intersections of the straight line segment $(\mathbf{x}, \mathbf{y})$ with three boundaries l_1, l_2, l_3, set

$$s_{\mathbf{x},\mathbf{y}} = (-1)^{n_{\mathbf{x},\mathbf{y}}}. \tag{3.46}$$

We call this gauge "insert half fluxes along the boundaries". While P is a projection, Q no longer is. Actually, we have

$$(Q^2 - Q)_{\mathbf{x},\mathbf{y}} = \sum_{\mathbf{z}} s_{\mathbf{x},\mathbf{z}} s_{\mathbf{z},\mathbf{y}} P_{\mathbf{x},\mathbf{z}} P_{\mathbf{z},\mathbf{y}} - s_{\mathbf{x},\mathbf{y}} P_{\mathbf{x},\mathbf{y}} = -2 s_{\mathbf{x},\mathbf{y}} \sum_{\mathbf{z}}{}' P_{\mathbf{x},\mathbf{z}} P_{\mathbf{z},\mathbf{y}}. \tag{3.47}$$

where $\sum'$ means sum under constraint $s_{\mathbf{x}\mathbf{y}\mathbf{z}} = -1$. Denote $V = Q^2 - Q$. Since matrix elements of P decays exponentially, V is mainly supported around the vertex (hence the notation V) due to the constraint. To be specific, we have the following:

Proposition 3.1. $\exists C_1', C_2'$, such that $|V_{\mathbf{x},\mathbf{y}}| < C_1' e^{-C_2' r}$ where $r = \max\{|\mathbf{x}|, |\mathbf{y}|\}$.

Proof. Let us calculate $V_{\mathbf{x},\mathbf{y}}$:

$$|V_{\mathbf{x},\mathbf{y}}| = |2 \sum_{\mathbf{z}}{}' P_{\mathbf{x},\mathbf{z}} P_{\mathbf{z},\mathbf{y}}| < 2 C_1^2 \sum_{\mathbf{z}}{}' e^{-C_2(|\mathbf{x}-\mathbf{z}|+|\mathbf{z}-\mathbf{y}|)}. \tag{3.48}$$

From geometry, it is obvious that $|\mathbf{x} - \mathbf{z}| + |\mathbf{z} - \mathbf{y}| > r$ if $s_{\mathbf{x}\mathbf{y}\mathbf{z}} = -1$, so the summation can be controlled by

$$2 C_1^2 e^{-\frac{C_2}{2} r} \sum_{\mathbf{z}} e^{-\frac{C_2}{2}(|\mathbf{x}-\mathbf{z}|+|\mathbf{z}-\mathbf{y}|)} < C_1' e^{-C_2' r}. \tag{3.49}$$

(This is a pretty crude estimation but is enough.) $\qquad \square$

In the following, we will refer to this property as the "exponential decay property" (EDP). Intuitively, $Q^2 - Q$ satisfies EDP means the deviation of Q from a projection mainly comes from states near the vertex point. If we spectral flatten Q to $\overline{Q}$ (for eigenvalues $\lambda \leq \frac{1}{2}$, convert it to 0, otherwise convert it to 1), we anticipate that $Q - \overline{Q}$ is mainly supported near the vertex. Actually, $Q - \overline{Q}$ also obeys EDP, but we do not need this result. We only need the following:

Proposition 3.2. $Q - \overline{Q}$ is trace class.

Proof. $|x - \bar{x}| \leq 2|x^2 - x|$ for $\forall x \in \mathbb{R}$, so $|Q - \overline{Q}| \leq 2|Q^2 - Q| = 2|V|$ as an operator (note that they commute). Since V obeys EDP, V must be trace class (see the corollary after Lemma C.2 in appendix C.1.1), so is $Q - \overline{Q}$. $\square$

Therefore, it is legal to define a "trace over vertex states" as

$$\mathrm{Tr}^v(Q) = \mathrm{Tr}(Q - \overline{Q}). \tag{3.50}$$

Note that in the definition of $\overline{Q}$ we can arbitrarily choose the chemical potential $\mu \in (0, 1)$, so the $\mathrm{Tr}^v(Q)$ should be naturally understood as mod 1. In the case of topological insulators, Q has time-reversal symmetry, every state is Kramers paired, so $\mathrm{Tr}^v(Q)$ can be naturally understood as mod 2. We will see in the following that it is $\mathrm{Tr}^v(Q)$ mod 2 [instead of $\mathrm{Tr}^v(Q)$ itself for a fixed "chemical potential"] that has good properties. Also note that Q is not trace class in general, so we cannot define $\mathrm{Tr}^v(Q)$ as $\mathrm{Tr}(Q)$ mod 2.

According to the above analysis, this expression is well-defined and the contributions mainly come from states near the vertex; it is a local expression. Interestingly, this local expression turns out to be independent of the flux-insertion point we choose; it only depends on the state itself. Moreover, it is an integer and is topologically invariant. Our main proposition is as follows:

Main Proposition $\mathrm{Tr}^v(Q)$ equals to the Kane-Mele invariant.

The derivation of our proposition is in Sec. 3.4.5 and the appendix C.1. Before going on, we give three comments on our formula.

Firstly, there is another construction of Q, closely related to the one given by Eq. (3.45):

$$Q = \begin{bmatrix} AAA & -AB & -AC \\ -BA & BB & -BC \\ -CA & -CB & CC \end{bmatrix}, \tag{3.51}$$

where AB means P_{AB}, a block in the original matrix P. If we consider a circle with many sites on it, it still gives us a total phase -1. In this case,

$$Q^2 - Q = 2 \begin{bmatrix} 0 & ACB & ABC \\ BCA & 0 & CAB \\ CBA & BAC & 0 \end{bmatrix}, \tag{3.52}$$

where ACB means $P_{AC}P_{CB}$, etc. It is still concentrated near the vertex (satisfies EDP), as long as the partition is good[7]. So we can follow the same procedure to define a new $\text{Tr}^v(Q)$. We note that the Q defined here is *not* unitary equivalent to the one in Eq. (3.45)—they have different spectra in general. However, in Sec. 3.4.5 we will show that $\text{Tr}^v(Q)$ defined from them are equal (mod 2). We call the Q in Eq. (3.51) the topological one, denoted by Q^t, because its definition does not depend on the geometric information such as "straight line segments". The Q in Eq. (3.45) will be called the geometric one, denoted by Q^g. It has the advantage of gauge invariance and many quantities [like $\text{spec}(Q)$] defined from it are manifestly independent of the partition.

Secondly, for systems in the DIII class ($\text{TRS}^2 = -1$, $\text{PHS}^2 = 1$ where TRS is time-reversal symmetry and PHS is particle-hole symmetry), our formula can be simplified. Indeed, since the original system has PHS:

$$K_{ph}^{\dagger} \overline{(2P-1)} K_{ph} = 2P - 1, \tag{3.53}$$

where $(2P-1)$ is the spectral-flattened Hamiltonian with spectrum=$\{\pm 1\}$. K_{ph} is an onsite action, and commutes with the operation from P to Q, so the same equation holds for Q. Therefore the spectra of Q is symmetric with respect to $1/2$:

$$\sigma(Q) = 1 - \sigma(Q). \tag{3.54}$$

---

[7]For example, the one in Fig. 3(b) is good. However, if we rotate l_2 towards l_1 and deform it a little bit so they are parallel at infinity, then $Q^2 - Q$ does not satisfy EDP and convergence problem will occur.

Now, for a spectrum q such that $q \neq \frac{1}{2}$, the Kramers degeneracy and PHS provides us a four-fold $\{q, q, 1-q, 1-q\}$, which contributes 0 to $\text{Tr}^v(Q)$ (mod 2). So:

$$\nu = \text{Tr}^v Q = \text{No. } \{\text{Kramers pairs at } \tfrac{1}{2}\} \pmod 2. \tag{3.55}$$

Thirdly, the input P is the correlation matrix for an infinite system. If we start with a finite system, say a topological insulator on the sphere, then our formula always gives 0. Mathematically, this is because both $\text{Tr}(\overline{Q})$ and $\text{Tr}(Q) = \text{Tr}(P)$ are even due to time-reversal symmetry. Physically, it is because when inserting a flux at some point, it is unavoidable to insert another flux at somewhere else for a closed geometry, then our formula counts the vertex states at both points. To get the right invariant, we need to "isolate" the physics at one vertex.

3.4.3 Approximation from Finite System

Although the input of our formula is an infinite-dimensional operator P, our formula is a trace of vertex states, which should only depend on the physics near the origin. Let us truncate the plane with a circle r [see Fig. 3(c)]. Denote P_N and Q_N to be the truncation of P and Q, where N is the number of sites inside the circle, $N \sim r^2$. We expect that one can approximate the invariant with data near the origin, i.e. with matrix elements of P_N or equivalently Q_N.

However, a naive limit $\lim_{N \to \infty} \text{Tr}(Q_N - \overline{Q_N})$ is wrong: it will give $\lim \text{Tr}(P_N)$ (mod 2) since $\text{Tr}(\overline{Q_N})$ is even. This is because $\overline{Q_N} \neq (\overline{Q})_N$. Physically, Q_N and Q do have similar "vertex states". However, unlike Q, Q_N also includes boundary contributions [see Eq. (3.57)], which need to be excluded.

We claim that we can use the following algorithm to approximate our invariant.

- Construct a matrix V_N by

$$V_N = -2s_{\mathbf{x},\mathbf{y}} \sum_{\substack{\mathbf{z} \in (ABC) \\ s_{\mathbf{x}\mathbf{y}\mathbf{z}}=-1}} P_{\mathbf{x},\mathbf{z}} P_{\mathbf{z},\mathbf{y}}. \tag{3.56}$$

V_N will be almost commuted with Q_N and it will tell us whether a state is near the vertex or the boundary.

- Find approximations Q'_N, V'_N for Q_N, V_N so that they indeed commute[8].

- Simultaneously diagonalize Q'_N and V'_N to get pairs of eigenvalues (q', v'). Sum over all the eigenvalues q' such that $v' \neq 0$.

  The summation will converge to $\mathrm{Tr}^v(Q)$ as $N \to \infty$.

In the following we explain the algorithm in detail. First of all, we have:

$$(Q_N^2 - Q_N)_{\mathbf{x},\mathbf{y}} = -s_{\mathbf{x},\mathbf{y}}[2 \sum_{\substack{\mathbf{z} \in ABC \\ s_{\mathbf{xyz}}=-1}} P_{\mathbf{x},\mathbf{z}} P_{\mathbf{z},\mathbf{y}} + \sum_{\mathbf{z} \in D} P_{\mathbf{x},\mathbf{z}} P_{\mathbf{z},\mathbf{y}}] \stackrel{\text{def}}{=} (V_N)_{\mathbf{x},\mathbf{y}} + (W_N)_{\mathbf{x},\mathbf{y}}. \qquad (3.57)$$

Here, V_N is supported near the center, while W_N is supported near the boundary. This means the deviation of Q_N to a projection happens both near the vertex and the boundary.

We can also work in the topological construction of Q. In this case,

$$Q_N^2 - Q_N = 2 \begin{bmatrix} 0 & ACB & ABC \\ BCA & 0 & CAB \\ CBA & BAC & 0 \end{bmatrix} - \begin{bmatrix} ADA & ADB & ADC \\ BDA & BDB & BDC \\ CDA & CDB & CDC \end{bmatrix}$$

$$= V_N + W_N. \qquad (3.58)$$

In both constructions, Q_N, V_N, W_N should almost commute, and V_N, W_N are almost orthogonal, since they are mainly supported in different regions ("almost" means relevant expressions approach 0 as $N \to \infty$).

Proposition 3.3. (1) Q_N, V_N, W_N defined above satisfies

$$\|[Q_N, V_N]\| < \epsilon, \quad \|[Q_N, W_N]\| < \epsilon,$$
$$\|V_N W_N\| < \epsilon, \quad \|W_N V_N\| < \epsilon, \qquad (3.59)$$

where the norm $\|\cdot\|$ is the L^2 norm (maximal singular value), $\epsilon \sim p(r)e^{-r}$ where $p(r)$ is a polynomial of r.

(2) There exist Hermitian matrices Q'_N, V'_N, W'_N as approximations of Q_N, V_N, W_N in the sense that

$$\|Q_N - Q'_N\| < \rho^2, \quad \|V_N - V'_N\| < \rho, \quad \|W_N - W'_N\| < \rho, \qquad (3.60)$$

---

[8]In practice, there are some arbitrariness to find Q'_N, V'_N. What we do is a joint approximation diagonalization (JAD) and then make them commute according to some rules. For example, one may make all v' such that $|v'| > \epsilon$ to zero. Another rule is indicated in Sec. 3.4.4.

such that

$$[Q'_N, V'_N] = [Q'_N, W'_N] = V'_N W'_N = W'_N V'_N = 0 \qquad (3.61)$$

$$Q'^2_N - Q'_N = V'_N + W'_N. \qquad (3.62)$$

Here ρ can be chosen as $F(\epsilon)\epsilon^{1/10}$ (independent of N) where the function $F(x)$ grows slower than any power of x.

Proof. (1) Straight forward calculation.

(2) It is easy to check $||Q_N||$ and $||V_N||$ are finite, independent of N (one way to do this is to prove it for the topological construction Q in Eq. (3.51) and use the relationship between two constructions as in property 3.6). According to Lin's theorem [70], $\exists Q'_N, V'_N$ such that $||Q_N - Q'_N||, ||V_N - V'_N|| < \delta$ and $[Q'_N, V'_N] = 0$. Moreover [71], we can choose $\delta = E(1/\epsilon)\epsilon^{1/5}$ where the function $E(x)$ grows slower than any power of x, independent of N.

Define $W'_N = Q'^2_N - Q'_N - V'_N$, then W'_N, Q'_N, V'_N can be simultaneously diagonalized. Since $W_N = Q^2_N - Q_N - V_N$, $||Q_N - Q'_N||, ||V_N - V'_N|| < \delta$, so we have $||W_N - W'_N|| \lesssim \delta$ and

$$||V'_N W'_N|| = ||(V'_N - V_N + V_N)(W'_N - W_N + W_N)|| \lesssim \epsilon + \delta \sim \delta. \qquad (3.63)$$

This means for each pair of eigenvalues (v'_N, w'_N), at least one of them should be smaller than $\sqrt{\delta}$. We manually make these eigenvalues to be 0, while fixing $v'_N + w'_N$.

The new V'_N and W'_N would be strictly orthogonal, and still commute with Q'_N, and still obeys $Q'^2_N - Q'_N = V'_N + W'_N$. Moreover, now $||V_N - V'_N|| \sim \delta + \sqrt{\delta} \sim \sqrt{\delta} \overset{\text{def}}{=} \rho$.

$\square$

Having Q'_N, V'_N, W'_N exactly commute, and V'_N, W'_N exactly orthogonal, we use them to distinguish vertex contributions and boundary contributions. We simultaneously diagonalize them and get triples (q', v', w'). Different contributions are then identified as follows (the reason for this identification is evident) [see Fig. 7]:

- $v' \neq 0, w' = 0$: vertex states
- $v' = 0, w' \neq 0$: boundary states
- $q' = 0$ or $1, v' = w' = 0$: bulk states

We anticipate that the summation of q' over vertex states will be a good approximation of $\text{Tr}^v(Q)$.

Proposition 3.4 (finite size approximation). After the above procedure,

$$\lim_{N\to\infty} \sum_{\substack{\text{vertex} \\ \text{states}}} q' = \text{Tr}^v(Q). \tag{3.64}$$

The proof is in appendix C.1.2.

3.4.4 Numerical Results

For our numerical results we use the Bernevig-Hughes-Zhang (BHZ) model [14] on a square lattice with Rashba coupling and scalar/valley disorder:

$$\begin{aligned}
H &= \int_{\mathbf{k}} (H_0 + H_R) \, d^2\mathbf{k} + \sum_{\mathbf{r}} H_D(\mathbf{r}), \\
H_0(\mathbf{k}) &= v(\tau^x \sigma^z \sin k_x + \tau^y \sin k_y) \\
&\quad + (m - t \cos k_x - t \cos k_y)\tau^z, \\
H_R(\mathbf{k}) &= r(\sigma^x \sin k_y - \sigma^y \sin k_x), \\
H_D(\mathbf{r}) &= V(\mathbf{r}, +)\frac{1 + \tau^z}{2} + V(\mathbf{r}, -)\frac{1 - \tau^z}{2}.
\end{aligned} \tag{3.65}$$

Here there are four degrees of freedom per site, with τ and σ acting on valley and spin space respectively.

In Figs. 7(b) and 7(c), we show the computation of the topological invariant of this model for $v = t = 1$, $r = 1/2$, with the disorder $V(\mathbf{r}, \pm)$ sampled uniformly from the interval $[-0.4, 0.4]$. Fig. 7(b) shows a topological phase with $m = 1.6$, while Fig. 7(c) shows a trivial phase with $m = 2.4$.

These plots show the eigenvalues (q', v') of the matrices Q'_N and V'_N respectively (q' is along the x-axis and v' is along y-axis). Recall that we have $(q')^2 - q' = v' + w'$ and $v'w' \approx 0$, hence points (q', v') either lives on the parabola $y = x^2 - x$ (if $v' \neq 0$) or along the x-axis (if $v' = 0$). According to our analysis, points along the x-axis represent boundary states; points near $(0,0)$ and $(1,0)$ represent bulk states; all other points on the parabola corresponds to vertex states. As a comparison, Fig. 7(c) shows the trivial region where there are (mostly)
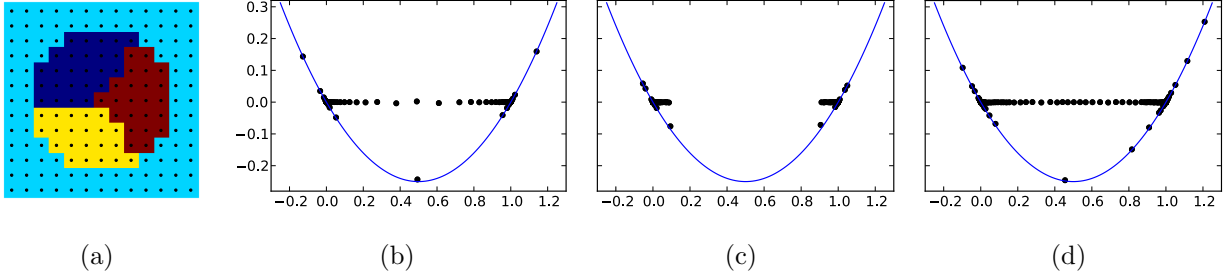
Figure 7: (a) The geometry for computing the topological invariants. The regions A, B, and C are represented by colours yellow, red, and navy blue respectively. (Region D is represented by cyan.) (b)–(c) Numerical results for the Hamiltonian Eq. (3.65) with (b) $m = 1.6$ and (c) $m = 2.4$. Shown in the plot are eigenvalues of V'_N vs. Q'_N. These results are generic; dots along the x-axis represent boundary states; dots near $(0,0)$ and $(1,0)$ are bulk states; dots on the parabola represent vertex states. (d) Numerical result from the Hamiltonian Eq. (3.66), which strongly breaks particle-hole symmetry.

only have bulk states. The goal of the numerical procedure outlined in the previous section is to isolate the vertex states which lives near the intersection of A, B, and C.

As the model Eq. (3.65) (without disorder) is particle-hole symmetric, the resulting eigenvalues are reflection symmetric ($q' \to 1 - q'$). Disorder only breaks this symmetry very weakly. To break this mirror symmetry, we construct a spinful model with three valleys,

$$
\begin{aligned}
H_0 = {} & 0.3\lambda^3 + 0.4\lambda^8 + (0.5\lambda^1 + 0.6\lambda^4)\sigma^z \sin k_x + (1.2\lambda^2 - 0.3\lambda^5) \sin k_y \\
& + (0.5\lambda^1 - 0.7\lambda^3 - 0.3\lambda^4 + 1.1\lambda^6 - 0.6\lambda^8) \cos k_x \\
& + (0.5\lambda^1 - 0.7\lambda^3 - 0.4\lambda^4 + 1.0\lambda^6 - 0.6\lambda^8) \cos k_y,
\end{aligned}
\tag{3.66}
$$

where $\lambda^1, \ldots, \lambda^8$ are the Gell-Mann matrices acting on valley space. We retain the Rashba term with $r = 0.1$, and disorder (for three valleys independently) sampled from $[-0.4, 0.4]$. The spectrum (q', v') is shown in Fig. 7(d), with ν evaluating to 1.02 indicating a QSH phase.

In Fig. 8, we plot the result of our formula Eq. (3.64) for model Eq. (3.65) as a function of m. (The data is computed for a single disorder realization.) For the computation of $\mathrm{Tr}^v Q$, we distinguished the vertex states (from the bulk and edge states) by only considering points
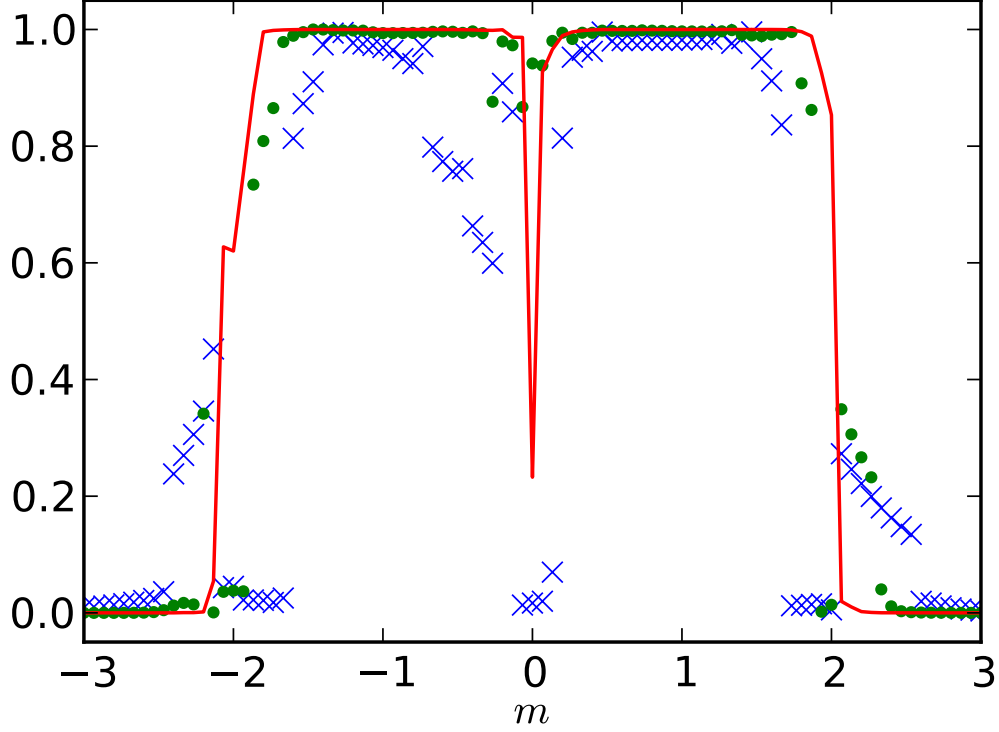
	total system size	radius of ABC region
blue crosses	7×7	2.4
green dots	13×13	4.5
red line	25×25	8.9

Figure 8: The sum $\mathrm{Tr}^v Q$ (approximating the invariant ν) of a finite system for various m. The system sizes are shown in the table. (For example, the green crosses shows data computed with Fig. 7(a)'s geometry.)
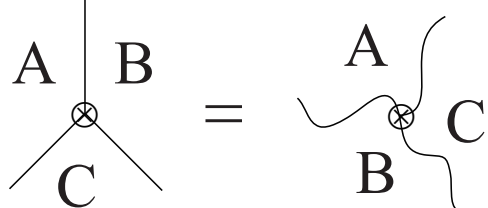
satisfying $q' < 0$, $q' > 1$, or $v' < \frac{(q')^2 - q'}{2}$. We see that the system is in the Quantum spin Hall (QSH) phase for the bulk of $-2 \lesssim m \lesssim 2$. As the Hamiltonian $H_0 + H_R$ is gapless (Dirac-type) at $m = 0$, we expect a small sliver of metallic phase near $m \approx 0$ from disorder. (In general, the metallic phase is stable in the AII class, hence we do not expect direct transition between the QSH and trivial phases.) We see that as the system size increases (so that it is large compared with the correlation length ξ), the invariant approaches 0 or 1 to

the gapped phases.

3.4.5 Property and Proof

In this section, we will investigate the property of $\mathrm{Tr}^v(Q)$ and derive our main proposition step by step.

Proposition 3.5 (Gauge invariance)**.** Fixing the position of the flux and working in the geometric definition, then $\mathrm{Tr}^v(Q)$ does not depend on the actual partition of the plane. For example, the following partition and the ordering of A, B, C will give the same $\mathrm{Tr}^v(Q)$.

$$\tag{3.67}$$

This is because different partitions correspond to different gauge choices in the Pierls substitution. Indeed, fix a reference point $*$, define $u_\mathbf{x} = s_{*,\mathbf{x}}/s'_{*,\mathbf{x}}$ where s, s' are the phases for two partitions. Since $s_{*,\mathbf{x}}s_{\mathbf{x},\mathbf{y}}s_{\mathbf{y},*} = s_{*\mathbf{x}\mathbf{y}} = s'_{*,\mathbf{x}}s'_{\mathbf{x},\mathbf{y}}s'_{\mathbf{y},*}$, we have:

$$s'_{\mathbf{x},\mathbf{y}} = u_\mathbf{x} s'_{\mathbf{x},\mathbf{y}} \bar{u}_\mathbf{y} \tag{3.68}$$

Thus $Q' = UQU^\dagger$ and they have the same spectra.

Proposition 3.6. $\mathrm{Tr}^v(Q^t)$ defined from topological Q (for good partitions) and $\mathrm{Tr}^v(Q^g)$ defined from geometric Q are equal (mod 2).

Proof. We calculate $Q^t - Q^g$ and find that

$$(Q^t - Q^g)_{\mathbf{x},\mathbf{y}} = \begin{cases} -2P_{\mathbf{x},\mathbf{y}}, & \mathbf{x}, \mathbf{y} \text{ belong to different regions} \\ & \text{and } (\mathbf{x}, \mathbf{y}) \text{ intersects 2 boundaries} \\ 0, & \text{otherwise} \end{cases} \tag{3.69}$$

From geometry we can see if $|\mathbf{x}| > r$, then the first condition is satisfied only if $|\mathbf{y}-\mathbf{x}| > \mathcal{O}(r)$ where $r = \max\{|\mathbf{x}|, |\mathbf{y}|\}$. So $Q^t - Q^g$ satisfies a EDP: $|(Q^t - Q^g)_{\mathbf{x},\mathbf{y}}| < C_1 e^{-C_2 r}$ and thus is trace class. Therefore,

54

- $\text{Tr}(Q^t - Q^g) = \lim_{N \to \infty} \text{Tr}(Q^t_N - Q^g_N) = 0$, since they always have the same diagonal elements (note that we need trace class condition for the first equation evolving limit [80]).

- $\overline{Q^t} - \overline{Q^g} = (Q^t - \overline{Q^t}) - (Q^g - \overline{Q^g}) - (Q^t - Q^g)$ is also trace class.

Due to time-reversal symmetry,

$$
\begin{aligned}
\text{Tr}(\overline{Q^t} - \overline{Q^g}) &= \text{Ind}(\overline{Q^t}, \overline{Q^g}) \\
&= \dim \text{Ker}(\overline{Q^t} - \overline{Q^g} - 1) - \dim \text{Ker}(\overline{Q^t} - \overline{Q^g} + 1) \\
&= 0 \ (\text{mod } 2),
\end{aligned}
\tag{3.70}
$$

where $\text{Ind}(\cdot, \cdot)$ is the index for a pair of projections [27]. So we have

$$
\text{Tr}^v(Q^t) - \text{Tr}^v(Q^g) = \text{Tr}(Q^t - \bar{Q}^t - Q^g - \bar{Q}^g) = \text{Tr}(Q^t - Q^g) - \text{Tr}(\bar{Q}^t - \bar{Q}^g) = 0 \ (\text{mod } 2). \tag{3.71}
$$

$\square$

Now we insert two $\frac{1}{2}$-fluxes at different positions far away from each other. We divide the plane into four regions, as in Fig. 9. Again, we "insert half fluxes along the boundaries" and write the Hamiltonian as

$$
S_{\mathbf{x},\mathbf{y}} = s_{\mathbf{x},\mathbf{y}} P_{\mathbf{x},\mathbf{y}}, \tag{3.72}
$$

where $s_{\mathbf{x},\mathbf{y}}$ are defined similar to Eq. (3.46) by the new partition. We have:

$$
S^2 - S = -2s_{\mathbf{x},\mathbf{y}} \sum_{\substack{\mathbf{z} \\ s_{\mathbf{xyz}}=-1}} P_{\mathbf{x},\mathbf{z}} P_{\mathbf{z},\mathbf{y}} = -2s_{\mathbf{x},\mathbf{y}} \Big(\sum_{\substack{\mathbf{z} \\ O_1 \in (\mathbf{xyz}) \\ O_2 \notin (\mathbf{xyz})}} + \sum_{\substack{\mathbf{z} \\ O_1 \notin (\mathbf{xyz}) \\ O_2 \in (\mathbf{xyz})}} \Big) P_{\mathbf{x},\mathbf{z}} P_{\mathbf{z},\mathbf{y}} \overset{\text{def}}{=} (V_1)_{\mathbf{x},\mathbf{y}} + (V_2)_{\mathbf{x},\mathbf{y}}.
\tag{3.73}
$$

Here V_i ($i = 1, 2$) is the "vertex" term for two junctions respectively. As in Sec. 3.4.2, V_i ($i = 1, 2$) satisfies EDP for vertex i and $S - \overline{S}$ is trace class, so $\text{Tr}^v(S)$ is well-defined.

As $\text{dist}(1, 2) \to \infty$, we have $V_1 V_2 = V_2 V_1 \to 0$. In the limiting case where $V_1 V_2 = V_2 V_1 = 0$ exactly, one can simultaneously diagonalize them and at least one eigenvalue for a common eigenstate should be 0. This means each "vertex state" of S (those states with $S \neq 0, 1$) is located at junction 1 or 2. Moreover, define Q_1 as the matrix corresponding to a 1/2-flux insertion at point 1 with partition $A + B + CD$, Q_2 corresponding to the insertion at point
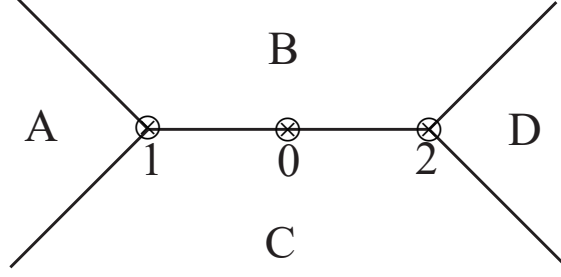
Figure 9: Divide the plane into 4 regions $A + B + C + D$. Insert a $\frac{1}{2}$-flux for each vertex (1 and 2). We will show that it is "equal" to insert a unit flux at the middle (point 0).

2 with partition $AB + C + D$, then the effect of S for a state near junction i will be close to the effect of Q_i, so one anticipates that

$$\mathrm{Tr}^v(S) \approx \mathrm{Tr}^v(Q_1) + \mathrm{Tr}^v(Q_2). \tag{3.74}$$

In the case where $\mathrm{dist}(1, 2)$ is large but not infinity, some vertex states of S may come from the coupling of two vertex states at different fluxes. However, it is not difficult to convince that Eq.(3.74) still holds. The physics here is similar to that for the two-states systems: due to the weak but nonzero coupling (off diagonal elements), the eigenstates will be approximately

$$|\phi\pm\rangle = \frac{1}{\sqrt{2}}(|1\rangle \pm |2\rangle). \tag{3.75}$$

Here, we cannot say a vertex states of R is located at one of the fluxes. However, the summation of eigenvalues for $|\phi\pm\rangle$ is still equal to that for $|1\rangle$ and $|2\rangle$.

Proposition 3.7 (Additivity). Under technical assumptions, as the distance between two fluxes goes to infinity, the vertex spectrum of S "decouples":

$$\lim_{\mathrm{dist}(1,2)\to\infty} \mathrm{Tr}^v(S) - (\mathrm{Tr}^v(Q_1) + \mathrm{Tr}^v(Q_2)) = 0. \tag{3.76}$$

The proof is in appendix C.1.1.

Proposition 3.8. $\mathrm{Tr}^v(S) = 0 \mod 2$. This is an exact equation, no matter whether $\mathrm{dist}(1, 2)$ is large or not.

56

The idea is, if one looks from a large distance, inserting two $\frac{1}{2}$-fluxes is approximately equivalent to insert a 1-flux, which is (singularly) gauge equivalent to 0-flux, so that no vertex states appear in the spectrum at all.

Proof. We works in the AB gauge, where the vector potential of a flux satisfies

$$|\mathbf{A}(\mathbf{r})| = \frac{\text{flux}}{2\pi r}, \quad \mathbf{A}(\mathbf{r}) \perp \mathbf{r}. \tag{3.77}$$

We still use S to denote the Hamiltonian in this gauge. Denote T to be the Hamiltonian for the case of inserting 1-flux at the center of two half-fluxes. S and T should be close outside the center. We will prove that $S - T$ is trace class in the Appendix C.1.3. Then, similar to the proof of property 3.6,

$$\text{Tr}(S - T) = \lim_{N \to \infty} \text{Tr}(S_N - T_N) = 0, \tag{3.78}$$

since they have the same diagonal elements. $\overline{S} - T = (\overline{S} - S) + (S - T)$ is also trace class, so

$$\text{Tr}(\overline{S} - T) = \text{Ind}(\overline{S}, T) = \dim \text{Ker}(\overline{S} - T - 1) - \dim \text{Ker}(\overline{S} - T + 1) = 0 \ (\text{mod } 2), \tag{3.79}$$

due to time reversal symmetry. Therefore,

$$\text{Tr}^v(S) = \text{Tr}(S - \overline{S}) = \text{Tr}(S - T) - \text{Tr}(\overline{S} - T) = 0 \ (\text{mod } 2). \tag{3.80}$$

$\square$

Proposition 3.9. $\text{Tr}^v(Q)$ is an integer (mod 2) independent of the position of the flux.

Proof. For every pair of points 1 and 2, we have

$$\text{Tr}^v(Q_1) - \text{Tr}^v(Q_2) = [\text{Tr}^v(Q_1) + \text{Tr}^v(Q_3)] - [\text{Tr}^v(Q_2) + \text{Tr}^v(Q_3)]. \tag{3.81}$$

Due to Properties 3.7 and 3.8, it can be arbitrarily close to 0 (mod 2) as $\text{dist}(1,3)$ and $\text{dist}(2,3)$ goes to infinity. So we must have

$$\text{Tr}^v(Q_1) = \text{Tr}^v(Q_2) \ (\text{mod } 2). \tag{3.82}$$

Plug this into Eq.(3.76) and use again property 3.8, we obtain that $\text{Tr}^v(Q_1) = \text{Tr}^v(Q_2) \in \mathbb{Z}_2$. $\square$

This property already shows that $\mathrm{Tr}^v(Q)$ is an $\mathbb{Z}_2$ invariant for topological insulators which only depends on the state itself. The only natural identification is the Kane-Mele invariant.

Proposition 3.10. $\mathrm{Tr}^v(Q)$ is equal to the Kane-Mele invariant.

Proof. Denote our invariant as ν. For two gapped time-reversal-symmetric systems A and B, we stack them (without hopping/interaction) and denote the new system $A \oplus B$. Obviously $\nu(A \oplus B) = \nu(A) + \nu(B)$. From the classification of topological insulator [17, 18, 19, 21] for AII class, the Kane-Mele invariant ν_{KM} is the only invariant with this property. It follows that

$$\nu = k\nu_{\mathrm{KM}}, \tag{3.83}$$

where $k = 0$ or $k = 1$.

To prove $k = 1$, it is enough to verify the existence of one system with $\nu = 1$. To this end, consider a translational invariant system in the DIII class with nontrivial $\mathbb{Z}_2$ invariant. In this case, according to Eq. (3.55), we have

$$\nu = \mathrm{No.}\ \{\mathrm{Kramers\ pairs\ at}\ \frac{1}{2}\} = 1\ (\mathrm{mod}\ 2). \tag{3.84}$$

The last equation can be obtained by considering the band structure, due to translational invariance: A Kramers pair at $1/2$ correspond to the a band crossing. $\qquad\square$

3.5   Summary

In this chapter, we have argued the necessity of real-space topological invariants for systems with boundaries or disorders. Starting with the filled-band projection, one can calculate the real-space invariants either based on some index theorems or almost commuting matrices.

For topological insulators, we proposed a formula Eq. (3.50) for the $\mathbb{Z}_2$ Kane-Mele invariant in 2D, which remains valid with disorder. The intuition behind our formula is flux-insertion-induced spectral flow, which manifests itself as the difference of numbers of

electrons in the ground states. The formula works by taking the single-body projection matrix P (or ground state correlation function) as the input, performing a Peierls substitution (either geometrical or topological), and then take the "trace over vertex states". Our formula is a local expression, in the sense that the contribution mainly comes from quantities near an arbitrarily but fixed point. The validity of this formula is proved rigorously, by showing its properties (gauge invariance, addictivity, integrality, etc).

Due to the local property of our formula, it can be well approximated with partial knowledge of the projection matrix. In this case, we construct "vertex matrix" and "boundary matrix" which almost commute. Using an interesting parabola, the vertex contributions are separated out. The validity of this algorithm is proved and verified numerically.

Similar ideas may be used in the case of other symmetries and other dimensions. It would be interesting to work out other cases to see if one can get (and prove) a new formula. Moreover, the flux-insertion idea also works in some interacting cases, for example, Ref. [83]. It would be interesting to explore such generalizations of our $\mathbb{Z}_2$ formula.

4.0 Homotopical Classification of Non-Hermitian Band Structures

While we are used to assuming the Hermiticity of Hamiltonians, as required by the axioms of quantum mechanics, there has been growing interest in non-Hermitian Hamiltonians these years. Indeed, in the Hermitian quantum mechanics framework, non-Hermitian Hamiltonian can emerge as an effective description of open system with gain and loss [41, 84, 85, 86, 87, 88, 89, 90, 91, 92, 93, 94, 95, 96, 97, 98, 99, 100, 101, 102, 103] or systems with finite-lifetime quasiparticles/non-Hermitian self energy [104, 105, 106], which can be experimental realized in atomic or optical systems [107, 108, 109, 110, 111, 112, 113]. Moreover, non-Hermitian Hamiltonians with certain properties can serve as an extension of conventional Hermitian quantum mechanics [42, 43, 44].

Inspired by the great success in topological phases for Hermitian systems, there has been lots of works focusing on the topological aspects of non-Hermitian systems [45, 46, 114, 47, 48, 49, 115]. On the one hand, many familiar constructions for topological phases can be extended in the case of non-Hermiticity. For example, people have constructed the non-hermitian counterparts for Su-Schrieffer-Heeger model [87, 116, 102, 117, 118, 119], Chern insulators [120, 121, 122, 123, 124], and quantum spin hall effects [125]. On the other hand, non-Hermitian systems also exhibit many unusual phenomena with no counterpart in the Hermitian world. These include exceptional points [126, 127, 128], anomalous bulk-edge correspondence [129, 102, 130, 131, 132], non-Hermitian skin effect [133, 120] and sensitivity to boundary conditions [129, 134]. For a recent review, see Ref. [135] and references therein.

There have been some works [45, 46, 114, 47, 48] on the general classification of non-Hermitian systems, aiming at a generalization of the Hermitian periodicity table. In these works, the authors first determined reasonable symmetry classes in the non-Hermitian setting (a generalization of Ref. [17]), then use a unitarization/Hermitianization map to reduce the problem into the Hermitian setting where one can apply K-theory.

In this chapter, we discuss a more conceptually straightforward homotopical [136, 62, 59, 78, 63, 137, 138] framework towards the topological classification of non-Hermitian band structures, which enables us to see more topological invariants beyond K-theoretical ap-

proaches. With rigorous algebraic-topological calculation, we implemented our idea in detail for systems with no symmetry.

We will also consider the stability issue of these new invariants, in the sense that whether adding other bands will trivialize these invariants (even if the band has no crossing with previous bands). Similar to the $\mathbb{Z}$ invariants of Hopf insulators [59], our torsion invariants are unstable. We will give a combinatorial proof for the instability in general.

4.1 Classification Results

4.1.1 Principle of Classification

As discussed in Sec. 2.3.1, one needs to specify the set and the equivalence relation before talking about classification.

For Hermitian systems, there is no subtlety regarding the meaning of the gap, since all eigenvalues of a Hermitian Hamiltonian are real and the meaning of a gap on the real line is clear. For non-Hermitian systems (interacting or not), however, the eigenvalues can be complex. Therefore, the meaning of a "gap" need to be further clarified [123, 46, 139].

Consider a non-interacting non-Hermitian system with translational invariance. Standard second quantization and band theory give rise to momentum-dependent one-body Hamiltonians $H(k)$. In this paper, we will call $\{H(k)\}$ ($k \in$ BZ, the Brillouin zone) a band structure, which contains information of both their spectrum $E_i(k)$ and associated eigenstates $|\psi_i(k)\rangle$.

One has at least the following different notions of the gap:

- **line gap** [46, 140]. There exists a (maybe curved) line l in the complex energy plane which separates the plane into two disconnected pieces. We require $E_i(k) \notin l$ for all i and k, and both connected component have some spectral points in them.

- **point gap** [45, 46, 114, 48]. $E_i(k) \neq 0$ for all i and k. Here, 0 is a reference point which can be altered to any E_0.

- **separable band** [123, 121]. A specific band $E_i(k)$ is called separable if $E_j(k) \neq E_i(k)$ for all $j \neq i$ and k.

- **isolated band** [123]. A specific band $E_i(k)$ is called isolated if $E_j(k') \neq E_i(k)$ for all $j \neq i$ and k, k'.

Note that these notions are not mutually exclusive. For example, an isolated band is always separable; systems with isolated bands always have line gaps and hence always have point gaps. Also note that, the first two notions are applicable to general non-Hermitian systems, while the last two notions are specific to translational-invariant non-interacting cases by definition.

In our paper, we will consider the classification of separable band structures, since other cases were solved [45, 46, 114, 47, 48] by mapping back to the Hermitian case. However, there is one more problem with the definition of separability that needs to be discussed: the above mentioned $E_i(k)$ may not be a well-defined function of k.

For example, consider a one-dimensional systems with two bands, satisfying $E_1(k) \neq E_2(k)$ for all k. It is possible that $E_1(2\pi) = E_2(0)$: if one follow the spectrum when k goes around the Brillouin zone (a circle in this case) starting from $E_1(0)$, one may go to $E_2(0)$ instead of going back to $E_1(0)$, see Fig. 10. In this case, the notation "$E_i(k)$" (and therefore its separability) for a specific i may not be well-defined. Instead, it is better to define separability in a global manner: for any k, $E_i(k)$ ($i = 1, \cdots, n$) are all different. This definition of separability automatically rules out exceptional points, i.e., $H(k)$ is not diagonalizable under similarity transformations, since it requires (algebraically) degenerated spectra.

To summarize, we will consider the following problem: classify the band structure $\{H(k)\}$ where spectrum of $H(k)$ are non-degenerated and $\{H_0(k)\}$ and $\{H_1(k)\}$ are equivalent if and only if they can be continuously connected by $\{H_t(k)\}$ for $t \in [0, 1]$ and the spectra of $H_t(k)$ for any t and k are always non-degenerated. Let us consider the general problem of classifying band structures with n bands on a m-dimensional lattice. Denote

$$X_n = \text{the space of } H(k). \tag{4.1}$$
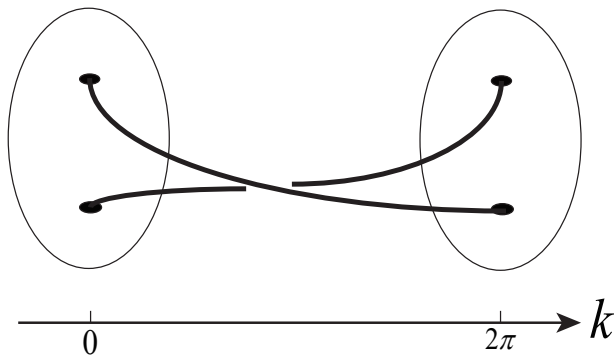
Figure 10: $\mathbb{Z}_2$ braiding of energy levels. In this figure, the disk is the complex energy plane, with two spectra points in it; k is the Bloch momentum, $k = 0$ and $k = 2\pi$ should be identified.

Namely, it is the space of $n \times n$ matrices with non-degenerated spectra. Here the Brillouin zone will be the m-dimensional torus T^m. Mathematically speaking, we want to find the homotopy equivalent classes of non-based maps from the Brillouin zone T^m to X_n, denoted by $[T^m, X_n]$.

It will be important to distinguish T^m and S^m since they will give different answers. It is also important to distinguish based maps and non-based maps: the former requires a chosen point in T^m to be mapped to a chosen point in X_n while the latter has no such requirement[1].

To calculate the classification, we are going to use some standard methods in algebraic topology. For an introduction, see Ref. [8].

4.1.2 The Space X_n and Its Homotopy Groups

An element H of X_n is an $n \times n$ matrix with non-degenerated spectrum, which can be represented as $(\lambda_1, \cdots, \lambda_n, \alpha_1, \cdots, \alpha_n)$. Here, $(\lambda_1, \cdots, \lambda_n)$ are ordered eigenvalues satisfying $\lambda_i \neq \lambda_j$, i.e.,

$$(\lambda_1, \cdots, \lambda_n) \in \mathrm{Conf}_n(\mathbb{C}), \tag{4.2}$$

---

[1]On the other hand, for continuous systems the appropriate choice the based map from S^m to X_n since the Brillouin zone here is S^n with the requirement that infinite momentum maps to some fixed point [18].

63

where $\text{Conf}_n(\mathbb{C})$ is the configuration space of *ordered* n-tuples in $\mathbb{C}$. $(\alpha_1, \cdots, \alpha_n)$ are corresponding eigenvectors (up to complex scalar multiplications), which are linearly indenpendent. Denote the space of linearly indenpendent ordered n-vectors (up to scalar) in $\mathbb{C}^n$ as F_n. We have

$$F_n \cong GL(n)/\mathbb{C}^{*n}, \tag{4.3}$$

since $GL(n)$ acts transitively on F_n and the stabilizer group is $\mathbb{C}^{*n}$, where $\mathbb{C}^* = \mathbb{C} - \{0\}$, the group of nonzero complex numbers. Another way to understand this equation is to consider the columns of a $GL(n)$ matrix, which are ordered n-vectors in $\mathbb{C}^n$, while "up to scalar" is taken care of by n independent scalar multiplications $\mathbb{C}^{*n}$. The space F_n is actually homotopic to the full flag manifold of $\mathbb{C}^n$.

This representation has some redundancies: one can permute (λ_i, α_i) and get the same matrix H. Therefore,

$$X_n \cong (\text{Conf}_n \times F_n)/S_n, \tag{4.4}$$

where S_n is the permutation group acting on $\text{Conf}_n \times F_n$ as simultaneous permutations of (λ_i, α_i).

Consider $\pi_1(\text{Conf}_n)$, whose elements are (equivalence classes of) paths in Conf_n, which correspond to some pure braidings of n mutually different points in $\mathbb{C}$. Here, "pure" means each point goes back to itself after the braiding. This is true since we are considering ordered n-tuples. Therefore,

$$\pi_1(\text{Conf}_n) = \text{PB}_n, \tag{4.5}$$

where PB_n is the pure braiding group of n points [141, 142].

It turns out [143] that $\text{Conf}_n = K(PB_n, 1)$, the classifying space of the group PB_n. Therefore,

$$\pi_m(\text{Conf}_n) = 0, \quad m \geq 2. \tag{4.6}$$

The homotopy groups $\pi_m(F_n)$ can be obtained by the long exact sequence of homotopy groups [8], based on the fibration Eq. (4.3). For $m = 1$, we have:

$$\pi_1(\mathbb{C}^{*n}) \to \pi_1(GL(n)) \to \pi_1(F_n) \to \pi_0(\mathbb{C}^{*n}) = 0. \tag{4.7}$$

64

Here, $\pi_1(\mathbb{C}^{*n}) = \mathbb{Z}^n$, $\pi_1(GL(n)) = \mathbb{Z}$, which is essentially the determinant. The map $\pi_1(\mathbb{C}^{*n}) \to \pi_1(GL(n))$ is exactly summing over n components in $\mathbb{Z}^n$, which is surjective. Therefore $\pi_1(F_n) = 0$. For $m = 2$, we have:

$$0 = \pi_2(GL(n)) \to \pi_2(F_n) \xrightarrow{\partial} \pi_1(\mathbb{C}^{*n}) \to \pi_1(GL(n)). \tag{4.8}$$

Therefore, $\pi_2(F_n)$, as the kernel, is represented by n integers with summation equals 0:

$$\{(t_1, \cdots, t_n) \in \mathbb{Z}^n | \sum t_i = 0\}, \tag{4.9}$$

which is isomorphic to $\mathbb{Z}^{n-1}$. This representation with n integers will be useful later. For $m \geq 3$, we have

$$0 = \pi_m(\mathbb{C}^{*n}) \to \pi_m(GL(n)) \to \pi_m(F_n) \to \pi_{m-1}(\mathbb{C}^{*n}) = 0, \tag{4.10}$$

therefore $\pi_m(F_n) = \pi_m(GL(n)) = \pi_m(U(n))$.

To summarize, the result is as follows:

$$\pi_m(F_n) = \begin{cases} 0, & m = 1 \\ \mathbb{Z}^{n-1}, & m = 2 \\ \pi_m(U(n)), & m \geq 3 \end{cases} \tag{4.11}$$

Now consider the space X_n. According to Eq. (4.4) and the fact that S_n is discrete, higher homotopy groups $\pi_{m \geq 2}(X_n)$ are the same as those of $\mathrm{Conf}_n \times F_n$, therefore the same as Eq. (4.11), due to the fact in Eq. (4.6).

For the fundamental group π_1, one can take advantage of the fact that $\pi_1(F_n) = 0$ and show that:

$$\pi_1(X_n) = \pi_1(\mathrm{Conf}_n / S_n) = B_n. \tag{4.12}$$

Here S_n acts on Conf_n by permutations, giving the configuration space Conf_n / S_n of *non-ordered* n-tuples in $\mathbb{C}$, whose fundamental group is B_n, the braiding group including "non-pure" braidings.

This is because a loop in X_n corresponds to a path $p(t) = (p_1(t), p_2(t))$ in $\mathrm{Conf}_n \times F_n$ such that $p_1(1) = gp_1(0)$ and $p_2(1) = gp_2(0)$ for the same $g \in S_n$. Note that g is uniquely determined by $p_1(1)$ (the initial point $(p_1(0), p_2(0))$ is a fixed lifting) and F_n is simply connected,

the path one-to-one (homotopically) corresponds to a path in Conf_n with $p_1(1) = gp_1(0)$ and therefore a loop in Conf_n / S_n. A more algebraic proof is to note that the actions of S_n on $\mathrm{Conf}_n \times F_n$ and Conf_n are consistent, which gives the following pullback:

$$
\begin{array}{ccc}
\mathrm{Conf}_n \times F_n & \longrightarrow & \mathrm{Conf}_n \\
\downarrow & & \downarrow \\
X_n & \longrightarrow & \mathrm{Conf}_n / S_n
\end{array}
\qquad (4.13)
$$

and then apply the homotopy exact sequence for this pullback square.

The appearance of braiding group B_n is easy to understand. Consider a one-dimensional band structure and follow the evolution of spectrum $\{E_i\}$ along the Brillouin zone circle. Similar to $n = 2$ case in Sec. 4.1.1 as shown in Fig. 10, in general points in $\{E_i\}$ will braid with each other during this evolution and may become other points after one cycle. The evolution of n disjoint points is topologically classified by the braiding group B_n.

4.1.3 The Set $[T^m, X_n]$

The equivalent classes $[T^m, X_n]$ is related but may not equal to the homotopy groups π_m, which is, by definition, $\langle S^m, X_n \rangle$. Here, $\langle -, - \rangle$ is used for based maps, while $[-, -]$ is used for non-based maps. In general, $[T, X]$ is just a set with no extra structures, even if T is a sphere, in which case $\langle T, X \rangle$ is exactly a homotopy group. The relation between $[T, X]$ and $\langle T, X \rangle$ for general spaces T and X is as follows [8]: There is a right action of $\pi_1(X)$ on $\langle T, X \rangle$, and $[T, X] \cong \langle T, X \rangle / \pi_1(X)$, the orbit set of the action.

We will first calculate $\langle T^m, X_n \rangle$ and then use the above connection to obtain $[T^m, X_n]$.

In the case $m = 1$, $\pi_1(X_n)$ acts on $\langle T^1, X_n \rangle = \pi_1(X_n)$ by conjugate:

$$
[f][\gamma] = [\gamma^{-1} \circ f \circ \gamma],
\qquad (4.14)
$$

therefore $[T^1, X_n]$ is the set of conjugacy classes of group B_n. Determine the conjugacy classes of braiding group B_n is a difficult problem[2] except $n \leq 2$.

---

[2] For a review of the conjugacy problem in braiding group, see Ref. [144]. It relies on the "Garside structure" [145].

In the case $m = 2$, the set $\langle T^2, X \rangle$ is given by [146] (see also Appendix C.2.1):

$$\{(a, b) \in \pi_1(X)^2 | ab = ba\} \times \pi_2(X)/\langle t - t^a, t - t^b \mid t \in \pi_2 \rangle, \tag{4.15}$$

where t^a is the result of $a \in \pi_1(X)$ acting on $t \in \pi_2(X)$. Note that this is a noncanonical identification. In our problem, the result is:

$$\bigcup_{\substack{a,b \in B_n \\ ab=ba}} \mathbb{Z}^{n-1}/\langle t - t^a, t - t^b \rangle \overset{\text{def}}{=} \bigcup_{\substack{a,b \in B_n \\ ab=ba}} Q(n, a, b). \tag{4.16}$$

In other words, the classification of based maps is decomposed into several sectors, denoted by a pair of commuting braidings[3] $a, b \in B_n$; classification within each sector (a, b) is given by the quotient $Q(n, a, b)$, a finite-generated abelian group, by identifying t with t^a and t^b.

Physically, the braidings a, b is given by following two nontrivial circles l_a, l_b in the Brillouin zone T^2. Since $l_a l_b l_a^{-1} l_b^{-1}$ is the boundary of the 2-cell of T^2, the corresponding braiding $aba^{-1}b^{-1}$ must be trivial, hence $ab = ba$. Fixing a, b, the map on the 2-cell is determined by $\pi_2(X_n) = \pi_2(F_n) = \mathbb{Z}^{n-1}$, which are enssentially $(n-1)$ Chern numbers, up to some ambiguities taken care of by the quotient.

The action $t \mapsto t^a$ here is determined as follows. Recall Eq. (4.9) that $\pi_2(X_n) = \mathbb{Z}^{n-1}$ can be represented by $\{(t_1, \cdots, t_n) \in \mathbb{Z}^n | \sum t_i = 0\}$. $a \in B_n$ induced a permutation $\tilde{a} \in S_n$ by forgetting the braiding. Then t^a is represented by a permutation of $(t_1, \cdots, t_n)$:

$$(t_1, \cdots, t_n) \mapsto (t_{a(1)}, \cdots, t_{a(n)}). \tag{4.17}$$

The proof of this statement is a bit technical. However, since it is the root of most novel classifications in this paper, we give a detailed proof in Appendix C.2.2.

Now consider the action of $\pi_1(X_n) = B_n$ on $\langle T^2, X_n \rangle$. Pick $c \in B_n$, then c act on (a, b) by conjugate:

$$(a, b) \to (c^{-1}ac, c^{-1}bc). \tag{4.18}$$

The action of c on $\bar{t} \in Q(n, a, b)$ is induced by the action of $\pi_1(X_n)$ on $\pi_2(X_n)$: under c, t goes to t^c, t^a goes to t^{ac}, therefore $t - t^a$ goes to $t^c - (t^c)^{c^{-1}ac}$, therefore the action of c on $\bar{t} \in Q(n, a, b)$ is well-defined as $\bar{t}^c = \overline{t^c} \in Q(n, c^{-1}ac, c^{-1}bc)$. Note that $Q(n, a, b) \cong$

---

[3]For a review of the centralizer problem in the braiding group, see Ref. [147]. The result heavily depends on the geometry of braiding, namely, the Nielsen-Thurston classification [148].

$Q(n, c^{-1}ac, c^{-1}bc)$, due to fact that Eq. (4.16) and Eq. (4.17) only care about the permutation structure of a, b, which is invariant under conjugation. We finally get:

$$[T^2, X_n] = \bigcup_{\substack{\overline{(a,b)} \\ ab=ba}} \overline{Q}(n, a, b), \tag{4.19}$$

where $\overline{(a,b)}$ means a conjugacy class of commuting pairs under Eq. (4.18), and $\overline{Q}(n, a, b) = Q(n, a, b)/\pi_1^s(X_n)$ is the orbit set (not quotient group) of $Q(n, a, b)$ under the stablizer subgroup $\pi_1^s(X_n)$ that keeps (a, b) invariant.

The reason for the appearance of this $\pi_1^s(X_n)$ action can be traced back to the difference between $[T, X]$ and $\langle T, X \rangle$. Physically, there is no natural way to label the bands (even if no braiding happens, namely, $a = b = \mathrm{id}$). In the Hermitian case, bands are naturally ordered according to their energy, which is not the case for complex energy levels. Therefore there are some redundancies corresponds to change the label of bands (see Sec. 4.2.2 for an example). Also note that, while $Q(n, a, b)$ is a finite generated abelian group, $\overline{Q}(n, a, b)$ is just a set.

4.2   Examples

4.2.1   Non-Hermitian Bands in One Dimension

In the case of $m = 1$, we know from Sec. 4.1.3 that band structures are classified by the conjugacy classes of group B_n.

Determine the conjugacy classes of braiding group B_n is only easy when the number of bands $n = 2$, where the braiding group B_2 is just $\mathbb{Z}$: $a \in \mathbb{Z}$ is the number of elementary braidings (half of a 2π rotation), with a even implies a pure braid and a odd implies a permutation. In this case, each conjugacy class only has one element, since $\mathbb{Z}$ is abelian. Therefore, the classification is given by:

$$[T^1, X_2] = \mathbb{Z}. \tag{4.20}$$

Same classification was found in Ref. [102, 123, 119]. Note that some authors use $\frac{1}{2}\mathbb{Z}$ instead of $\mathbb{Z}$: their spectral "vorticity" is exactly one half of the above invariant.

4.2.2 Two-Band Chern "Insulators"

Consider the case with $m = n = 2$, namely, band structures with two bands in two dimensional (2D) space. This corresponds to Chern insulators in the Hermitian case. However, it may not be a true insulator in the non-Hermitian case if there is no line gap (to place the chemical potential).

Let us calculate $Q(2, a, b)$ and $\overline{Q}(2, a, b)$, where $a, b \in B_2 = \mathbb{Z}$. There are four cases, depending on the even/odd of a and b.

- a, b even. Then $t^a = t^b = t$, therefore $Q(2, a, b) = \mathbb{Z}$. The action of $c \in \pi_1(X_n)$ on $Q(2, a, b)$ might be nontrivial: it acts as opposite if c is odd (see below), therefore $\overline{Q}(2, a, b) = \mathbb{N}$, the set of nonnegative integers.

- a even, b odd. Then $t^a = t$ while $t^b = -t$ in the sense that $(s, -s)^b = (-s, s)$. Therefore $Q(2, a, b) = \langle (s, -s) \rangle / \langle (2s, -2s) \rangle \cong \mathbb{Z}_2$. The action of $\pi_1(X_n)$ at most takes $(s, -s)$ to $(-s, s)$, which has no effects on $\mathbb{Z}_2$, therefore $\overline{Q}(2, a, b) = \mathbb{Z}_2$.

- a odd, b even. Same as above.

- a, b odd. Then $t^a = t^b = -t$, $Q(2, a, b) = \overline{Q}(2, a, b) = \mathbb{Z}_2$.

Therefore, band structures are classified by:

$$\bigcup_{a,b \in \mathbb{Z}} \mathbb{N} \text{ or } \mathbb{Z}_2. \tag{4.21}$$

The $\mathbb{N}$ classification (instead of $\mathbb{Z}$) comes from the fact that we have no natural way to identify "upper band" and "lower band" as in the Hermitian case, since there $\mathbb{C}$ is not naturally ordered as $\mathbb{R}$. This new feature of non-Hermitian classification will disappear if, for example, we have a *fixed* line gap, where the classification will go back to $\mathbb{Z}$.

The $\mathbb{Z}_2$ classification in some sectors is a more interesting phenomenon. It comes from the interplay between spectrum braiding and eigenvector topology (Chern band). Here, we provide a formula as well as heuristic arguments for this invariant.

We will concentrate on the case where (a, b) is (even, odd). The (odd, even) case is similar; the (odd, odd) case can be handled by a Dehn twist. Also note that the $\mathbb{Z}_2$ invariant essentially comes from the (odd, even) sector of $[T^2, F_2/S_2]$ (F_2/S_2 is the space of distinct pairs of states), as one can see by following the same calculations as above.

We claim the following formula for this invariant:

$$C = \frac{1}{2\pi} \int_{\text{BZ}} \epsilon_{ij} B_{ij}(k) d^2k + S_{WZW}(a, a'). \tag{4.22}$$

In the first term, the Berry curvature $B_{ij}(k)$ [123] is defined by following one band, therefore has discontinuity at boundary; the integral is over the conventional $2\pi \times 2\pi$ Brillouin zone. The second term $S_{WZW}(a, a')$ is a boundary Wess-Zumino-Witten (WZW) term[4], defined as follows. By following one band, one gets a map from a cylinder to the Bloch sphere S^2, such that for any point on the left boundary a, the corresponding point on the right boundary a' maps to different point on S^2 (since they corresponds to linear independent vectors), see Fig. 11. We then close two boundaries in a *consistent* way [62] such that the above condition is still satisfied on two "caps". This is always possible since $[\tilde{a}] = 0$ in $\pi_1(F_2/S_2)$ due to the assumption that a is even, where $\tilde{a}$ denotes the map from the nontrivial loop (boundary) to the space of pairs F_2/S_2. Then $S_{WZW}(a, a')$ is then defined as

$$\frac{1}{4\pi} \times \text{oriented area of caps on } S^2. \tag{4.23}$$

By adding the caps, we obtain a closed manifold, therefore Eq. (4.22) is an integer. As always, there are some ambiguities in the definition of S_{WZW}, corresponding to the ambiguities in adding the caps. Importantly, the consistency requirement for the caps implies that Eq. (4.22) can only be shifted by 2 (instead of 1) by the ambiguities[5]. To see this, note that we have a deformation retraction from F_2/S_2 to RP^2, as defined in Fig.11(b). After this deformation retraction, the consistency condition simply requires that corresponding points in two boundaries map to antipodal points. Therefore, two caps should always be antipodal to each other, and

$$S_{WZW}(a, a') = 2S_{WZW}(a). \tag{4.24}$$

Therefore, C is only defined mod 2 and we obtain a $\mathbb{Z}_2$ invariant.

---

[4]The boundary term is also known as a Berry phase term [149].
[5]Heuristically, one cannot just flip one cap while leaving the other unflipped in Fig.11(a), otherwise the Brouwer's fixed point theorem guarantees an inconsistent point.
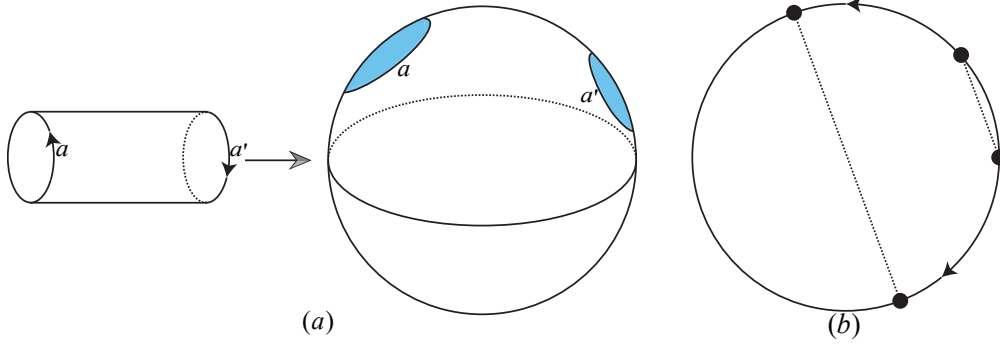
Figure 11: (a) Following one band, we get a map from the cylinder to S^2. To define the WZW term, one needs to close the cylinder with two caps in a consistent way (not necessarily antipodal in the non-Hermitian case). Here the arrow represents orientation, not to be confused with the way one identifies two boundaries. (b) A deformation retraction from F_2/S_2 to RP^2. Each point in F_2/S_2 corresponds to a pair of different points in S^2. We draw the great circle corresponds two that pair, and then gradually push the pair to an antipodal pair (corresponds to a point in RP^2). If a pair is already antipodal, nothing needs to be done. In this way, we have defined a deformation retraction.

Another way to understand the $\mathbb{Z}_2$ invariant is as follows. Using the above deformation retraction, we see that this $\mathbb{Z}_2$ can also be understood from $[T^2, RP_2]$. For the (odd, even) sector, we have the following diagram:

$$
\begin{array}{ccc}
2T^2 & \longrightarrow & S^2 \\
\downarrow & & \downarrow \\
T^2 & \longrightarrow & RP^2
\end{array}
\tag{4.25}
$$

therefore the classification amounts to classifying covariant maps from $2T^2$ to S^2. Here, $2T^2$ is a double cover of Brillouin zone T^2, by gluing two cylinders along b-direction, see Fig. 12; "covariant" means corresponding points in the left and right cylinder should map to antipodal points.

Now, we can add a "bump" of Berry curvature with positive 1 integral and a "bump" with negative 1 integral by deforming the eigenstates, both in the "upper band". It is

71
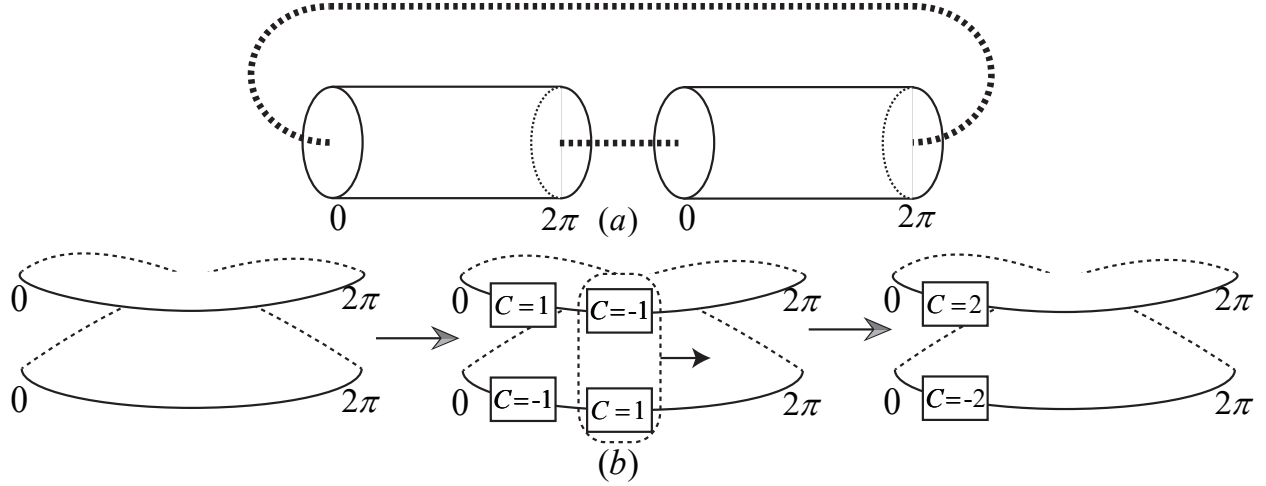
Figure 12: Physical origin of the $\mathbb{Z}_2$ invariant. (a) Due to energy level braiding, the Brillouin zone is better considered as a torus with size $4\pi \times 2\pi$ on which the energy $E(k)$ and wavefunction $\psi(k)$ is well-defined: if one follows one band on the conventional Brillouin zone of size $2\pi \times 2\pi$, then after 2π one goes to the other band. The dashed lines indicate this "gluing". (b) Each solid line represents a cylinder similar to those in figure (a), the dashed lines again indicate the "gluing". Starting with trivial bands, one adds ± 1 "bumps" to the upper band, and ∓ 1 "bumps" to the lower band, then move the right pair (circled by the dashed line) to the right. After 2π, they will switch, resulting in a $C = 2$ "bump" in the upper band and $C = -2$ "bump" in the lower band.

necessary to add opposite bumps due to the covariant constraint. We can then move a pair of bumps along b-direction for 2π. After this procedure, we effectively add a $C = 2$ bump to the "upper band" and a $C = -2$ bump to the "lower band". Therefore, C is again only well-defined mod 2.

4.2.3 Multiband Chern "Insulators"

The conjugacy classes and commuting pairs are hard to describe if $n > 2$. However, the quotient $Q(n, a, b)$ for given braiding sector (a, b) are not hard to calculate.

Recall from Eq. (4.17) that $\pi_2(X_n) = \mathbb{Z}^{n-1} = \{(t_1, \cdots, t_n) | \sum t_i = 0\}$ and $(t_1, \cdots, t_n)^a = (t_{a(1)}, \cdots, t_{a(n)})$ where $a(i)$ is the image of i under the permutation a. Therefore, the subgroup to be quotient out is (we only write down the t^a part):

$$\langle t - t^a \rangle = \langle (t_1 - t_{a(1)}, \cdots, t_n - t_{a(n)}) | \sum t_i = 0 \rangle. \tag{4.26}$$

There are only $(n-1)$ independent t_i: we can use $t_n = -\sum_{i=1}^{n-1} t_i$ to get rid of the constraint. Then the subgroup Eq. (4.26) is generated by $2(n-1)$ (not necessarily independent) generators. For example, take $t_1 = 1, t_2 = \cdots = t_{n-1} = 0, t_n = -1$ and consider the action of a, we get a generator $e_1 - e_{a^{-1}(1)} - e_n + e_{a^{-1}(n)}$, where $e_1 = (1, 0, \cdots, 0, -1), e_2 = (0, 1, 0, \cdots, 0, -1), e_{n-1} = (0, \cdots, 0, 1, -1), e_n = (0, \cdots, 0)$. Therefore, the $Q(n, a, b)$ is the quotient of $\langle e_1, \cdots, e_{n-1} \rangle$ with $2(n-1)$ relations $e_i - e_{a^{-1}(i)} - e_n + e_{a^{-1}(n)} (i = 1, \ldots, n-1)$. Its structure can be determined by standard procedure using Smith normal form.

As a simple example, consider the case where $a : 1 \to 2 \to 3 \to 4 \to 1$, $b : 1 \to 4 \to 3 \to 2 \to 1$. This is possible, say, by taking a to be a braiding with such permutation structure, then taking $b = a^{-1}$. The auxiliary "generators" given by $t_i = 1, t_1 = \cdots = t_{i-1} = t_{i+1} = \cdots = t_n = 0$ writen in terms of n-tuples is the ith columns of the following matrix

$$\begin{bmatrix} 1 & -1 & & \\ & 1 & -1 & \\ & & 1 & -1 \\ -1 & & & 1 \end{bmatrix}. \tag{4.27}$$

Since the true generators are given by taking $t_i = 1, t_n = -1, t_j = 0 (j = 1, \cdots, i-1, i+1, \cdots, n-1)$, we need to subtract the last column from all other columns and delete the last row. The matrix of true generators for $\langle t - t^a \rangle$ is:

$$\begin{bmatrix} 1 & -1 & \\ & 1 & -1 \\ 1 & 1 & 2 \end{bmatrix}, \tag{4.28}$$

and similarly for b:

$$\begin{bmatrix} 2 & 1 & 1 \\ -1 & 1 & \\ & -1 & 1 \end{bmatrix}. \tag{4.29}$$

Juxtapose those two matrices and calculate its Smith normal form, we get:

$$\begin{bmatrix} 1 & 0 & 0 & 0 & 0 & 0 \\ 0 & 1 & 0 & 0 & 0 & 0 \\ 0 & 0 & 4 & 0 & 0 & 0 \end{bmatrix}, \tag{4.30}$$

which means $Q(4, a, b) = \mathbb{Z}_4$.

Another example is when $b = \text{id}$, i.e., no permutation. We can decompose a into cycles: $a = (...)(...)...(...)$. Denote the length of each cycle to be $l_1, \cdots, l_k$ ($\sum_{i=1}^{k} l_i = n$) where k is the number of cycles. In this case, we can follow the above procedure and get an explicit formula for $Q(n, a, b)$.

Denote an $l \times l$ matrix of form Eq. (4.27) to be J_l, then the counterpart of Eq. (4.27) (where columns are auxiliary "generators") is:

$$\begin{bmatrix} J_{l_1} & & & \\ & J_{l_2} & & \\ & & \ddots & \\ & & & J_{l_k} \end{bmatrix}, \tag{4.31}$$

and the counterpart of Eq. (4.28) by subtraction and deleting is:

$$\left[\begin{array}{cc|c|cc|c} J_{l_1} & & & & & \\ \hline & J_{l_2} & & & & \\ \hline & & \ddots & & & \\ \hline & & & & & \bar{J}_{l_k} \\ 1 & 1 & 1 & 1 & 1 & 1 \end{array} \right], \tag{4.32}$$

where $\bar{J}_{l_k}$ is an $(l_k - 1) \times (l_k - 1)$ matrix of form Eq. (4.28). To clarify, the last row of the above big matrix is $(1, 1, \ldots, 1, 2)$. It is easy to perform row transformation on the above matrix and get:

$$
\begin{bmatrix}
K_{l_1} & & & & \\
 & K_{l_2} & & & \\
 & & \ddots & & \\
 & & & & \overline{K}_{l_k} \\
0 & l_1 & 0 & l_2 & \cdots \; \cdots
\end{bmatrix},
\tag{4.33}
$$

where $K_l = \mathrm{diag}\{1, \cdots, 1, 0\}$ (size l), $\overline{K}_l = \mathrm{diag}\{1, \cdots, 1, l\}$ (size $l - 1$). To clarify, the last row of the above big matrix is $(0, \cdots, 0, l_1, 0, \cdots, 0, l_2, \cdots, 0, \cdots, 0, l_k)$. Therefore, the structure of $Q(n, a, b)$ is:

$$
Q(n, a, b) = \mathbb{Z}^{k-1} \oplus \mathbb{Z}_{\mathrm{gcd}\,(l_1, \ldots, l_k)},
\tag{4.34}
$$

where $\mathbb{Z}_{\mathrm{gcd}\,(l_1, \ldots, l_k)}$ is the greatest common divisor and $\mathbb{Z}_1$ means trivial group $\{0\}$ if $\mathrm{gcd} = 1$.

The $\mathbb{Z}^{k-1}$ comes from the fact that we have k groups of bands (bands that transfer to each other under braidings are in the same group). Each band has an integer Chern number, with summation equals 0. This is the same as the Hermitian case. However, there is an extra $\mathbb{Z}_{\mathrm{gcd}}$. We also see that the extra torsion part is determined by *all band groups* as a whole, not from any specific band group. It shows some complicated interplay between energy braiding and eigenstates topology.

With other permutations $a, b(a, b \neq \mathrm{id})$, it is possible to get more than one torsions. An example is $a : 1 \leftrightarrow 2, 3 \leftrightarrow 4$ with $b : 1 \leftrightarrow 3, 2 \leftrightarrow 4$. The algorithm will give us $\mathbb{Z}_2 \oplus \mathbb{Z}_2$.

4.3   Instability

Examples in Sec. 4.2 show that our homotopical approach reveals more topological invariants than the traditional K-theory approach. For example, a 2-band Chern "insulator"

in 2D may reveal some Z_2 classification due to nontrivial topology of the spectrum.

Similar phenomena also happen in the Hermitian world. For example, in three dimensions (3D), insulators in class A are always trivial according to the periodicity table. However, one can still have a $\mathbb{Z}$ classification if the number of bands is fixed to be 2, due to the fact that $\pi_3(\mathbb{C}P^1) = \mathbb{Z}$. This is called the Hopf insulator [59], which is *unstable* against adding more bands. Indeed, as long as one adds one more band above and below the Fermi surface respectively, the classification will be trivial due to $\pi_3(Gr_{\mathbb{C}}(3,1)) = 0$ (and similarly for more bands), where $Gr_{\mathbb{C}}(3,1)$ is the complex Grassmannian.

A natural question arises: is our new topological invariants stable against adding bands?

As an example, let us consider 2-band systems in 2D as in Sec. 4.2.2, and add one more band. Since the classification is decomposed into braiding sectors and each sector has its own classification set, it only makes sense to add a band with no permutation to previous bands (therefore it does not alter the braiding sectors). For each sector (a, b), adding a band without permutation is to add a length-1 cycle after previous a, b.

- a, b even. Then a' and b' are trivial permutations, therefore $Q(3, a, b) = \mathbb{Z}^2$, which are just two Chern numbers.

- a even, b odd. Then a' trivial while b' decomposes as $(12)(3)$. Eq. (4.34) shows that $Q(3, a', b') = \mathbb{Z}$.

- a odd, b even. Same as above.

- a, b odd. Then both a' and b' has the form $(12)(3)$. A Smith normal form calculation shows $Q(3, a', b') = \mathbb{Z}$.

In all cases, we see that the extra band contributes a Chern number $\mathbb{Z}$, as well as kills the old $\mathbb{Z}_2$ invariant it there is any, even if the $\mathbb{Z}_2$ comes from other bands that never intersect with the added band. This is possible since the $\mathbb{Z}_2$ not just comes from those two bands, but from all three bands as a whole, as noted at the end of Sec. 4.2.3.

The instability of $\mathbb{Z}_2$ can be understood as follows. Assuming a odd and b even, consider the procedure shown in Fig. 13: we start with three bands with Chern number $1, -1, 0$ respectively, where the first two bands switch to each other after 2π as in Fig. 12(a). Adding a negative bump and a positive bump in band 1, as well as a positive bump and a negative
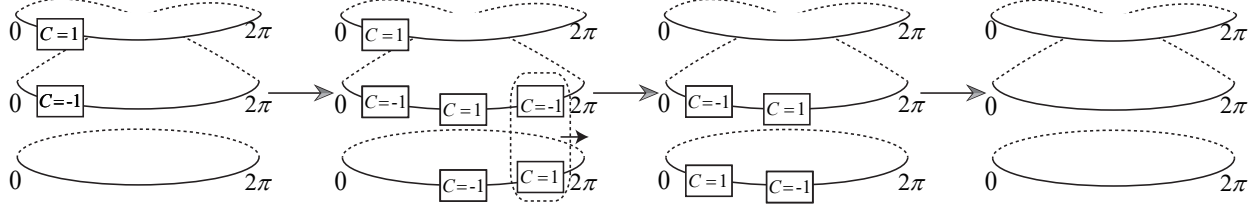
Figure 13: Physical origin of instability. Similar to Fig. 12, solid lines represent the Brillouin; dashed lines indicate the "gluing". We start with three bands with Chern number $1, -1, 0$ respectively, where the first two bands switch to each other after 2π. If we forget band 3, it will be nontrivial, indicated by a $\mathbb{Z}_2$ invariant. However, add band 3 and follow the procedure shown in the figure, we can make the band structure totally trivial.

bump in band 3; then move the rightmost bump pair in band 1 and 3, so that the positive bump cancels the negative bump in band 2; the remaining bumps in band 1 and 3 can be easily canceled, leaving three trivial bands. During the procedure, the local neutral condition is always satisfied. Note that it is essential to have the 3rd band for this to work.

Similarly, as long as $b = \mathrm{id}$, Eq. (4.34) shows that $Q(n+1, a', b')$ has no torsion part.

We can prove a general result regarding the instability, even if $b \neq \mathrm{id}$. For a system with n bands, consider the braiding sector labeled by the commuting pair (a, b). Let us add an extra no-permutation band, denote $a, b \to a', b'$. The matrix of auxiliary "generators" is:

$$\left[\begin{array}{cc|c} & & 0 \\ A & B & \\ & & 0 \\ \hline 0 \ \ 0 & 0 \ \ 0 & 0 \end{array} \right], \tag{4.35}$$

where A and B are of form Eq. (4.31) up to some congruent transformation by permutation matrices. The matrix of generators (counterpart of Eq. (4.28)) is therefore just

$$[A \mid B]. \tag{4.36}$$

We claim that the invariant factors in its Smith normal form must be 1. Indeed, we claim a more general statement:

77

Claim. Assuming a matrix has the following property: there are either 2 or 0 nonzero elements in each column; in the former case, there is exactly one 1 and one -1. Then the invariant factors of this matrix must be 1 (if there is any).

Proof. We prove by induction on the total number of nonzero elements N. From the assumption, N must be even. If $N = 0$, then the statement is trivially true.

Now assume the state is true for N and less, let us consider $N + 2$. Denote the matrix to be A. Without lose of generality, assume $A_{1,1} = 1$, $A_{2,1} = -1$, $A_{i,1} = 0$ for $i \geq 3$. Add row 1 to row 2, denote the new matrix as A', then $A'_{i,1} = 0$ for $i \geq 2$. Moreover, from the assumption on matrix A, there are only 7 possibilities happened to $\begin{bmatrix} A_{1,2} \\ A_{2,2} \end{bmatrix}$ (we only write 4 of them, the other 3 are obtained by adding negative sign):

$$\begin{bmatrix} 0 \\ 0 \end{bmatrix} \rightarrow \begin{bmatrix} 0 \\ 0 \end{bmatrix}, \begin{bmatrix} 1 \\ -1 \end{bmatrix} \rightarrow \begin{bmatrix} 1 \\ 0 \end{bmatrix}, \begin{bmatrix} 1 \\ 0 \end{bmatrix} \rightarrow \begin{bmatrix} 1 \\ 1 \end{bmatrix}, \begin{bmatrix} 0 \\ 1 \end{bmatrix} \rightarrow \begin{bmatrix} 0 \\ 1 \end{bmatrix}. \tag{4.37}$$

Therefore, the column $(A'_{2,2}, \cdots, A'_{n,2})^T$ satisfies the same assumption as columns of A. The number of nonzero elements in this shorter column is less or equal to that in $(A_{1,2}, \cdots, A_{n,2})^T$. Other columns are similar.

Then we use column transformations to make $A'_{1,i} = 0$ for $i \geq 2$, while keeping other elements. A' is of the form:

$$A' = \begin{bmatrix} 1 & 0 & 0 \\ \hline 0 & & \\ & A'' & \\ 0 & & \end{bmatrix}. \tag{4.38}$$

We can then apply the induction assumption on A'' and finish the proof. $\square$

Therefore, $Q(n + 1, a', b')$ is always of the form $\mathbb{Z}^k$. This means all torsion invariants $\mathbb{Z}_i (i \geq 2)$ are unstable against adding a no-permutation band.

4.4 Summary

For non-Hermitian free fermionic systems, we considered the homotopical classification of band structures from first principles. We found that, the whole classification set is decomposed into several sectors, based on the braiding of energy levels. Fix a braiding pattern, we considered the classification coming from nontrivial eigenstates topology. Due to the fact that different bands will transfer to each other under braidings, the classification of band topology is not just a direct summation of Chern numbers. Instead, the interplay between energy level braiding and eigenstates topology gives some new torsion invariants.

The torsion invariants come from all bands as a whole, instead of a specific band or a proper subset of bands: even if we add a band with no crossing with previous bands, the torsion invariants can in principle be changed. We found that those torsion invariants are unstable, in the sense that just adding one trivial band will trivialize them. This statement is proved based on an interesting combinatorial argument.

There are definitely many works that can be done in this framework. First of all, due to the complexity of the braiding group, it is complicated to describe its conjugacy classes and commuting pairs, let alone the conjugacy classes of commuting pairs. It will be useful to develop more explicit descriptions of the braiding sectors. On the other hand, in this thesis we only consider the case with no symmetry as an illustration. It is interesting to consider other symmetry classes using our framework.

5.0   Conclusions and Outlooks

Topological phases are important extensions of the Landau-Ginzburg paradigm regarding phases of matter. Free fermion systems provide interesting examples for topological phases, which are of both theoretical beauty and experimental relevance.

While the complete classification of topological phases is unknown, we have shown that it is possible to establish a formal theory for translationally invariant gapped free fermion systems, starting from first principles of quantum mechanics. The resulting theory, based on topological band theory, shows deep connections with some beautiful mathematics such as topological K theory and Bott periodicity.

In this thesis, we have discussed some extensions of topological band theory. We argued that, to capture systems with boundaries and/or disorders, it is necessary to define and calculate topological invariants in real space. We showed that it is indeed possible, and the resulting formula will be some nice local expressions in the sense that one can get a good approximation with only local information. We have also discussed the non-Hermitian extension of traditional topological band theory. The main novelty of non-Hermitian band theory lies in the fact that eigenvalues themself can possess interesting topological properties (braiding). Moreover, the eigenvalue topology has some interesting interplay between the conventional eigenvector topology, resulting in new or altered topological invariants.

While the basic properties of free fermion systems are relatively well understood, there is much work to be done.

First of all, this thesis only addresses free fermion systems. The classification of general interacting systems is still far from complete. For gapped systems, although a lot of progress has been made [4, 150, 151, 28, 152, 58, 153], the classification of two-dimensional systems is essentially still a conjecture in the sense that people cannot derive the result from first principles yet. Classification of three-dimensional systems and systems in higher dimensions is more incomplete. For example, the newly discovered fracton phases [154] tell us that our imagination based on conventional notions like quasiparticles is limited and sometimes even misleading. We believe it is safe to claim that nature will keep surprising us with more and

more exotic topological phases of matter.

Secondly, understanding the basic classification is far from understanding everything, just like understanding set theory is far from understanding mathematics. Even within the realm of noninteracting systems, there are lots of interesting problems. We have discussed the extensions to real space and non-Hermitian Hamiltonians. Some other extensions include Floquet topological phases [155, 156], higher-order topological phases [157] and extensions with other symmetries [158].

On the realistic side, it is always important to study the topological physics of real materials and experimentally realize the theoretical models and verify the theoretical predictions. It is also very interesting and useful to explore their potential utilities in, for example, quantum computations [151].

Appendix A Clifford Algebra, Symmetric Space, and K Theory

In this appendix, we briefly review Clifford algebra, symmetric space, K theory, and relations among them. See Ref. [56, 159, 160] for details and more information.

A.1 Clifford Algebra

Definition A.1 (Clifford algebra). The Clifford algebra $Cl(V, Q)$ associated with a vector space V and a quadratic form Q is the universal algebra such that $v \cdot v = Q(v)$ for $\forall x \in V$. In perticular, the real Clifford algebra $Cl_{p,q}$ is generated by $e_1, \cdots, e_p, \cdots, e_{p+q}$ over $\mathbb{R}$ subject to the relations:

$$(e_i)^2 = -1 \ (i \le p), \quad (e_i)^2 = -1 \ (p+1 \le i \le p+q), \quad \{e_i, e_j\} = 0 \ (i \ne j). \tag{A.1}$$

The complex Clifford algebra $\mathbb{C}l_n$ is generated by $e_1, \cdots, e_n$ such that:

$$(e_i)^2 = -1, \quad \{e_i, e_j\} = 0 \ (i \ne j). \tag{A.2}$$

The structure of real Clifford algebras can be obtained by the following theorem:

Theorem A.1. $Cl_{p+1,q+1} \cong Cl_{p,q} \otimes_{\mathbb{R}} Cl_{1,1}$ (isomorphic as algebra). $Cl_{1,1} \cong \mathbb{R}(2)$, the matrix algebra $M_2(\mathbb{R})$ over $\mathbb{R}$. Moreover,

$$Cl_{p+8,q} \cong Cl_{p,q+8} \cong Cl_{p,q} \otimes_{\mathbb{R}} \mathbb{R}(16). \tag{A.3}$$

According to this theorem, the structure of $Cl_{p,q}$ only depends on $p - q$ up to tensor product with matrix algebra, and have a mod 8 periodicity up to tensor product with matrix algebra.

Below we list 8 simplest Clifford algebras. The structure for higher p, q can be obtained by the above theorem.

$Cl_{0,3}$	$Cl_{0,2}$	$Cl_{0,1}$	$Cl_{0,0}$	$Cl_{1,0}$	$Cl_{2,0}$	$Cl_{3,0}$	$Cl_{4,0}$
$\mathbb{C}(2)$	$\mathbb{R}(2)$	$\mathbb{R} \oplus \mathbb{R}$	$\mathbb{R}$	$\mathbb{C}$	$\mathbb{H}$	$\mathbb{H} \oplus \mathbb{H}$	$\mathbb{H}(2)$

The structure of complex Clifford algebras can be obtained by complexifying the above results. We will get a mod 2 periodicity:

$$\mathbb{C}l_{n+2} \cong \mathbb{C}l_n \otimes_\mathbb{C} \mathbb{C}(2), \tag{A.4}$$

and $\mathbb{C}l_0 \cong \mathbb{C}$, $\mathbb{C}l_1 \cong \mathbb{C} \oplus \mathbb{C}$.

The periodicities here are simple algebraic facts. Yet they have deep connections with the profound Bott periodicity.

A.2   Symmetric Space

This section is a very brief review of symmetric spaces, from Lie theory point of view. The results here will not be used in an essential way in this thesis. The main purpose of this section is to explain the terminology.

In the following symmetric space means Riemannian Symmetric space: a Riemannian manifold M such that for $\forall p \in M$, there is an isometry σ of M which flips all geodesics through p.

For a Lie group G with an involution θ, assuming the fixed point group $K = \{g | \theta(g) = g\}$ is compact, then G/K will be a symmetric space since θ actually induces an isometry (after choosing a K, θ-invariant metric on G) of G/K and flips the geodesics through the "origin". Conversely, given a Riemannian symmetric space M, consider the isometry group G and an isotropy subgroup K, one can prove $M \cong G/K$. Moreover, K is indeed (with some cautions) the fixed point group of the following involution on G:

$$\sigma : g \mapsto s_p g s_p, \tag{A.5}$$

where s_p is the geodesic-flipping isometry at p. Therefore, the study of symmetric spaces reduces to the study of Lie groups.

Denote $\mathfrak{g}$ the Lie algebra of G. The $\theta = 1$ subspace $\mathfrak{k}$ is the Lie algebra of K, and we denote the $\theta = -1$ subspace as $\mathfrak{p}$. We have $\mathfrak{g} = \mathfrak{k} \oplus \mathfrak{p}$. Consider another Lie algebra:

$$\mathfrak{g}_c = \mathfrak{k} \oplus i\mathfrak{p}, \tag{A.6}$$

it will have the same complexification as $\mathfrak{g}$, denoted by $\mathfrak{g}_{\mathbb{C}}$. The involution θ can be extended on $\mathfrak{g}_c$ linearly:

$$K + iP \mapsto K - iP. \tag{A.7}$$

We assume the constructions above extends to Lie groups G, G_c, $G_{\mathbb{C}}$, $\theta : G_c \to G_c$, and also assume that G is noncompact while G_c is compact[1]. It is clear that θ on G_c has the fixed point group K. Therefore, this construction gives us a pair of symmetric spaces $X = G/K$ and $X_c = G_c/K$, which are said to be in duality to each other.

It turns out that under these assumptions, the fixed point group K will be a maximal compact subgroup of G, so the possibilities are really limited. In the following, we list the classification results.

On a coarse level, symmetric spaces are classified into four types:

- **Type-2**. If K is a compact Lie group, it is automatically a symmetric space.
- **Type-4**. If G is itself the complexification of a compact Lie group K and θ is the "complex conjugation", then G/K will be a noncompact symmetric space.
- **Type-1**. Compact symmetric spaces that is not of type-2.
- **Type-3**. Compact symmetric spaces that is not of type-4.

Type-2 and type-4 symmetric spaces are dual to each other: here $G_c = K \times K$ hence $X_c = G_c/K = K$. Therefore, the classification of type-2 and type-4 symmetric spaces reduces to the classification of compact Lie groups, which then reduces to the classification of simple complex Lie algebras and discrete subgroups. They are of type A, B, C, D, E_6, E_7, E_8, F_4 and G.

---

[1]Therefore $\mathfrak{g} = \mathfrak{k} \oplus \mathfrak{p}$ is a Cartan decomposition.

The classification of type-1 and type-3 symmetric spaces is first done by Cartan. In Tab. 6, we list symmetric spaces with corresponding G, G_c, K. The Cartan label starts with letter $A/B/C/D$ as the Lie algebra type of $\mathfrak{g}$ (or equivalently $\mathfrak{g}_c$ and $\mathfrak{g}_\mathbb{C}$) and then follows with Roman numerals which further classifies symmetric spaces within each Lie algebra class.

Cartan label	G	G_c	K
AI	$SL(n, \mathbb{R})$	$SU(n)$	$SO(n)$
AII	$SL(n, \mathbb{H})$	$SU(2n)$	$Sp(2n)$
AIII	$SU(p, q)$	$SU(p+q)$	$S(U(p) \times U(q))$
BI	$SO(p, q)$, $p + q$ odd	$SO(p+q)$	$S(O(p) \times O(q))$
DI	$SO(p, q)$, $p + q$ even	$SO(p+q)$	$S(O(p) \times O(q))$
DIII	$SO^*(2n)^2$	$SO(2n)$	$U(n)$
CI	$Sp(2n, \mathbb{R})$	$Sp(2n)$	$U(n)$
CII	$Sp(2p, 2q)$	$Sp(2p + 2q)$	$Sp(2p) \times Sp(2q)$

Table 6: Cartan's classification of classical type-1 and type-3 symmetric spaces. See Ref. [159] for a more complete form including exceptional cases.

Some final remarks are in order:

- The above table omits symmetric space from exceptional groups. Indeed, there are symmetric spaces of class EI-EIX, FI, FII, and G.

- Cartan's original classification also includes AIV, BII, and DII, which come from AIII, BI, and DI by restricting $q = 1$ (so we do not see DII between DI and DIII in many literatures).

- In some cases we need to take the $p, q \to \infty$ limit. Then BI and DI go to the same limit, denoted by BDI.

---

[2] The subgroup of $SO(2n, \mathbb{C})$ that fixes the form $\sum_{i=1}^{n} \text{Im}(x_i \overline{x_{n+1}})$.

A.3 From Clifford Algebra to Symmetric Space

In this section, we explain the following relation between Clifford algebras and symmetric spaces: the space of gradations of some $Cl_{p,q}$-modules is a symmetric space.

For a $Cl_{p,q}$-module M, an extension from the $Cl_{p,q}$ action to a $Cl_{p,q+1}$ action is called a gradation on E. Equivalently, we need a endomorphism η of M acts as the extra e_{p+q+1}:

$$\eta^2 = 1 \text{ and } \eta e_i + e_i \eta = 0, \quad \text{for } \forall i \leq p + q. \tag{A.8}$$

The terminology "gradation" comes from the fact that $\eta = \pm 1$ subspaces make M into a $\mathbb{Z}_2$-graded module. We denote the space of gradations on a $Cl_{p,q}$-module M as $\mathrm{Grad}^{p,q}(M)$

$p - q \bmod 8$	$\mathrm{Grad}^{p,q}$	Cartan label
0	$\mathbb{Z} \times O/O \times O$	BDI
1	U/O	AI
2	Sp/U	CI
3	Sp	C
4	$\mathbb{Z} \times Sp/Sp \times Sp$	CII
5	U/Sp	AII
6	O/U	DIII
7	O	D

Table 7: Symmetric spaces as gradations of modules of real Clifford algebras. Here we only present the limiting case.

By considering a transive group G action and the isotropy subgroup G_1, one can express $\mathrm{Grad}^{p,q}(M)$ as G/G_1 and check that they are symmetric spaces. In Tab. 7 we list the result for $\mathrm{Grad}^{p,q}$, defined as $\varinjlim \mathrm{Grad}(M_r)$ for any cofinal systems $\{M_r\}$ for finitely generated $Cl_{p,q}$-modules.

A quick way to remember Tab. 7 is to consider the following chain (most embeddings are obvious and $O \subset O \times O$ is the diagonal map):

$$O(16r) \supset U(8r) \supset Sp(4r) \supset Sp(2r) \times Sp(2r) \supset Sp(2r)$$
$$\supset U(2r) \supset O(2r) \supset O(r) \times O(r) \supset O(r) \supset \cdots \tag{A.9}$$

and then the symmetric spaces are successive quotients. This chain also illustrates the definition of the notations in the table. For example:

$$O/O \times O \overset{\text{def}}{=} \varinjlim_r O(2r)/O(r) \times O(r), \tag{A.10}$$

and it is also denoted by BO since it is the classifying space of real vector bundles (structure group O).

n mod 8	Grad^n	Cartan label
0	$\mathbb{Z} \times U/U \times U$	AIII
1	U	A

Table 8: Symmetric spaces as gradations of modules of complex Clifford algebras. Here we only present the limiting case.

For complex Clifford algebras, the story is similar, see Tab. 8. The corresponding group chain is:

$$U(2r) \supset U(r) \times U(r) \supset U(r) \supset \cdots \tag{A.11}$$

A.4 K Theory

Definition A.2 (Grothendieck group)**.** The Grothendieck group[3] of an abelian monoid M is the universal abelian group K such that there exists a monoid homomorphism $M \to K$. Explicitly, K can be defined as the group of formal subtractions $x - y$ where $x, y \in M$ such that:

$$x - y \sim x' - y' \iff \exists z : x + y' + z = x' + y + z. \tag{A.12}$$

---

[3]This is exactly how we obtain $\mathbb{Z}$ from $\mathbb{N}$.

Now consider all (complex or real) vector bundles over a fixed space X. Their equivalence classes form an abelian monoid by the Witney sum (fiber-wise direct sum). We take its Grothendieck group and denote it as $K(X)$ (for complex bundles) or $KO(X)$ (for real bundles). Elements in the K group is the stable equivalent class of vector bundles on X. In the following definitions, we only consider K theory. The extensions to KO theory will be obvious.

We also define $\tilde{K}(X) = \ker[K(X) \to K(pt) \cong \mathbb{Z}]$, where the homomorphism is induced by the injection $pt \to X$. It simply counts the dimension. So $\tilde{K}$ contains stable equivalent class of (virtual) vector bundles with dimension 0.

Definition A.3 (higher K and relative K). Suppose Y is a closed subspace of X, $n \in \mathbb{N}$, then define

$$
\begin{aligned}
\tilde{K}^{-n}(X) &= \tilde{K}(\Sigma^n(X)), \\
K^{-n}(X, Y) &= \tilde{K}^{-n}(X/Y), \\
K^{-n}(X) &= K^{-n}(X, \emptyset),
\end{aligned}
\tag{A.13}
$$

where Σ is the suspension.

The definition of K^{-n} is designed such that K^{-*} is a generalized cohomology theory. For example, one can prove the following exact sequence (as in any cohomology theory):

$$
\cdots \to K^{-n-1}(X) \to K^{-n-1}(Y) \to K^{-n}(X, Y) \to K^{-n}(X) \to K^{-n}(Y) \to \cdots \tag{A.14}
$$

A.5   From Clifford Algebra to K Theory

In this section, we review how Clifford algebras are connected to the K theory. Therefore the periodicity of Clifford algebras is ultimately connected to the Bott periodicity.

A.5.1 ABS Construction

To start, consider $K(D^n, S^{n-1}) \cong K^{-n}(pt)$. For any graded $Cl_{n,0}$ module $W = W^0 \oplus W^1$, we can define an element:

$$[E_0, E_0, \alpha] \in K(D^n, S^{n-1}), \tag{A.15}$$

where $E_i = D^n \times W^i$ is a trivial Clifford bundle, α is an isomorphism of E_0 and E_1 over S^{n-1}, defined by:

$$\alpha(x, w) = (x, x \cdot w), \tag{A.16}$$

where in $x \cdot w$ we regard $x \in S^{n-1}$ as an element in $Cl_{n,0}$ and act it on w (this is why we need a $Cl_{n,0}$-module). If W happens to be a graded $Cl_{n+1,0}$-module and regard it as a $Cl_{n,0}$-module by restriction of scalar (since there is a natural injection $Cl_{n,0} \to Cl_{n+1,0}$), then one can check that the K group element obtained in this way is 0.

Theorem A.2 (Atiyah-Bott-Shapiro isomorphism [161])**.** Define $\hat{M}_n$ to be the Grothendieck group of graded $Cl_{n,0}$-modules, $i^* : \hat{M}_{n+1} \to \hat{M}_n$ is the restriction of scalar map, then:

$$K^{-n}(pt) \cong \hat{M}_n / i^* \hat{M}_{n+1}. \tag{A.17}$$

Using this isomorphism and the structure of Clifford algebras, one can work out $K^*(pt)$ as follows:

$$K^{-n}(pt) \cong \begin{cases} \mathbb{Z}, & n \text{ even} \\ 0, & n \text{ odd} \end{cases}, \tag{A.18}$$

and

$$KO^{-n}(pt) \cong \mathbb{Z}, \mathbb{Z}_2, \mathbb{Z}_2, 0, \mathbb{Z}, 0, 0, 0, \quad \text{for } n = 0, 1, 2, 3, 4, 5, 6, 7 \pmod{8} \tag{A.19}$$

A.5.2 Karoubi's K Theory and Bott Periodicity

There is a more general connection between Clifford algebra and K theory, which will be useful in the classification of topological insulators.

Definition A.4. Denote $\mathcal{C}^{p,q}$ be the category of $Cl_{p,q}$ modules in category $\mathcal{C}$ (namely, each object of $\mathcal{C}^{p,q}$ is a object of $\mathcal{C}$ with a $Cl_{p,q}$ action). Define $K^{p,q}(\mathcal{C})$ to be[4] the abelian group generated by triples (E, η_1, η_2) where η_i are gradations on E, with the natural addition and the following identification:

$$(E, \eta_1, \eta_2) = 0 \text{ iff } \eta_1 \text{ is homotopic to } \eta_2 \text{ within gradations of } E.$$

According to the above definition, $K^{p,q}(\mathcal{C})$ is a Grothendieck group of "homotopy class of $Cl_{p,q}$-module $\to Cl_{p,q+1}$-module extensions", or "homotopy class of gradations on (ungraded) $Cl_{p,q}$-modules".

Since $Cl_{p+1,q+1} \cong Cl_{p,q} \otimes_{\mathbb{R}} \mathbb{R}(2)$, $Cl_{p+1,q+1}$ and $Cl_{p,q}$ has essentially the same representation theory[5]. Therefore, $K^{p,q}(\mathcal{C})$ only depends on $p - q$. Moreover, due to the periodicity Eq. (A.3), it only depends on $p - q$ mod 8. Similarly, substitute $Cl_{p,q}$ with $\mathbb{C}l_n$, we can define $K_{\mathbb{C}}^n(\mathcal{C})$ and it only depends on n mod 2.

The relation between Clifford algebras and K theory is given by the following:

Theorem A.3 (Karoubi). If $\mathcal{C} = \mathcal{E}(X)$, the category of vector bundles over X, then $K^{p,q}(\mathcal{C})$ is canonically isomorphic to $KO^{p-q}(X)$ if $p \leq q$. Similar result holds for relative K groups.

According to this theorem, we can also define $K^n(X)$ for $n > 0$. Moreover, we have understood the following celebrated:

Theorem A.4 (Bott Periodicity). $KO^n(X, Y)$ is periodic with respect to n with period 8. $K^n(X, Y)$ is periodic with respect to n with period 2.

---

[4]Equivalently, consider the functor $\phi : \mathcal{C}^{p,q+1} \to \mathcal{C}^{p,q}$, defined by "restriction of scalars": regard a $Cl_{p,q+1}$-module as a $Cl_{p,q}$-module. Define $K^{p,q}(\mathcal{C})$ to be the Grothendieck group of the functor ϕ. We will not need this definition.

[5]This is an example of the Morita equivalence. It is a generalization of the fact that matrix algebra has a unique simple module.

It is sometimes useful to consider a $Cl_{p,q}$-module as a $Cl_{p,q}$. To solve this problem, one just need to use the isomorphism:

$$Cl_{p,q} \otimes Cl_{0,2} \cong Cl_{q,p+2}, \tag{A.20}$$

and the problem will be equivalent to $Cl_{q,p+2} \to Cl_{q,p+3}$.

A.6 From K Theory to Symmetric Space

Karoubi's construction makes the connection between K theory and symmetric spaces explicit.

Let us consider an element in $K^{p,q}(X)$, represented as $[E, \eta, \eta']$, where E is a $Cl_{p,q}$-bundle, η and η' are gradations. It turns out one can make E trivial ($E \cong M$) by direction addition with some other Clifford bundle. Without loss of generality, one can also fix η for each E by assuming M has a given $Cl_{p,q+1}$-module structure. Therefore, the equivalent class of $[E, \eta, \eta']$ is determined by (the stable homotopy class of) η', which in turn should be determined pointwisely. Rigorously, we have the following[6]:

Theorem A.5. $K^{p,q}(X) \cong \varinjlim[X, \mathrm{Grad}^{p,q}(M)] \cong [X, \mathrm{Grad}^{p,q}]$.

As an example, let us consider $p = q = 0$. In this case, we have $\mathrm{Grad}^{0,0} \cong \mathbb{Z} \times BO$, therefore:

$$KO(X) \cong [X, \mathbb{Z} \times BO]. \tag{A.21}$$

One can check this relation is indeed correct using classfication of vector bundles. We know

$$\mathrm{Vect}(X) \cong [X, BO], \tag{A.22}$$

where $\mathrm{Vect}(X)$ is the set of stable equivalence classes of vector bundles over X. Dimensions are omitted in the above equation since trivial bundles of all dimensions are all represented by 0. Add the dimension back, we obtain Eq. (A.21).

The above representation theorem for K is a special case of the representability theorem for any generalized cohomology theory.

---

[6]In category theory, this means the functor K is representable. The spaces $\mathrm{Grad}^{p,q}$ are called classifying spaces.

Definition A.5 (Ω-spectrum). An Ω-spectrum is a sequence of spaces $K_1, K_2, \cdots$ together with weak homotopy equivalences $K_n \to \Omega K_{n+1}$. Here Ω means loop space.

Theorem A.6 (Brown's representability). The functor $X \to [X, K_n]$ is a generalized cohomology theory iff $\{K_n\}$ is an Ω-spectrum.

For the case of K theory, one can indeed directly check (this can be done in Morse theory) that $\mathrm{Grad}^{p,q}$ as listed in Tab. 7 are Ω-spectra:

$$\Omega(\mathrm{Grad}^{p,q}) \simeq \mathrm{Grad}^{p,q+1}. \tag{A.23}$$

A.6.1 Bott Periodicity for K Spectra and Homotopy Groups

In terms of the K theory spectra, the Bott periodicity can be expressed as periodicities in the spectra:

$$\Sigma^8 O \simeq O, \Sigma^2 U \simeq U. \tag{A.24}$$

A coralary is the periodicity of homotopy groups for O, U and Sp:

$$\pi_k(O) = \pi_{k+4}(Sp) = \pi_{k+8}(O), \quad \pi_k(U) = \pi_{k+2}(U) \tag{A.25}$$

with

k mod 8	0	1	2	3	4	5	6	7
$\pi_k(O)$	$\mathbb{Z}_2$	$\mathbb{Z}_2$	0	$\mathbb{Z}$	0	0	0	$\mathbb{Z}$
$\pi_k(U)$	0	$\mathbb{Z}$	0	$\mathbb{Z}$	0	$\mathbb{Z}$	0	$\mathbb{Z}$
$\pi_k(Sp)$	0	0	0	$\mathbb{Z}$	$\mathbb{Z}_2$	$\mathbb{Z}_2$	0	$\mathbb{Z}$

The homotopy groups are the same (with shifting) as K groups for pt in Eq. (A.18) and Eq. (A.19). This is because

$$KO^{-n}(pt) = \widetilde{KO}(S^n) = [S^n, \mathbb{Z} \times BO]_* = \pi_n(BO) = \pi_{n-1}(\Omega BO) = \pi_{n-1}(O), \tag{A.26}$$

and similarly for complex K. Moreover, the isomorphism between $\tilde{K}(S^n)$ and $\pi_{n-1}(O)$ has a simple geometric explaination: a G-bundle over S^n can be obtained by gluing two trivial bundles along the equator S^{n-1} and is classified by the homotopy class of gluing functions, which is simply $\pi_{n-1}(G)$.

A.7 KR and KQ

For classifications in higher dimensions or with more symmetries, one will need further "twist" the K theory. If some symmetries have nontrivial actions on the base manifold (the Brillouin zone), for example, crystalline symmetry or time-reversal symmetry in some cases, the symmetry will generally connect fibers on different points.

In this section, we briefly discuss the KR and KQ theory. One may also need other equivariant theories K_G for other symmetries.

Definition A.6. A Real space[7] X is a space with an involution c_X. A Real bundle over X is a complex bundle E with an anti-linear involution c_E that is compatible with c_X:

$$
\begin{array}{ccc}
E & \xrightarrow{\ c_E\ } & E \\
\downarrow{\scriptstyle\pi} & & \downarrow{\scriptstyle\pi} \\
X & \xrightarrow{\ c_X\ } & X
\end{array}
\tag{A.27}
$$

A morphism between two Real bundles over the same Real space (X, c_X) is a morphism over the underlying vector bundles (thus preserve base points) that is compatible with c_E. The set of all Real bundles over a Real space (X, c_X) is a monoid, and its Grothendieck group is called the KR group[8] of X, denoted by $KR(X)$.

For example, if c_X is trivial, then c_E acts fiberwise and determines a real structure for each fiber. So one is essentially classifying real bundles, therefore $KR(X) \cong KO(pt)$.

In the above definition, if one demands c_E to be anti-linear anti-involution instead, one will get KQ theory, with Q for quaternion, since c_E determines a quaternionic structure for fibers with fixed points of c_X. It is clearly the most suitable formalism for topological insulators.

One can also defines higher KR by suspensions. This time one needs spheres with Real space structure. Define $S^{p,q}$ (and similarly $B^{p,q}$) to be the sphere (and the ball) in $\mathbb{R}^{p+q}$, this time with involution $(x, y) \to (-x, y)$. Then define:

$$
KR^{r,s}(X, Y) = KR(X \times B^{r,s}, X \times S^{r,s} \cup Y \times B^{r,s}).
\tag{A.28}
$$

---

[7]Real$\neq$real!

[8]$KR \neq K_{\mathbb{R}}$, the latter usually means KO.

It is still a generalized cohomology theory. Note that suspension with spheres with -1, denoted by $\bar{S}^n$, has the involution has opposite effective on the indexes: suspension by $\bar{S}^n$ one gets $KR^{n,0}$, while suspension by S^n results in $KR^{0,n}$, as in Eq. (A.13).

Moreover, Karoubi's descreption on K theory using Clifford algebras still applies here. Formally, one considers $Cl_{p,q}$-modules in the Real bundle category, and the K-theoretical classification of extensions as $Cl_{p,q}$-modules will be exactly $KR^{p,q}(X)$. As a result, for KR theory one has the $(1,1)$-periodicty:

$$KR^{r+1,s+1}(X) \cong K^{r,s}(X), \tag{A.29}$$

and moreover the mod 8 periodicity:

$$KR^{r,s}(X) \quad \text{only depends on } (r-s) \text{ mod } 8. \tag{A.30}$$

Appendix B   A No-Go Theorem for Localized Wannier Functions

This appendix is based on the supplemental material of [68]. We will show that for Chern insulators there is no Wannier basis where all Wannier functions are strictly compacted supported.

First, we recall how the Chern number (or other topological invariants) is defined from the filled-band projection ($P_{\mathbf{x},\mathbf{y}}$) for translationally invariant systems.

In general the (minimal) unit cell C may contain several sites and several orbitals, we need to regard the matrix ($P_{\mathbf{x},\mathbf{y}}$) as a block matrix ($P_{\bar{\mathbf{x}}\lambda,\bar{\mathbf{y}}\mu}$) (here λ,μ are labels in a unit cell, $\lambda,\mu \in \{1,2,\cdots,N\}$), which only depends on $\bar{\mathbf{x}} - \bar{\mathbf{y}}$ and λ,μ. Then taking the Fourier transform with respect to $\bar{\mathbf{x}} - \bar{\mathbf{y}}$:

$$\mathcal{P} = \sum_{\bar{\mathbf{x}},\bar{\mathbf{y}}} \phi_{\bar{\mathbf{x}}}^{\dagger} P_{\bar{\mathbf{x}}-\bar{\mathbf{y}}} \phi_{\bar{\mathbf{y}}} = \int \frac{d^2\mathbf{k}}{(2\pi)^2} \phi_{\mathbf{k}}^{\dagger} P(\mathbf{k}) \phi_{\mathbf{k}}, \tag{B.1}$$

one obtains projection matrices $P(\mathbf{k}) = (P_{\lambda,\mu}(\mathbf{k}))$ and hence a map:

$$P : T^2 \rightarrow \mathrm{Gr}(N,q). \tag{B.2}$$

It induces a vector bundle over T^2 by pullback of the tautological bundle over $\mathrm{Gr}(N,q)$. The Chern number is a characteristic number [11] of this bundle, which is used to classify topologically inequivalent bundles.

As a remark to be used later, here we have embedded $\mathrm{Gr}(N,q)$ into $M(N,\mathbb{C})$, the space of $N \times N$ complex matrices. Indeed, a point of $\mathrm{Gr}(N,q)$ corresponds to a q-dimensional subspace, which uniquely corresponds to the orthogonal projection matrix onto this subspace.

In this appendix, our main result the following:

Theorem B.1. If $P_{\mathbf{x},\mathbf{y}} = 0$ for $\forall \mathbf{x}, \mathbf{y}$ such that $|\mathbf{x} - \mathbf{y}|$ is large enough, then $c(P) = 0$.

Proof. We want to show the existence of q everythere-linear-independent global sections of $P^*(\tau)$, hence the bundle $P^*(\tau)$ is trivial.

To proceed, write the matrix-valued map $P(\mathbf{k}) : T^2 \to \mathrm{Gr}(N, q) \subseteq M(N, \mathbb{C})$ in components $p_{ij}(\mathbf{k})$ ($i, j \in \{1, 2, \cdots, N\}$). Denote $x = e^{ik_1}$, $y = e^{ik_2}$, where $\mathbf{k} = (k_1, k_2)$. The condition "$P_{\mathbf{x}, \mathbf{y}} = 0$ for sufficiently large $|\mathbf{x} - \mathbf{y}|$" is now equivalent to "each $p_{ij}(x, y)$ is a Laurent polynomial of x, y", i.e: $p_{ij} \in R \overset{\mathrm{def}}{=} \mathbb{C}[x, x^{-1}, y, y^{-1}]$, the Laurent polynomial ring over x, y. From now on, we extend T^2 to its complexification $(\mathbb{C}^*)^2$. We extend the function $P(x, y)$ to $(\mathbb{C}^*)^2$ by the Laurent polynomials $p_{ij}(x, y)$ described above.

We still have $P^2 = P$ since it is an algebraic relation and is valid on the real torus. The rank of P on the entire $(\mathbb{C}^*)^2$ is always q since $P^2 = P$ implies that $\mathrm{rank}(P) = \mathrm{Tr}(P)$ and $\mathrm{Tr}(P)$ is continuous.

Denote

$$S = \{u \in R^N | Pu = u\}, \tag{B.3}$$

which is the R-module of global Laurent sections (each component is a Laurent polynomial of x, y).

Remark: For any (x, y), $\{u \in \mathbb{C}^N | P(x, y)u = u\}$ is the fiber of $P^*(\tau)$ at (x, y), which is of dimension q. The purpose to construct S is that we want to find a global basis of the bundle $P^*(\tau)$ made of Laurent polynomials. The below lemma tells us that we can do it at least locally.

Lemma (local structure): For $\forall (x_0, y_0) \in (\mathbb{C}^*)^2$, there exists $u_1, \cdots, u_q \in S$ such that $u_1(x, y), \cdots, u_q(x, y)$ are linear independent in a neighbourhood of (x_0, y_0).

Proof of Lemma: For a fixed (x_0, y_0), choose a basis of $\mathbb{C}^N$ so that

$$P(x_0, y_0) = \mathrm{diag}(1, \cdots, 1, 0, \cdots, 0). \tag{B.4}$$

Under this basis, we write $1 - P(x, y)$ as a block matrix:

$$1 - P(x, y) = \frac{1}{x^a y^b} \begin{bmatrix} A(x, y) & B(x, y) \\ C(x, y) & D(x, y) \end{bmatrix}, \tag{B.5}$$

96

where A, B, C, D are matrixes with polynomial elements. By continuity, D is nonsigular on a neighbourhood of (x_0, y_0). On this neighbourhood,

$$
\begin{bmatrix} A & B \\ C & D \end{bmatrix} = \begin{bmatrix} I_q & B \\ 0 & D \end{bmatrix} \begin{bmatrix} A - BD^{-1}C & 0 \\ D^{-1}C & I_{N-q} \end{bmatrix},
\tag{B.6}
$$

where I_q denotes the identity matrix of size q, etc. Since $\text{rank}(1 - P) = N - q$, we know $A - BD^{-1}C = 0$. Therefore, a basis of in $\ker(1 - P)$ (dim=q) is given by the columns of the following $N \times q$ matrix:

$$
\begin{bmatrix} (\det D)I_q \\ -(\det D)D^{-1}C \end{bmatrix}.
\tag{B.7}
$$

Here we keep $\det(D)$ so that each element of the above matrix is a polynomial (no denominator), as required by the lemma.

The above lemma and its proof tell us S is a locally free module. Indeed, $(\mathbb{C}^*)^2$ is an affine variety with coordinate ring R, so according to the Hilbert's nullstellensatz, each maximal ideal of R corresponds to a point in $(\mathbb{C}^*)^2$ (The correspondence of ideal and point is the basic idea of algebraic geometry. Readers who are not familar with these notions may refer to [162].) For the maximal ideal $\mathfrak{m}$ corresponds point (x_0, y_0), consider $S_{\mathfrak{m}} = \{\frac{s}{f} | s \in S, f \in R, f(x_0, y_0) \neq 0\}$, the localization [162] of S at $\mathfrak{m}$. Then every $v \in S_{\mathfrak{m}}$ can be uniquely written as a linear combination of v_i (the image of u_i in $S_{\mathfrak{m}}$) with coefficients in $R_{\mathfrak{m}}$. So $S_{\mathfrak{m}}$ is a free $R_{\mathfrak{m}}$-module with rank q.

Back to the original question. Since $S \subseteq R^N$ and R (as a quotient of a polynomial ring) is a Noetherian ring, S is a Noetherian R-module. Thus S is a projective module[1]. According to a generalization of the Quillen-Suslin theorem[2] on the Laurent polynomial ring [164], S must be a free module. Fix a basis of S, then each element s_i of the basis must be an everywhere-nonzero section, otherwise, the lemma breaks down at points where s_i vanishes (as a vector in $\mathbb{C}^N$). So we have found the desired set of global sections. $\qquad\square$

---

[1]A finite-generated module over a Noetherian ring is projective iff it is locally free. Moreover, it is enough to verify this for the localization at every maximal ideal. See, for example, [163].

[2]A finite-generated projective module over the polynomial ring $k[x_1, \cdots, x_n]$ is free. See, for example, [53].

Geometrically, any such $P_{\mathbf{x},\mathbf{y}}$ gives rise to bundle $P^*(\tau)$ with algebraic structure. The Quillen-Suslin theorem confirms that such an "algebraic bundle" over certain base manifold (also with algebraic structure) must be trivial.

Corollary B.1. If the Chern number is nonzero, then there is no Wannier basis where all Wannier functions are strictly compacted supported.

Proof. Assuming there exist a set of compacted-supported Wannier basis, denoted as $|v^a\rangle$. Then:

$$P_{\mathbf{x},\mathbf{y}} = \langle\mathbf{x}|\,P\,|\mathbf{y}\rangle = \sum_a \langle\mathbf{x}|v^a\rangle\,\langle v^a|\mathbf{y}\rangle. \tag{B.8}$$

If $|\mathbf{x}-\mathbf{y}|$ is large enough (larger than twice the largest range of $|v^a\rangle$), there will be no $|v^a\rangle$ contributes to the summation. Therefore $P_{\mathbf{x},\mathbf{y}} = 0$. According to the above theorem, the Chern number must be 0. □

Note: compacted support Wannier functions cannot exist even if they are allowed to be overcompleted [69]. To prove this result, one cannot just proceed as above, since the module generated by (Fourier transformation of) Wannier functions is not free, even if localized on the real torus it is. For example, the module generated by x, y over $\mathbb{C}[x,y]$ is not a free module. Nevertheless, one can to use Hilbert's Syzygy theorem [53] to make sure that the bundle is (topologically but may not algebraically) trivial on the real torus.

98

Appendix C   Technical Details

C.1   More Technicalities for Sec. 3.4

C.1.1   Proof of Additivity

In this appendix, we will prove property 3.7 in Sec. 3.4.5. The proof is a little bit technical, but the physics idea is simple: vertex states of S comes from those of Q_1 and Q_2.

Lemma C.1 (Almost orthogonal vectors). For N unit vectors u_n in a d-dimensional linear space s.t. $|(u_i, u_j)| < \sigma$ for each $i \neq j$. If $\sigma < \frac{1}{\sqrt{2d}}$, then $N < 2d - 1$.

Proof. Let $A = (A_{i,j}) = ((u_i, u_j))$ to be the Gram matrix of $\{u_i\}$. Denote $\lambda_1, \cdots, \lambda_N$ the eigenvalues of A. Since $u_i \in \mathbb{C}^d$, $\text{rank}(A) \leq d$, at most d of them are nonzero. By Cauchy inequality, $\sum \lambda_i^2 \geq (\sum \lambda_i)^2/d = (\text{Tr } A)^2/d = N^2/d$. On the other hand, $\sum \lambda_i^2 = \text{Tr}(A^2) = \sum |(u_i, u_j)|^2 < N + N(N-1)\sigma^2$. Therefore,

$$\frac{N^2}{d} < N + N(N-1)\sigma^2 < N + N(N-1)\frac{1}{2d}. \tag{C.1}$$

Solving this inequality, we find $N < 2d - 1$. □

Lemma C.2 (an estimation of the eigenvalue distribution). Assume a Hermitian matrix A satisfying the exponential decay property (EDP) $|A_{\mathbf{i},\mathbf{j}}| < C_1 p(t) e^{-C_2 t}$ where $t = \max\{|\mathbf{i}|, |\mathbf{j}|\}$, $p(t)$ is a monic (leading coefficient=1) polynomial. The number of eigenvalues outside $(-\epsilon, \epsilon)$ is bounded by $\mathcal{O}(\frac{1}{C_2^2} \ln^2 \frac{C_1}{C_2^\alpha \epsilon})$, where $\alpha = 2 + \deg p$.

Proof. For an unit eigenvector x: $Ax = ax$, $|a| > \epsilon$, we separate x into two parts $x = y \oplus z$ according to whether the label is inside or outside a circle: $y_{\mathbf{i}} = 0$ if $|\mathbf{i}| > r$, $z_{\mathbf{i}} = 0$ if $|\mathbf{i}| < r$. The radius r will be determined later (depend on ϵ).

We claim that $\|z\| < \delta \overset{\text{def}}{=} \frac{C_1 r^{3/2} p(r) e^{-C_2 r}}{\epsilon}$. Indeed, $ay \oplus az = Ax$, $\|x\| = 1$. According to the Cauchy inequality we have

$$\|\epsilon z\|^2 < \|az\|^2 < \sum_{|\mathbf{i}| > r, \mathbf{j}} |A_{\mathbf{i},\mathbf{j}}|^2 \lesssim [C_1 r^{\frac{3}{2}} p(r) e^{-C_2 r}]^2. \tag{C.2}$$

Here, $\lesssim$ (means inequality up to constant) can be verified by doing integral. Denote the number of eigenvalues larger than ϵ to be N: $Ax_n = a_n x_n$, $n = 1, \cdots, N$. Without loss of generality, we can assume they are orthogonal, so

$$(x_i, x_j) = 0 \Rightarrow |(y_i, y_j)| = |(z_i, z_j)| < \delta^2. \tag{C.3}$$

Now we have N unit vectors $u_n = \frac{y_n}{\sqrt{1-z_n^2}}$ in dimension $d \propto r^2$ whose inner products with each other are less than $\sigma \overset{\text{def}}{=} \frac{\delta^2}{1-\delta^2}$. We choose r large enough so that

$$\sigma < \frac{1}{\sqrt{2d}} \sim \frac{1}{r}. \tag{C.4}$$

According to Lemma C.1, $N < 2d = \mathcal{O}(r^2)$. We can solve Eq. (C.4) to estimate r (thus N). Roughly, set $\sigma \sim (\frac{C_1 r^{3/2} p(r) e^{-C_2 r}}{\epsilon})^2 = \frac{1}{r}$, let $x = C_2 r$, we find $e^x = \frac{C_1}{C_2^\alpha \epsilon} x^\alpha$, where $\alpha = 2 + \deg p$. The exact solution can be expressed using the Lambert W function [165]. Here we only need the asymptotic expansion. Denote $\beta = \frac{C_1}{C_2^\alpha \epsilon}$, take logarithm, we have the following iteration:

$$x = \ln \beta + \alpha \ln x = \ln \beta + \alpha \ln(\ln \beta + \alpha \ln x) = \cdots = \mathcal{O}(\ln \beta). \tag{C.5}$$

Thus, it is enough to choose $r = \mathcal{O}(\frac{1}{C_2} \ln \frac{C_1}{C_2^\alpha \epsilon})$, and $N < 2d = \mathcal{O}(r^2) = \mathcal{O}(\frac{1}{C_2^2} \ln^2 \frac{C_1}{C_2^\alpha \epsilon})$. $\qquad \square$

As a corollary, it follows that

$$\sum_{|a|<\epsilon} |a| = \sum_{|a|<\epsilon} \int_0^\epsilon \theta(|a| - x) dx = \int_0^\epsilon \sum_{|a|<\epsilon} \theta(|a| - x) dx < \int_0^\epsilon \frac{1}{C_2^2} \ln^2 \frac{C_1}{C_2^\alpha x} dx, \tag{C.6}$$

which converges to 0 as $\epsilon \to 0$. Therefore any EDP operator is trace class.

Lemma C.3. Assume A is Hermitian. If $\exists x \neq 0$ s.t. $\|(A - \lambda)x\| < \|\epsilon x\|$, then A has an eigenvalue $a \in (\lambda - 2\epsilon, \lambda + 2\epsilon)$. Moreover, decompose $x = x^\| + x^\perp$ with respect to subspace $(\lambda - 2\epsilon, \lambda + 2\epsilon)$, then $\|x^\perp\| < \frac{1}{2}$. If A is of finite size $N \times N$, then an eigenvector x_a of A with eigenvalue $a \in (\lambda - 2\epsilon, \lambda + 2\epsilon)$ satisfies $|(x, y)| > \sqrt{\frac{3}{4N}}$.

Proof. Denote $B = A - \lambda$, then $\|Bx\| < \|\epsilon x\|$. Without loss of generality, assume $\|x\| = 1$. Let us diagonalize B, so that $B = \text{diag}\{b_1, \cdots, b_n\}$. Then we have

$$\epsilon^2 > \sum b_i^2 |x_i|^2 = \sum_{|b_i| \geq 2\epsilon} b_i^2 |x_i|^2 + \sum_{|b_i| < 2\epsilon} b_i^2 |x_i|^2 > 4\epsilon^2 \sum_{|b_i| \geq 2\epsilon} |x_i|^2 + \sum_{|b_i| < 2\epsilon} b_i^2 |x_i|^2. \qquad \text{(C.7)}$$

So we must have $\sum_{|b_i| \geq 2\epsilon} |x_i|^2 < \frac{1}{4}$, thus $\|x^\perp\| < \frac{1}{2}$ and $\exists i$ such that $|b_i| < 2\epsilon$. If N is finite, then from $\sum_{|b_i| < 2\epsilon} |x_i|^2 < \frac{3}{4}$ we know $\exists i$ such that $|b_i| < 2\epsilon, |x_i| > \sqrt{\frac{3}{4N}}$. $\qquad \square$

Go back to the original proposition. We want to find a correspondence between vertex eigenvalues of S and those of Q_1 and Q_2. To make the notation simple, in the following e^{-r} means $C_1 p(r) e^{-C_2 r}$ and C_1, C_2 can change.

For each vertex state x of Q_1: $Q_1 x = qx$, $\|x\| = 1$ ($q \neq 0, 1$), separate x as $x = y + z$ with respect to the disk $B(1, r)$. As in Eq.(C.2), we still have $\|z\| < \frac{e^{-r}}{|q^2 - q|}$. It is not difficult to show that

$$\|(S - q)x\| = \|(S - Q_1)x\| \leq \|(S - Q_1)y\| + \|(S - Q_1)z\| \lesssim (1 + \frac{1}{|q^2 - q|}) e^{-r} \overset{\text{def}}{=} \delta. \quad \text{(C.8)}$$

According to Lemma C.3, S has an eigenvalue in $(q - 2\delta, q + 2\delta)$. The same argument also applies to Q_2. Thus, for each vertex eigenvalue q of Q_1, Q_2, we get an eigenvalue of S in a neighbourhood of q.

Denote $U_\epsilon \overset{\text{def}}{=} (-\epsilon, \epsilon) \cup (1 - \epsilon, 1 + \epsilon)$. For $q \notin U_\epsilon$, $|q^2 - q| > \epsilon/2$, so that $\delta < \frac{e^{-r}}{\epsilon}$. As $r \to \infty$, we will adjust ϵ accordingly so that δ is still small enough such that spectral gaps outside U_ϵ are always greater than δ. Then we can describe the spectra structure of Q_1, Q_2 in Fig. 14. The shaded windows have width$\sim \delta$ and are of three types. For types 1 and 2, we already get the correspondence. For type 3, we claim the dimension of the subspace X corresponding to eigenvalues (of S) in such window is at least 4. Indeed, denote x_1, x_2 the eigenstates of Q_1, x_3, x_4 the the eigenstates of Q_2, then $|(x_i, x_j)| < \delta$. Let $x_i = u_i + v_i$ where $u_i \in X$ and $v_i \perp X$, then

$$|(y_i, y_j)| \leq |(x_i, x_j)| + |(z_i, z_j)| < \delta + \frac{1}{4}. \qquad \text{(C.9)}$$

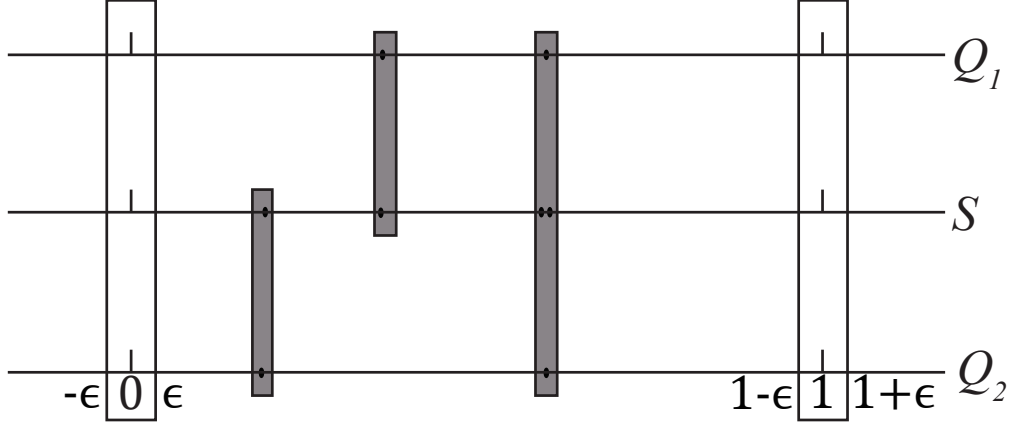Similar to Eq. (C.1) (here $N = 4$), we get $d \geq 4$.

Figure 14: Spectra structure of Q_i and S. We only consider eigenvalues outside $(-\epsilon, \epsilon) \cup (1 - \epsilon, 1 + \epsilon)$. The dots $\bullet$ are eigenvalues. Each dots represents a Kramers pair due to time reversal symmetry. The shaded windows are of width $\delta \sim \frac{e^{-r}}{\epsilon}$ and are (from left to right) of three types.

Moreover, each eigenstate of S with $s \in U_\epsilon$ is generated in this way. Indeed, assume $Sx = sx$, $\|x\| = 1$ ($s \neq 0, 1$), then

$$x = \frac{1}{s^2 - s}(V_1 x + V_2 x) \tag{C.10}$$

is a decomposition of x. At least one of $\|V_i x\|$ should be larger than $|s^2 - s|/2$, say $V_1 x$. Note that $V_i x$ and $(S - s)V_i x$ are mainly supported near vertex i, and

$$(S - s)V_1 x + (S - s)V_2 x = (S - s)(S^2 - S)x = 0, \tag{C.11}$$

and both terms must be small:

$$\|(S - s)V_i x\| < e^{-r}. \tag{C.12}$$

Therefore,

$$\|(Q_1 - s)V_1 x\| \leq \|(S - s)V_i x\| + \|(S - Q_1)V_1 x\| < e^{-r} \leq \frac{e^{-r}}{|s^2 - s|}\|V_1 x\| \stackrel{\text{def}}{=} \delta'\|V_1 x\|. \tag{C.13}$$

102

According to Lemma C.3, Q_1 has an eigenvalue in $(s - 2\delta', s + 2\delta')$. Therefore, s must be near (within $\sim \delta$) a window, and an argument similar to (C.9) shows that x cannot be a new eigenstate.

Due to this correspondence, the last term in the decomposition

$$|\operatorname{Tr}^v(S) - (\operatorname{Tr}^v(Q_1) + \operatorname{Tr}^v(Q_2))| \leq |\sum_{s \in U_\epsilon} s| + |\sum_{q_1 \in U_\epsilon} q_1| + |\sum_{q_2 \in U_\epsilon} q_2| + |\sum_{s \notin U_\epsilon} s - \sum_{q_1 \notin U_\epsilon} q_1 - \sum_{q_2 \notin U_\epsilon} q_2|,$$
$$(C.14)$$

is bounded by $\delta \ln^2 \frac{1}{\epsilon}$ and goes to 0 as $r \to \infty$. The second and third term can be bounded due to Eq. (C.6), since $Q_i - \overline{Q_i}$ obeys EDP with the same C_1 and C_2. For the first term, $S^2 - S$ also obeys EDP (with respect to the central point 0), however with a new constant $C_1' \sim C_1 e^r$. This is because (see Eq. (3.73)) the EDP of V_i is with respect to vertex i, so the decay property of $S^2 - S$ with respect to vertex 0 need to be estimated by $e^{-\operatorname{dist}(\mathbf{x},0)} < e^r e^{-\operatorname{dist}(\mathbf{x},1)}$. Luckily, similar to Eq. (C.6), we still have

$$|\sum_{s \in U_\epsilon} s| < \int_0^\epsilon \frac{1}{C_2^2} \ln^2 \frac{C_1 e^r}{C_2^\alpha x} dx \to 0, \tag{C.15}$$

as $r \to \infty$ as long as $\epsilon = o(\frac{1}{r^2})$. Thus we have proved that

$$\lim_{r \to \infty} \operatorname{Tr}^v(S) - (\operatorname{Tr}^v(Q_1) + \operatorname{Tr}^v(Q_2)) = 0. \tag{C.16}$$

Note that we have assumed that the requirement $\epsilon = o(\frac{1}{r^2})$ is compatible with $\delta = \frac{e^{-r}}{\epsilon} < \operatorname{gap}$. This technical assumption is reasonable. Indeed, according to Lemma C.2, the spectral gap at ϵ is roughly $(\frac{d}{d\epsilon} \ln^2 \frac{1}{\epsilon})^{-1} \sim \frac{\epsilon}{\ln \epsilon}$ in average. In order for $\delta < \frac{\epsilon}{\ln \epsilon}$, it is enough to set $\epsilon > \Omega(e^{-C'r})$, which is exponentially smaller than $\frac{1}{r^2}$ for large r. Even if we consider the fluctuation of the spectral gaps and even if the level statistics is Poissonian (so that no level repulsion), the probability for this to be true is 1 from the following estimation:

$$\Pr(\text{at least one gap} < \frac{p(r)e^{-r}}{\epsilon}) < \sum_{x > \epsilon} \frac{p(r)e^{-r}/\epsilon}{x/\ln x} < \frac{p(r)e^{-r} \ln \epsilon}{\epsilon^2} \times \ln^2 \frac{1}{\epsilon} \to 0 \tag{C.17}$$

C.1.2 Proof of the Finite Size Approximation

In this section, we prove Proposition 3.4. The technique used will be similar to the above section. We need to compare vertex eigenvalues of Q and Q'_N. Recall that $\|Q'_N - Q_N\| \le \rho^2, \|V'_N - W_N\| < \rho, \|V'_N - W_N\| < \rho$ where $\rho \sim e^{-Cr}$.

Temporarily fix ϵ, and only consider eigenvalues outside $U_\epsilon \overset{\text{def}}{=} (-\epsilon, \epsilon) \cup (1 - \epsilon, 1 + \epsilon)$. For any $\alpha \notin U$, $|\alpha^2 - \alpha| > \epsilon/2$.

For $(Q - q)x = 0$, $q \notin U_\epsilon$, we separate it as $x = y + z$ with respect to circle $r/2$, again $\|z\| < \frac{p(r)e^{-Cr}}{\epsilon} \overset{\text{def}}{=} \delta$. In the following δ means "everything that goes like $\frac{p(r)e^{-Cr}}{\epsilon}$ with perhaps different C". Thus

$$
\begin{aligned}
\|(Q'_N - q)x\| &= \|(Q'_N - Q_N + Q_N - Q)x\| \\
&\le \|(Q'_N - Q_N)x\| + \|(Q_N - Q)y\| + \|(Q_N - Q)z\| \\
&\lesssim \delta,
\end{aligned}
\tag{C.18}
$$

so Q'_N has an eigenvalue $q' \in (q - 2\delta, q + 2\delta)$ with eigenstate x' satisfies $|(x, x')| > \sqrt{\frac{3}{4N}}$ (Lemma C.3). This implies x' must contain a vertex eigenstate. Indeed, if not, we have $V'_N x' = 0$ so $x' = \frac{1}{q'^2 - q'} W'_N x'$ which is concentrated near boundary r, thus

$$
|(x, x')| = \frac{1}{|q'^2 - q'|}(x, W'_N x') < \frac{2}{\epsilon}[|(y, W'_N x')| + |(z, W'_N x')|] \lesssim \delta,
\tag{C.19}
$$

a contradiction as $r \to \infty$.

On the other hand, if $(Q'_N - a)x = 0(a \ne 0, 1)$, and x is a vertex state: $W'_N x = 0$, then $x = \frac{V'_N x}{a^2 - a}$. We have

$$
(Q - a)x = \frac{1}{a^2 - a}(Q - Q'_N)V'_N x = \frac{1}{a^2 - a}[(Q - Q_N)V_N x + (Q_N - Q'_N)V'_N x] \lesssim \delta.
\tag{C.20}
$$

So, Q has an eigenvalue in $(a - 2\delta, a + 2\delta)$.

Now we choose r according to the same technical assumption above, so that there is a correspondence outside region U_ϵ for $\forall \epsilon$. Then, similarly we have

$$
|\sum_{\text{vertex}} q' - \text{Tr}^v(Q)| \le |\sum_{q \in U_\epsilon} q| + |\sum_{q' \in U_\epsilon} q'| + |\sum_{q \notin U_\epsilon} q - \sum_{q' \notin U_\epsilon} q'|.
\tag{C.21}
$$

The last term is bounded by $\delta \ln^2 \frac{1}{\epsilon}$ which goes to 0 as $\epsilon \to 0$. The first term also goes to 0 since $Q - \overline{Q}$ is trace class. The second term is bounded by No. $\{q'\}\epsilon$. Obviously No. $\{q'\} < \dim Q_N \sim r^2$, so this term also converges to 0 since $\epsilon = o(\frac{1}{r^2})$.

104

C.1.3   Proof that $S - T$ is Trace Class

In this section, we prove the claim used in Property 3.8.

The first step is to figure out the decay behaviour of the matrix elements of $S - T$. According to the Peierls substitution [82],

$$S_{ij} = P_{ij}e^{i\int_i^j \mathbf{A}\cdot d\mathbf{r}}, \quad T_{ij} = P_{ij}e^{i\int_i^j \mathbf{A}'\cdot d\mathbf{r}}, \tag{C.22}$$

where $\mathbf{A}$ and $\mathbf{A}'$ are the vector potential for the two flux configurations. See Fig. 15(a) (all angles here are directed), we have:

$$\mathbf{A} \cdot d\mathbf{r} \propto 2\theta, \quad \mathbf{A}' \cdot d\mathbf{r} \propto \theta_1 + \theta_2,$$
$$(S - T)_{\mathbf{x},\mathbf{y}} \sim P_{\mathbf{x},\mathbf{y}}e^{i(\theta_1+\theta_2)}(e^{i(2\theta-\theta_1-\theta_2)} - 1). \tag{C.23}$$
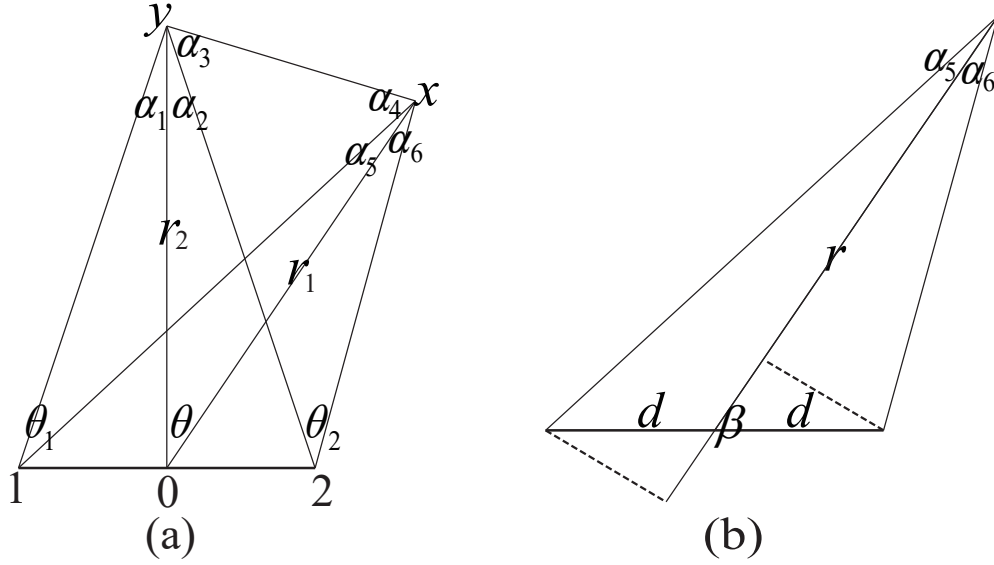

Figure 15: Relevant geometries in the proof. (a) Position 0 is the position for 1-flux insertion; position 1 and 2 are the positions for half-flux insertions. (b) To calculate $(\alpha_5 - \alpha_6)$, we draw to dashed lines perpendicular to the middle solid line.

From geometry, $2\theta - \theta_1 - \theta_2 = (\alpha_1 - \alpha_2) - (\alpha_5 - \alpha_6)$. Let us calculate $(\alpha_5 - \alpha_6)$. See Fig. 15(b), we have:

$$
\begin{aligned}
\alpha_5 - \alpha_6 &= \arctan \frac{d \sin \beta}{r + d \cos \beta} - \arctan \frac{d \sin \beta}{r - d \cos \beta} \\
&= \arctan \frac{\frac{d \sin \beta}{r + d \cos \beta} - \frac{d \sin \beta}{r - d \cos \beta}}{1 + \frac{d \sin \beta}{r + d \cos \beta} \frac{d \sin \beta}{r - d \cos \beta}} \\
&= -\arctan \frac{d^2 \sin 2\beta}{r^2 - d^2} \\
&= -\frac{d^2 \sin 2\beta}{r^2} + \mathcal{O}(\frac{1}{r^4}).
\end{aligned}
\tag{C.24}
$$

Due to the energy gap, $|A_{\mathbf{x},\mathbf{y}}| \lesssim e^{-C|\mathbf{x}-\mathbf{y}|}$. Assuming $r_1 \geq r_2$, we claim that

$$
e^{-C|\mathbf{x}-\mathbf{y}|} |e^{i(2\theta - \theta_1 - \theta_2)} - 1| < e^{-\frac{C}{2}|\mathbf{x}-\mathbf{y}|} \mathcal{O}(\frac{1}{r_1^3}).
\tag{C.25}
$$

Indeed, if $e^{-\frac{C}{2}|\mathbf{x}-\mathbf{y}|} < \frac{1}{(r_1+r_2)^3}$, there is nothing needed to prove. If not, then $|\mathbf{x}-\mathbf{y}| < \frac{6}{C} \ln(r_1 + r_2) < \frac{7}{C} \ln r_1$ (asymptotically). In this case, from geometry, we know $|\beta_i - \beta_j| = |\theta| \lesssim \frac{|\mathbf{x}-\mathbf{y}|}{r_1}$. Then $2\theta - \theta_1 - \theta_2 = (\alpha_1 - \alpha_2) - (\alpha_5 - \alpha_6) = \frac{\sin 2\beta_1}{r_1^2} - \frac{\sin 2\beta_2}{r_2^2} + \mathcal{O}(\frac{1}{r_2^4})$ will be of order $\mathcal{O}(\frac{|\mathbf{x}-\mathbf{y}|}{r_1^3})$ as can be seen from Taylor expansion. Then it is easy to see that the claim also holds.

The result is (in a more symmetric fashion, ignore constants) as follows: the operator $A = S - T$ satisfies the following decay property:

$$
|A_{\mathbf{x},\mathbf{y}}| < \frac{1}{(|\mathbf{x}| + |\mathbf{y}|)^3} e^{-|\mathbf{x}-\mathbf{y}|}.
\tag{C.26}
$$

Now, we prove this kind of operator must be trace class. Let us denote the nth singular value (decreasing order) to be s_n. According to the Courant min-max principle [80], we have

$$
s_n = \min_{Y_{n-1}} \max_{u \perp Y_{n-1}} \frac{(Au, Au)}{(u, u)},
\tag{C.27}
$$

where Y_{n-1} means a subspace of dimension $n-1$. Thus, for any given n-dimensional subspace Y_{n-1}, we have

$$
s_n^2 \leq \max_{u \perp Y_{n-1}} \frac{(Au, Au)}{(u, u)} = \max_{\substack{u \perp Y_{n-1} \\ ||u||=1}} ||Au||^2.
\tag{C.28}
$$

Let us choose the subspace Y_{n-1} to be spanned by the n components nearest to the center (so that the label of the components are approximately in the disk of radius $r \sim \sqrt{n}$). Denote

106

the columns of A to be $v_\mathbf{x}$ ($v_\mathbf{x} = Ae_\mathbf{x}$, $\mathbf{x} \in \mathbb{Z}^2$ is the label). With Eq. (C.26) it is easy to show (note that here $e^{-|\mathbf{x}-\mathbf{y}|}$ means $e^{-C|\mathbf{x}-\mathbf{y}|}$ for a different C)

$$|(v_\mathbf{x}, v_\mathbf{y})| = |(A^2)_{\mathbf{x},\mathbf{y}}| \lesssim \frac{e^{-|\mathbf{x}-\mathbf{y}|}}{|\mathbf{x}|^3|\mathbf{y}|^3}. \tag{C.29}$$

Thus,

$$\|Au\|^2 = \left\|\sum_{|\mathbf{x}|>r} u_\mathbf{x} v_\mathbf{x}\right\|^2 = \sum_{|\mathbf{x}|,|\mathbf{y}|>r} \bar{u}_\mathbf{x} u_\mathbf{y} (v_\mathbf{x}, v_\mathbf{y}) = \left(\sum_{\substack{|\mathbf{x}-\mathbf{y}|\geq l \\ |\mathbf{x}|,|\mathbf{y}|>r}} + \sum_{\substack{|\mathbf{x}-\mathbf{y}|<l \\ |\mathbf{x}|,|\mathbf{y}|>r}}\right) \bar{u}_\mathbf{x} u_\mathbf{y} (v_\mathbf{x}, v_\mathbf{y}). \tag{C.30}$$

Here, l will be of the order $\ln r$, to be specific later.

The first summation is (crude but enough) controlled by e^{-l} due to Eq. (C.29) and Cauchy inequality. For the second summation, we have

$$\left|\sum \bar{u}_\mathbf{x} u_\mathbf{y} (v_\mathbf{x}, v_\mathbf{y})\right| < \frac{1}{4}\sum (|u_\mathbf{x}|^2 + |u_\mathbf{y}|^2)|(v_\mathbf{x}, v_\mathbf{y})| \lesssim \frac{l^2}{r^6}. \tag{C.31}$$

Let us choose l such that $e^{-l} = \frac{1}{r^6}$, we finally have

$$s_n^2 \leq e^{-l} + \frac{l^2}{r^6} < \frac{\ln^2 r}{r^6} \sim \frac{\ln^2 n}{n^3}. \tag{C.32}$$

so $\sum s_n = \sum \frac{\ln n}{n^{3/2}}$ converges, which means A is trace class.
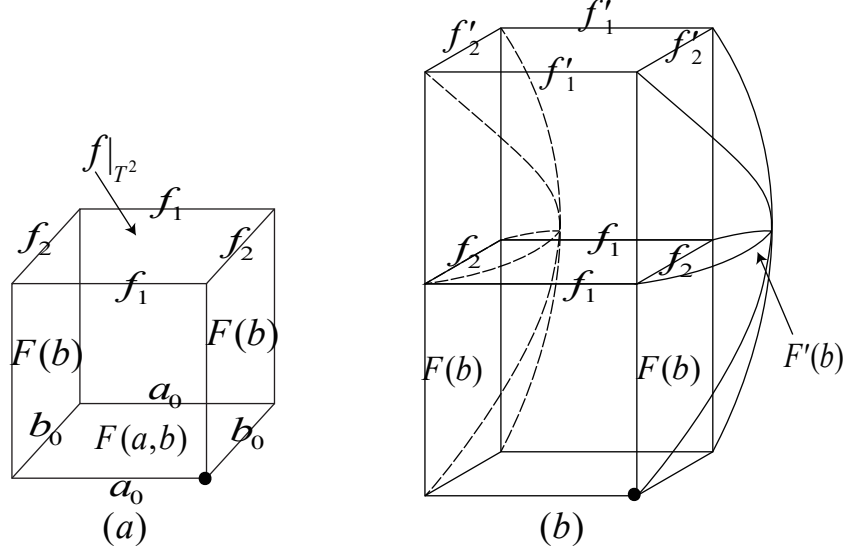
Figure 16: (a) The definition of $h \in \pi_2(X)$. It is defined by the surface of the cube, made of $f|_{T^2}, F(a), F(b)$ and the pre-chosen $F(a, b)$. (b) $\bar{h}$ is well-defined. The "cap" attached to the right surface (another one in the left denoted with dashed line) is the other homotopy $F'(b)$. Here, $F(b), F'(b)$ and the homotopy between f_2 and f_2' defined an element $s \in \pi_2(X)$. Pictorially it is the right "cap"+right surface. The one on the left corresponds to s^a, since we have to fixed a base point when defining $\pi_2(X)$, say the one denoted by $\bullet$.

C.2   Some Algebraic Topology Details for Sec. 4.1

C.2.1   Homotopy Class $\langle T^2, X \rangle$–Proof of Eq. (4.15)

In this section, we prove Eq. (4.15) in detail:

$$\langle T^2, X \rangle = \{(a, b) \in \pi_1(X)^2 | ab = ba\} \times \pi_2(X)/\langle t - t^a, t - t^b \mid t \in \pi_2 \rangle. \tag{C.33}$$

Namely, a homotopy class $[f] \in \langle T^2, X \rangle$ one-to-one corresponds to an element in set at right hand side of Eq. (C.33).

For each pair $(a, b) \in \pi_1(X)^2$ such that $ab = ba$, we choose and fix two loops[1] a_0, b_0, and also choose and fix a homotopy from $a_0 b_0 a_0^{-1} b_0^{-1}$ to 0, denoted by $F(a, b)$. Note that $a_0, b_0, F(a, b)$ are arbitrarily chosen. But once they are chosen, they are fixed for all.

Given $[f] \in \langle T^2, X \rangle$, we choose a map $f : T^2 \to X$ in this class. There are two nontrivial loops (fixed) in T^2, denoted by l_1, l_2, with the same base point. The restriction of f on l_1 defines a map (loop) $f_1 : S^1 \to X$ and therefore an element $a \in \pi_1(X)$. Similarly we have $b \in \pi_1(X)$. Since the loop $l_1 l_2 l_1^{-1} l_2^{-1}$ is homotopic to 0 in T^2, we know $ab = ba$ in $\pi_1(X)$. Obviously a, b are well-defined function of $[f]$.

Since loop f_1 is homotopic to a_0, there exists (not unique) a homotopy $F(a)$ from f_1 to a_0; the same for b and we have a $F(b)$. Now define an element h in $\pi_2(X)$ as in Fig. 16(a). In this way we get an element $\bar{h} \in \pi_2(X)/\langle t - t^a, t - t^b \mid t \in \pi_2 \rangle$.

We need to prove that $\bar{h}$ does not depend on the choice of $f, F(a), F(b)$. To do this, assume we choose a different f' and therefore different loops l'_1, l'_2 in X, different homotopy $F'(a)$ and $F'(b)$, and different element $h' \in \pi_2(X)$. To compare h and h' we need to fix a base point. Defined t to be the element in $\pi_2(X)$ determined by $F(a), F'(a)$ and the homotopy between f, f', see Fig. 16(b). Also from this figure, we know that

$$h' = h + t - t^b + s - s^a, \tag{C.34}$$

therefore $\bar{h} = \bar{h}'$.

The inverse map is easy to define. Therefore we have proved Eq. (C.33).

C.2.2 The Action of $\pi_1(X_n)$ on $\pi_2(X_n)$–Proof of Eq. (4.17)

In this section, we prove that the action $t \mapsto t^a$ is determined by Eq. (4.17), which we rewrite here for convenience:

$$(t_1, \cdots, t_n) \mapsto (t_{a(1)}, \cdots, t_{a(n)}). \tag{C.35}$$

To see this, consider the projection

$$X_n = (\mathrm{Conf}_n \times F_n)/S_n \xrightarrow{j} F_n/S_n, \tag{C.36}$$

---

[1]Note the notations here: a, b are homotopy class of loops, a_0, b_0 are loops.

which induces an isomorphism on π_2 and a surjection $B_n \to S_n$ on π_1. Therefore, the action of $\pi_1(X_n)$ on $\pi_2(X_n)$ factorizes through the action of $\pi_1(F_n/S_n) = S_n$ on $\pi_2(F_n/S_n)$:

$$
\begin{array}{ccc}
\pi_2(X_n) & \xrightarrow{B_n} & \pi_2(X_n) \\
\Big\downarrow{\cong} & & \Big\downarrow{\cong} \\
\pi_2(F_n/S_n) & \xrightarrow{S_n} & \pi_2(F_n/S_n)
\end{array}
\qquad (C.37)
$$

Geometrically, the action of $[\gamma] \in \pi_1(X_n)$ on $\pi_2(X_n)$ is given by any homotopy $f_t : S^2 \to X_n$ such that $f_t(s_0) = \gamma(t)$ (here s_0 is a base point on S^2); under projection j, $j \circ f_t$ gives a homotopy $S^2 \to F_n/S_n$ and therefore an action of $p([\gamma]) \in S_n$ on $\pi_2(F_n/S_n)$.

We now show the action of $\pi_1(F_n/S_n) = S_n$ on $\pi_2(F_n/S_n)$ is given by Eq. (C.35). Indeed, assuming the loop γ in F_n/S_n is lifted to $\tilde{\gamma}$ in F_n, $\tilde{\gamma}(1) = g\tilde{\gamma}(0)$ where $g \in S_n$. Then a homotopy $S^2 \to F_n/S_n$ corresponding to the $[\gamma]$ action will be lifted to a homotopy that deforms the map $\tilde{f}_0 : S^2 \to F_n$ to $\tilde{f}_1 : S^2 \to F_n$ such that $\tilde{f}_1(s_0) = \tilde{\gamma}(1), \tilde{f}_0(s_0) = \tilde{\gamma}(0)$. In order to identify the corresponding element of $\tilde{f}_1$ in $\pi_2(F_n/S_n)$, one just need to consider $g^{-1} \circ \tilde{f}_1$ since they ($g^{-1} \circ \tilde{f}_1$ and $\tilde{f}_1$) are the same map after projection to F_n/S_n and $g^{-1}\tilde{f}_1(s_0) = \tilde{f}_0(s_0)$ is the correct base point, see Fig. 17 for illustration of above argument.

Now we identify $g^{-1} \circ \tilde{f}_1$ in $\pi_2(F_n) = \mathbb{Z}^{n-1}$ according to the injection $\pi_2(F_n) \xrightarrow{\partial} \pi_1(\mathbb{C}^{*n})$ in Eq. (4.8). Recall that the boundary map ∂ is defined by a homotopy lifting. For example, to identify $\partial(\tilde{f}_1)$, one regard $\tilde{f}_0 : S^2 \to F_n$ as a map $I^2 \to F_n$, where $\tilde{f}_0(\partial I^2) = \{b_0\}$; then as a homotopy $H_t : I^1 \to F_n$. Then lift H_0 along into $GL(n)$. This is just the trivial map to a point, say e_0. They use relative homotopy lifting property to lift H_t for $t \in I$. $H_1(I)$, which is the lift of $\tilde{f}_0$ on $I \times \{1\}$, is now a loop based on e_0, which induces as an element in $\pi_1(\mathbb{C}^{*n})$.

In our case, $g^{-1} \circ \tilde{f}_1$ is just given by Fig. 17(b). We can construct the lifting explicitly. First note that S_n has an action on $GL(n)$ by column transformation, which is the lift of its action on F_n. We lift the path $g^{-1}(\tilde{\gamma})$ in F_n to a path β in $GL(n)$ starting at e_0. We can make it end at $e_{-1} = g^{-1}e_0$ by gradually changing the phases of each column vector along the path. Now the homotopy lifting is defined as follows (see Fig. 17(c)). For $t \in [0, 1]$, scan the square in Fig. 17(b) from bottom to up. For small t (before touching the inner square), just lift the homotopy it along β. Then one lifts the homotopy inside the inner square by
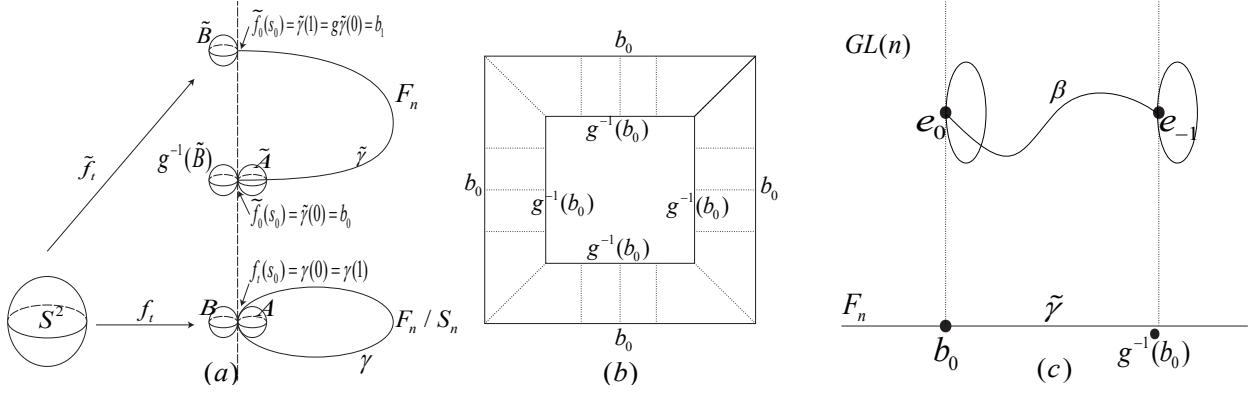
Figure 17: (a) An illustration for the proof of Eq. (4.17). Assuming $[\gamma]$ action takes an element in $\pi_2(F_n/S_n)$ (represented by A) to B, then the lift $\tilde{f}_t$ will be a homotopy from $\tilde{A}$ to $\tilde{B}$. To identify the corresponding element of $\tilde{B}$ in $\pi_2(F_n/S_n)$, just consider $g^{-1}(\tilde{B})$ since it is the same as $\tilde{B}$ under projection. (b) The definition of $g^{-1} \circ \tilde{f}_1$ (corresponds to $g^{-1}(\tilde{B})$ in Fig. 17). One regard S^2 as I^2 with boundary points identified, then draw a smaller square inside it. Define the map on the inner square as $g^{-1} \circ \tilde{f}_0$ (would be $g^{-1}(\tilde{A})$ in the notation of Fig. 17), so that the inner boundary maps to $g^{-1}(b_0)$. Then one connects the inner and outer boundary by the paths $g^{-1}(\tilde{\gamma})$. One gets a well-defined map from I^2 to F_n, with the outer boundary maps to b_0. (c) Illustration of the homotopy lifting process.

$g^{-1} \circ$ the homotopy lifting of $\tilde{f}_0$. After one passes the inner square, one can just move e_{-1} to e_0 by shrinking the line β. The homotopy class (n integers) of the loops on fibers is invariant (For example, since we are only looking at the bundle over an open path $\tilde{\gamma}$, we can regard it as a trivial bundle). The final lifting is a loop on the fiber over b_0 with base point e_0. It is easy to see this loop corresponds to Eq. (4.17).

111

Bibliography

[1]   L. D. Landau. Zur Theorie der phasenumwandlungen II. *Phys. Z. Sowjetunion*, 11:26–35, 1936.

[2]   L.D. Landau and E.M. Lifshitz. *Statistical Physics: Volume 5*. Butterworth-Heinemann, New York, 2013.

[3]   D. J. Thouless, M. Kohmoto, M. P. Nightingale, and M. den Nijs. Quantized Hall conductance in a two-dimensional periodic potential. *Phys. Rev. Lett.*, 49:405–408, Aug 1982.

[4]   F. D. M. Haldane. Nonlinear field theory of large-spin Heisenberg antiferromagnets: Semiclassically quantized solitons of the one-dimensional easy-axis Néel state. *Phys. Rev. Lett.*, 50:1153–1156, Apr 1983.

[5]   K. v. Klitzing, G. Dorda, and M. Pepper. New method for high-accuracy determination of the fine-structure constant based on quantized Hall resistance. *Phys. Rev. Lett.*, 45:494–497, Aug 1980.

[6]   A.N. W, N.W. Ashcroft, N.D. Mermin, N.D. Mermin, and Brooks/Cole Publishing Company. *Solid State Physics*. HRW international editions. Holt, Rinehart and Winston, 1976.

[7]   Michael A. Nielsen and Isaac L. Chuang. *Quantum Computation and Quantum Information: 10th Anniversary Edition*. Cambridge University Press, 2010.

[8]   A. Hatcher. *Algebraic Topology*. Cambridge University Press, 2002.

[9]   Clifford Taubes. *Differential Geometry: Bundles, Connections, Metrics and Curvature*. Oxford University Press, New York, Oxford, 2011.

[10]   Dale Husemller, Siegfried Echterhoff, Stefan Fredenhagen, and Bernhard Krtz. *Basic bundle theory and K-cohomology invariants*. Springer, New York; Berlin, 2008.

[11]   J.W. Milnor and J.D. Stasheff. *Characteristic Classes*. Annals of mathematics studies. Princeton University Press, 1974.

[12]   F. D. M. Haldane. Model for a quantum hall effect without landau levels: Condensed-matter realization of the "parity anomaly". *Phys. Rev. Lett.*, 61:2015–2018, Oct 1988.

[13]   C. L. Kane and E. J. Mele. Z_2 topological order and the quantum spin Hall effect. *Phys. Rev. Lett.*, 95:146802, Sep 2005.

[14] B. Andrei Bernevig, Taylor L. Hughes, and Shou-Cheng Zhang. Quantum spin Hall effect and topological phase transition in hgte quantum wells. *Science*, 314(5806):1757–1761, 2006.

[15] Markus König, Steffen Wiedmann, Christoph Brüne, Andreas Roth, Hartmut Buhmann, Laurens W. Molenkamp, Xiao-Liang Qi, and Shou-Cheng Zhang. Quantum spin Hall insulator state in HgTe quantum wells. *Science*, 318(5851):766–770, 2007.

[16] C. L. Kane and E. J. Mele. Quantum spin Hall effect in graphene. *Phys. Rev. Lett.*, 95:226801, Nov 2005.

[17] Alexander Altland and Martin R. Zirnbauer. Nonstandard symmetry classes in mesoscopic normal-superconducting hybrid structures. *Phys. Rev. B*, 55:1142–1161, Jan 1997.

[18] A. Kitaev. Periodic table for topological insulators and superconductors. In V. Lebedev and M. Feigel'Man, editors, *American Institute of Physics Conference Series*, volume 1134 of *American Institute of Physics Conference Series*, pages 22–30, May 2009.

[19] Andreas P. Schnyder, Shinsei Ryu, Akira Furusaki, and Andreas W. W. Ludwig. Classification of topological insulators and superconductors in three spatial dimensions. *Phys. Rev. B*, 78:195125, Nov 2008.

[20] Daniel S. Freed and Gregory W. Moore. Twisted equivariant matter. *Annales Henri Poincaré*, 14(8):1927–2023, Dec 2013.

[21] Ching-Kai Chiu, Jeffrey C. Y. Teo, Andreas P. Schnyder, and Shinsei Ryu. Classification of topological quantum matter with symmetries. *Rev. Mod. Phys.*, 88:035005, Aug 2016.

[22] A. Connes. *Noncommutative Geometry*. Elsevier Science, 1995.

[23] Emil Prodan. Non-commutative tools for topological insulators. *New Journal of Physics*, 12(6):065003, Jun 2010.

[24] Emil Prodan. Disordered topological insulators: a non-commutative geometry perspective. *Journal of Physics A: Mathematical and Theoretical*, 44(11):113001, Feb 2011.

[25] Emil Prodan, Bryan Leung, and Jean Bellissard. The non-commutative nth-Chern number ($n \geqslant 1$). *Journal of Physics A: Mathematical and Theoretical*, 46(48):485202, Nov 2013.

[26] I. C. Fulga, F. Hassler, and A. R. Akhmerov. Scattering theory of topological insulators and superconductors. *Phys. Rev. B*, 85:165409, Apr 2012.

[27]   Joseph E. Avron, Ruedi Seiler, and Barry Simon. Charge deficiency, charge transport and comparison of dimensions. *Comm. Math. Phys.*, 159(2):399–422, 1994.

[28]   Alexei Kitaev. Anyons in an exactly solved model and beyond. *Annals of Physics*, 321(1):2 – 111, 2006. January Special Issue.

[29]   Zhi Li and Roger S. K. Mong. Local formula for the Z_2 invariant of topological insulators. *Phys. Rev. B*, 100:205101, Nov 2019.

[30]   T. A. Loring and M. B. Hastings. Disordered topological insulators via C*-algebras. *EPL (Europhysics Letters)*, 92(6):67004, Dec 2010.

[31]   Matthew B. Hastings and Terry A. Loring. Almost commuting matrices, localized wannier functions, and the quantum Hall effect. *Journal of Mathematical Physics*, 51(1):015214, 2010.

[32]   Matthew B. Hastings and Terry A. Loring. Topological insulators and C*-algebras: Theory and numerical practice. *Annals of Physics*, 326(7):1699 – 1759, 2011. July 2011 Special Issue.

[33]   Terry A. Loring. K-theory and pseudospectra for topological insulators. *Annals of Physics*, 356:383 – 416, 2015.

[34]   Giuseppe De Nittis and Hermann Schulz-Baldes. Spectral flows associated to flux tubes. *Annales Henri Poincaré*, 17(1):1–35, Jan 2016.

[35]   Hosho Katsura and Tohru Koma. The Z_2 index of disordered topological insulators with time reversal symmetry. *Journal of Mathematical Physics*, 57(2):021903, 2016.

[36]   Yutaka Akagi, Hosho Katsura, and Tohru Koma. A new numerical method for Z_2 topological insulators with strong disorder. *Journal of the Physical Society of Japan*, 86(12):123710, 2017.

[37]   Raffaello Bianco and Raffaele Resta. Mapping topological order in coordinate space. *Phys. Rev. B*, 84:241106, Dec 2011.

[38]   Huaqing Huang and Feng Liu. Quantum spin Hall effect and spin bott index in a quasicrystal lattice. *Phys. Rev. Lett.*, 121:126401, Sep 2018.

[39]   J. Bellissard. K-theory of C^*–Algebras in solid state physics. In T. C. Dorlas, N. M. Hugenholtz, and M. Winnink, editors, *Statistical Mechanics and Field Theory: Mathematical Aspects*, volume 257 of *Lecture Notes in Physics, Berlin Springer Verlag*, pages 99–156, 1986.

[40]   J. Bellissard, A. van Elst, and H. Schulz̃Baldes. The noncommutative geometry of the quantum Hall effect. *Journal of Mathematical Physics*, 35(10):5373–5451, 1994.

[41] Nimrod Moiseyev. *Non-Hermitian Quantum Mechanics*. Cambridge University Press, 2011.

[42] Carl M. Bender and Stefan Boettcher. Real spectra in non-Hermitian Hamiltonians having PT symmetry. *Phys. Rev. Lett.*, 80:5243–5246, Jun 1998.

[43] Carl M. Bender, Dorje C. Brody, and Hugh F. Jones. Complex extension of quantum mechanics. *Phys. Rev. Lett.*, 89:270401, Dec 2002.

[44] Carl M Bender. Making sense of non-Hermitian Hamiltonians. *Reports on Progress in Physics*, 70(6):947–1018, May 2007.

[45] Zongping Gong, Yuto Ashida, Kohei Kawabata, Kazuaki Takasan, Sho Higashikawa, and Masahito Ueda. Topological phases of non-Hermitian systems. *Phys. Rev. X*, 8:031079, Sep 2018.

[46] Kohei Kawabata, Ken Shiozaki, Masahito Ueda, and Masatoshi Sato. Symmetry and Topology in Non-Hermitian Physics. *arXiv e-prints*, page arXiv:1812.09133, Dec 2018.

[47] Kohei Kawabata, Takumi Bessho, and Masatoshi Sato. Classification of exceptional points and non-Hermitian topological semimetals. *Phys. Rev. Lett.*, 123:066405, Aug 2019.

[48] Hengyun Zhou and Jong Yeon Lee. Periodic table for topological bands with non-Hermitian symmetries. *Phys. Rev. B*, 99:235112, Jun 2019.

[49] Ananya Ghatak and Tanmoy Das. New topological invariants in non-Hermitian systems. *Journal of Physics: Condensed Matter*, 31(26):263001, Apr 2019.

[50] Zhi Li and Roger S. K. Mong. Homotopical classification of non-hermitian band structures, 2019.

[51] Eugene P. Wigner. *Gruppentheorie und ihre Anwendung auf die Quantenmechanik der Atomspektren. Mit 12 Abbildungen*. F. Vieweg & Sohn Akt.-Ges, Braunschweig, 1931.

[52] V. Bargmann. On unitary ray representations of continuous groups. *Annals of Mathematics*, 59(1):1–46, 1954.

[53] S. Lang. *Algebra*. Graduate Texts in Mathematics. Springer New York, 2005.

[54] Eugene P. Wigner. Characteristic vectors of bordered matrices with infinite dimensions. *Annals of Mathematics*, 62(3):548–564, 1955.

[55] Freeman J. Dyson. The Threefold Way. Algebraic Structure of Symmetry Groups and Ensembles in Quantum Mechanics. *Journal of Mathematical Physics*, 3(6):1199–1215, November 1962.

[56] Max Karoubi. *K-theory: an introduction.* Springer-Verlag, New York, Berlin, 1977.

[57] Zheng-Cheng Gu and Xiao-Gang Wen. Tensor-entanglement-filtering renormalization approach and symmetry-protected topological order. *Phys. Rev. B*, 80:155131, Oct 2009.

[58] Xie Chen, Zheng-Cheng Gu, Zheng-Xin Liu, and Xiao-Gang Wen. Symmetry protected topological orders and the group cohomology of their symmetry group. *Phys. Rev. B*, 87:155114, Apr 2013.

[59] Joel E. Moore, Ying Ran, and Xiao-Gang Wen. Topological surface states in three-dimensional magnetic insulators. *Phys. Rev. Lett.*, 101:186805, Oct 2008.

[60] A Yu Kitaev. Unpaired majorana fermions in quantum wires. *Physics-Uspekhi*, 44(10S):131–136, Oct 2001.

[61] Liang Fu, C. L. Kane, and E. J. Mele. Topological insulators in three dimensions. *Phys. Rev. Lett.*, 98:106803, Mar 2007.

[62] J. E. Moore and L. Balents. Topological invariants of time-reversal-invariant band structures. *Phys. Rev. B*, 75:121306, Mar 2007.

[63] Rahul Roy. Topological phases and the quantum spin Hall effect in three dimensions. *Phys. Rev. B*, 79:195322, May 2009.

[64] G.E. Volovik. *The Universe in a Helium Droplet.* International Series of Monographs on Physics. OUP Oxford, 2009.

[65] J. Avron, R. Seiler, and B. Simon. The index of a pair of projections. *Journal of Functional Analysis*, 120(1):220 – 237, 1994.

[66] C. Davis. Separation of two linear subspaces. *Acta Sci. Math. (Szeged)*, 19:172–187, 1958.

[67] Christian Brouder, Gianluca Panati, Matteo Calandra, Christophe Mourougane, and Nicola Marzari. Exponential localization of wannier functions in insulators. *Phys. Rev. Lett.*, 98:046402, Jan 2007.

[68] Zhi Li and Roger S. K. Mong. Entanglement renormalization for chiral topological phases. *Phys. Rev. B*, 99:241105, Jun 2019.

[69] J. Dubail and N. Read. Tensor network trial states for chiral topological phases in two dimensions and a no-go theorem in any dimension. *Phys. Rev. B*, 92:205307, Nov 2015.

[70] Huaxin Lin. Almost commuting selfadjoint matrices and applications. *Fields Institute Commun.*, 13, 01 1997.

[71] M. B. Hastings. Making almost commuting matrices commute. *Communications in Mathematical Physics*, 291(2):321–345, Oct 2009.

[72] Terry A. Loring. K-theory and asymptotically commuting matrices. *Canadian Journal of Mathematics*, 40(1):197216, 1988.

[73] Terry A. Loring. When matrices commute. *Mathematica Scandinavica*, 82(2):305–319, 1998.

[74] Jonathan M. Rosenberg. *Algebraic K-theory and its applications*, volume 147. Springer-Verlag, New York, 1994.

[75] Liang Fu and C. L. Kane. Time reversal polarization and a Z_2 adiabatic spin pump. *Phys. Rev. B*, 74:195312, Nov 2006.

[76] Liang Fu and C. L. Kane. Topological insulators with inversion symmetry. *Phys. Rev. B*, 76:045302, Jul 2007.

[77] Xiao-Liang Qi, Taylor L. Hughes, and Shou-Cheng Zhang. Topological field theory of time-reversal invariant insulators. *Phys. Rev. B*, 78:195424, Nov 2008.

[78] Rahul Roy. Z_2 classification of quantum spin Hall systems: An approach using time-reversal invariance. *Phys. Rev. B*, 79:195321, May 2009.

[79] D. J. Thouless. Quantization of particle transport. *Phys. Rev. B*, 27:6083–6087, May 1983.

[80] P.D. Lax. *Functional Analysis*. Pure and Applied Mathematics: A Wiley Series of Texts, Monographs and Tracts. Wiley, 2014.

[81] Matthew B. Hastings and Tohru Koma. Spectral gap and exponential decay of correlations. *Communications in Mathematical Physics*, 265(3):781–804, Aug 2006.

[82] R. Peierls. Zur Theorie des Diamagnetismus von Leitungselektronen. *Zeitschrift fur Physik*, 80:763–791, November 1933.

[83] Sven Bachmann, Alex Bols, Wojciech De Roeck, and Martin Fraas. Many-body Fredholm index for ground-state spaces and abelian anyons. *Phys. Rev. B*, 101:085138, Feb 2020.

[84] H. J. Carmichael. Quantum trajectory theory for cascaded open systems. *Phys. Rev. Lett.*, 70:2273–2276, Apr 1993.

[85] Ingrid Rotter. A non-Hermitian hamilton operator and the physics of open quantum systems. *Journal of Physics A: Mathematical and Theoretical*, 42(15):153001, Mar 2009.

[86] Sebastian Diehl, Enrique Rico, Mikhail A. Baranov, and Peter Zoller. Topology by dissipation in atomic quantum wires. *Nature Physics*, 7:971 EP –, Oct 2011. Article.

[87] Kenta Esaki, Masatoshi Sato, Kazuki Hasebe, and Mahito Kohmoto. Edge states and topological phases in non-Hermitian systems. *Phys. Rev. B*, 84:205128, Nov 2011.

[88] Alois Regensburger, Christoph Bersch, Mohammad-Ali Miri, Georgy Onishchukov, Demetrios N. Christodoulides, and Ulf Peschel. Parity-time synthetic photonic lattices. *Nature*, 488:167 EP –, Aug 2012. Article.

[89] Bo Zhen, Chia Wei Hsu, Yuichi Igarashi, Ling Lu, Ido Kaminer, Adi Pick, Song-Liang Chua, John D. Joannopoulos, and Marin Soljacic. Spawning rings of exceptional points out of dirac cones. *Nature*, 525:354 EP –, Sep 2015.

[90] Liang Feng, Ramy El-Ganainy, and Li Ge. Non-Hermitian photonics based on parity-time symmetry. *Nature Photonics*, 11(12):752–762, 2017.

[91] Hui Cao and Jan Wiersig. Dielectric microcavities: Model systems for wave chaos and non-Hermitian physics. *Rev. Mod. Phys.*, 87:61–111, Jan 2015.

[92] Ramy El-Ganainy, Konstantinos G. Makris, Mercedeh Khajavikhan, Ziad H. Musslimani, Stefan Rotter, and Demetrios N. Christodoulides. Non-Hermitian physics and pt symmetry. *Nature Physics*, 14:11 EP –, Jan 2018. Review Article.

[93] K. G. Makris, R. El-Ganainy, D. N. Christodoulides, and Z. H. Musslimani. Beam dynamics in $\mathcal{PT}$ symmetric optical lattices. *Phys. Rev. Lett.*, 100:103904, Mar 2008.

[94] Shachar Klaiman, Uwe Günther, and Nimrod Moiseyev. Visualization of branch points in $\mathcal{PT}$-symmetric waveguides. *Phys. Rev. Lett.*, 101:080402, Aug 2008.

[95] A. Guo, G. J. Salamo, D. Duchesne, R. Morandotti, M. Volatier-Ravat, V. Aimez, G. A. Siviloglou, and D. N. Christodoulides. Observation of $\mathcal{PT}$-symmetry breaking in complex optical potentials. *Phys. Rev. Lett.*, 103:093902, Aug 2009.

[96] S. Longhi. Bloch oscillations in complex crystals with $\mathcal{PT}$ symmetry. *Phys. Rev. Lett.*, 103:123601, Sep 2009.

[97] Youngwoon Choi, Sungsam Kang, Sooin Lim, Wookrae Kim, Jung-Ryul Kim, Jai-Hyung Lee, and Kyungwon An. Quasieigenstate coalescence in an atom-cavity quantum composite. *Phys. Rev. Lett.*, 104:153601, Apr 2010.

[98] Zin Lin, Hamidreza Ramezani, Toni Eichelkraut, Tsampikos Kottos, Hui Cao, and Demetrios N. Christodoulides. Unidirectional invisibility induced by $\mathcal{PT}$-symmetric periodic structures. *Phys. Rev. Lett.*, 106:213901, May 2011.

[99] S. Bittner, B. Dietz, U. Günther, H. L. Harney, M. Miski-Oglu, A. Richter, and F. Schäfer. PT symmetry and spontaneous symmetry breaking in a microwave billiard. *Phys. Rev. Lett.*, 108:024101, Jan 2012.

[100] M. Liertzer, Li Ge, A. CerJan, A. D. Stone, H. E. Türeci, and S. Rotter. Pump-induced exceptional points in lasers. *Phys. Rev. Lett.*, 108:173901, Apr 2012.

[101] Simon Malzard, Charles Poli, and Henning Schomerus. Topologically protected defect states in open photonic systems with non-Hermitian charge-conjugation and parity-time symmetry. *Phys. Rev. Lett.*, 115:200402, Nov 2015.

[102] Tony E. Lee. Anomalous edge state in a non-Hermitian lattice. *Phys. Rev. Lett.*, 116:133903, Apr 2016.

[103] Daniel Leykam, Konstantin Y. Bliokh, Chunli Huang, Y. D. Chong, and Franco Nori. Edge modes, degeneracies, and topological numbers in non-Hermitian systems. *Phys. Rev. Lett.*, 118:040401, Jan 2017.

[104] Vladyslav Kozii and Liang Fu. Non-Hermitian Topological Theory of Finite-Lifetime Quasiparticles: Prediction of Bulk Fermi Arc Due to Exceptional Point. *arXiv e-prints*, page arXiv:1708.05841, Aug 2017.

[105] Tsuneya Yoshida, Robert Peters, and Norio Kawakami. Non-Hermitian perspective of the band structure in heavy-fermion systems. *Phys. Rev. B*, 98:035141, Jul 2018.

[106] A. A. Zyuzin and A. Yu. Zyuzin. Flat band in disorder-driven non-Hermitian weyl semimetals. *Phys. Rev. B*, 97:041203, Jan 2018.

[107] C. Dembowski, H.-D. Gräf, H. L. Harney, A. Heine, W. D. Heiss, H. Rehfeld, and A. Richter. Experimental observation of the topological structure of exceptional points. *Phys. Rev. Lett.*, 86:787–790, Jan 2001.

[108] Christian E. Rüter, Konstantinos G. Makris, Ramy El-Ganainy, Demetrios N. Christodoulides, Mordechai Segev, and Detlef Kip. Observation of parity-time symmetry in optics. *Nature Physics*, 6:192 EP –, Jan 2010.

[109] Liang Feng, Ye-Long Xu, William S. Fegadolli, Ming-Hui Lu, José E. B. Oliveira, Vilson R. Almeida, Yan-Feng Chen, and Axel Scherer. Experimental demonstration of a unidirectional reflectionless parity-time metamaterial at optical?frequencies. *Nature Materials*, 12:108 EP –, Nov 2012.

[110] Long Chang, Xiaoshun Jiang, Shiyue Hua, Chao Yang, Jianming Wen, Liang Jiang, Guanyu Li, Guanzhong Wang, and Min Xiao. Parity-time symmetry and variable optical isolation in active-passive-coupled microresonators. *Nature Photonics*, 8:524 EP –, Jun 2014.

[111] Hossein Hodaei, Mohammad-Ali Miri, Matthias Heinrich, Demetrios N. Christodoulides, and Mercedeh Khajavikhan. Parity-time–symmetric microring lasers. *Science*, 346(6212):975–978, 2014.

[112] T. Gao, E. Estrecho, K. Y. Bliokh, T. C. H. Liew, M. D. Fraser, S. Brodbeck, M. Kamp, C. Schneider, S. Höfling, Y. Yamamoto, F. Nori, Y. S. Kivshar, A. G.

Truscott, R. G. Dall, and E. A. Ostrovskaya. Observation of non-Hermitian degeneracies in a chaotic exciton-polariton billiard. *Nature*, 526:554 EP –, Oct 2015.

[113] Hossein Hodaei, Absar U. Hassan, Steffen Wittek, Hipolito Garcia-Gracia, Ramy El-Ganainy, Demetrios N. Christodoulides, and Mercedeh Khajavikhan. Enhanced sensitivity at higher-order exceptional points. *Nature*, 548:187 EP –, Aug 2017.

[114] Chun-Hui Liu, Hui Jiang, and Shu Chen. Topological classification of non-Hermitian systems with reflection symmetry. *Phys. Rev. B*, 99:125103, Mar 2019.

[115] Xiao-Qi Sun, Charles C. Wojcik, Shanhui Fan, and Tom Bzduek. Non-trivial braiding of band nodes in non-Hermitian systems, 2019.

[116] Baogang Zhu, Rong Lü, and Shu Chen. $\mathcal{PT}$ symmetry in the non-Hermitian su-schrieffer-heeger model with complex boundary potentials. *Phys. Rev. A*, 89:062102, Jun 2014.

[117] Simon Lieu. Topological phases in the non-Hermitian su-schrieffer-heeger model. *Phys. Rev. B*, 97:045106, Jan 2018.

[118] Chuanhao Yin, Hui Jiang, Linhu Li, Rong Lü, and Shu Chen. Geometrical meaning of winding number and its characterization of topological phases in one-dimensional chiral non-Hermitian systems. *Phys. Rev. A*, 97:052115, May 2018.

[119] Hui Jiang, Rong Lü, and Shu Chen. Topological invariants, zero mode edge states and finite size effect for a generalized non-reciprocal Su-Schrieffer-Heeger model. *arXiv e-prints*, page arXiv:1906.04700, Jun 2019.

[120] Shunyu Yao, Fei Song, and Zhong Wang. Non-Hermitian chern bands. *Phys. Rev. Lett.*, 121:136802, Sep 2018.

[121] Timothy M. Philip, Mark R. Hirsbrunner, and Matthew J. Gilbert. Loss of Hall conductivity quantization in a non-Hermitian quantum anomalous Hall insulator. *Phys. Rev. B*, 98:155430, Oct 2018.

[122] Yu Chen and Hui Zhai. Hall conductance of a non-Hermitian chern insulator. *Phys. Rev. B*, 98:245130, Dec 2018.

[123] Huitao Shen, Bo Zhen, and Liang Fu. Topological band theory for non-Hermitian Hamiltonians. *Phys. Rev. Lett.*, 120:146402, Apr 2018.

[124] Kohei Kawabata, Ken Shiozaki, and Masahito Ueda. Anomalous helical edge states in a non-Hermitian chern insulator. *Phys. Rev. B*, 98:165148, Oct 2018.

[125] Kohei Kawabata, Sho Higashikawa, Zongping Gong, Yuto Ashida, and Masahito Ueda. Topological unification of time-reversal and particle-hole symmetries in non-Hermitian physics. *Nature Communications*, 10(1):297, 2019.

[126] M V Keldysh. On the completeness of the eigenfunctions of some classes of non-selfadjoint linear operators. *Russian Mathematical Surveys*, 26(4):15–44, Aug 1971.

[127] M.V. Berry. Physics of nonhermitian degeneracies. *Czechoslovak Journal of Physics*, 54(10):1039–1047, Oct 2004.

[128] W D Heiss. The physics of exceptional points. *Journal of Physics A: Mathematical and Theoretical*, 45(44):444016, Oct 2012.

[129] Ye Xiong. Why does bulk boundary correspondence fail in some non-hermitian topological models. *Journal of Physics Communications*, 2(3):035043, Mar 2018.

[130] V. M. Martinez Alvarez, J. E. Barrios Vargas, and L. E. F. Foa Torres. Non-Hermitian robust edge states in one dimension: Anomalous localization and eigenspace condensation at exceptional points. *Phys. Rev. B*, 97:121401, Mar 2018.

[131] Flore K. Kunst, Elisabet Edvardsson, Jan Carl Budich, and Emil J. Bergholtz. Biorthogonal bulk-boundary correspondence in non-Hermitian systems. *Phys. Rev. Lett.*, 121:026808, Jul 2018.

[132] Heinrich-Gregor Zirnstein, Gil Refael, and Bernd Rosenow. Bulk-boundary correspondence for non-Hermitian Hamiltonians via Green functions. *arXiv e-prints*, Jan 2019.

[133] Shunyu Yao and Zhong Wang. Edge states and topological invariants of non-Hermitian systems. *Phys. Rev. Lett.*, 121:086803, Aug 2018.

[134] Ching Hua Lee and Ronny Thomale. Anatomy of skin modes and topology in non-Hermitian systems. *Phys. Rev. B*, 99:201103, May 2019.

[135] V. M. Martinez Alvarez, J. E. Barrios Vargas, M. Berdakin, and L. E. F. Foa Torres. Topological states of non-Hermitian systems. *The European Physical Journal Special Topics*, 227(12):1295–1308, Dec 2018.

[136] J. E. Avron, R. Seiler, and B. Simon. Homotopy and quantization in condensed matter physics. *Phys. Rev. Lett.*, 51:51–53, Jul 1983.

[137] Ari M. Turner, Yi Zhang, Roger S. K. Mong, and Ashvin Vishwanath. Quantized response and topology of magnetic insulators with inversion symmetry. *Phys. Rev. B*, 85:165120, Apr 2012.

[138] Krishanu Roychowdhury and Michael J. Lawler. Classification of magnetic frustration and metamaterials from topology. *Phys. Rev. B*, 98:094432, Sep 2018.

[139] Luis E. F. Foa Torres. Perspective on topological states of non-Hermitian lattices. *Journal of Physics: Materials*, 2019.

[140] Dan S. Borgnia, Alex Jura Kruchkov, and Robert-Jan Slager. Non-Hermitian Boundary Modes. *arXiv e-prints*, page arXiv:1902.07217, Feb 2019.

[141] Joan S. Birman and James Cannon. *Braids, Links, and Mapping Class Groups. (AM-82)*. Princeton University Press, 1974.

[142] Louis H Kauffman. *Knots and Physics*. World Scientific, 3rd edition, 2001.

[143] Edward Fadell and Lee Neuwirth. Configuration spaces. *MATHEMATICA SCANDINAVICA*, 10:111–118, Jun. 1962.

[144] C. Kassel, O. Dodane, and V. Turaev. *Braid Groups*. Graduate Texts in Mathematics. Springer New York, 2008.

[145] F. A. Garside. The Braid Group and Other Groups. *The Quarterly Journal of Mathematics*, 20(1):235–254, 01 1969.

[146] Grigory M (https://math.stackexchange.com/users/152/grigory m). How to compute homotopy classes of maps on the 2-torus? Mathematics Stack Exchange.

[147] Juan Gonzlez-Meneses. Basic results on braid groups. *Annales mathmatiques Blaise Pascal*, 18:15–59, Jun 2011.

[148] William P. Thurston. On the geometry and dynamics of diffeomorphisms of surfaces. *Bulletin of the American Mathematical Society*, 19(2):417–431, 1988.

[149] Eduardo Fradkin. *Field Theories of Condensed Matter Physics*. Cambridge University Press, 2 edition, 2013.

[150] X. G. Wen and Q. Niu. Ground-state degeneracy of the fractional quantum hall states in the presence of a random potential and on high-genus riemann surfaces. *Phys. Rev. B*, 41:9377–9396, May 1990.

[151] A.Yu. Kitaev. Fault-tolerant quantum computation by anyons. *Annals of Physics*, 303(1):2 – 30, 2003.

[152] Michael A. Levin and Xiao-Gang Wen. String-net condensation: A physical mechanism for topological phases. *Phys. Rev. B*, 71:045110, Jan 2005.

[153] Daniel S. Freed and Michael J. Hopkins. Reflection positivity and invertible topological phases, 2016.

[154] Rahul M. Nandkishore and Michael Hermele. Fractons. *Annual Review of Condensed Matter Physics*, 10(1):295–313, 2019.

[155] Jrme Cayssol, Balzs Dra, Ferenc Simon, and Roderich Moessner. Floquet topological insulators. *physica status solidi (RRL) Rapid Research Letters*, 7(12):101–108, 2013.

[156] Marin Bukov, Luca D'Alessio, and Anatoli Polkovnikov. Universal high-frequency behavior of periodically driven systems: from dynamical stabilization to floquet engineering. *Advances in Physics*, 64(2):139–226, 2015.

[157] Frank Schindler, Ashley M. Cook, Maia G. Vergniory, Zhijun Wang, Stuart S. P. Parkin, B. Andrei Bernevig, and Titus Neupert. Higher-order topological insulators. *Science Advances*, 4(6), 2018.

[158] Liang Fu. Topological crystalline insulators. *Phys. Rev. Lett.*, 106:106802, Mar 2011.

[159] Daniel Bump. *Lie Groups*, volume 225. Springer, New York, 2004.

[160] H. B. Lawson and M. Michelsohn. *Spin Geometry*, volume 38. Princeton University Press, Princeton, N.J, 1989.

[161] M.F. Atiyah, R. Bott, and A. Shapiro. Clifford modules. *Topology*, 3:3 – 38, 1964.

[162] Miles Reid. *Undergraduate Algebraic Geometry*. London Mathematical Society student texts. Cambridge University Press, 2001.

[163] Pete L. Clark. *Commutative Algebra*.

[164] Richard G Swan. Projective modules over laurent polynomial rings. *Transactions of the American Mathematical Society*, 237:111–120, 1978.

[165] R. M. Corless, G. H. Gonnet, D. E. G. Hare, D. J. Jeffrey, and D. E. Knuth. On the Lambert-W function. *Advances in Computational Mathematics*, 5(1):329–359, Dec 1996.